Neural circuits mediating innate and learned behavior

Felicity Gore

Submitted in partial fulfillment of the
requirements for the degree of
Doctor of Philosophy
under the Executive Committee
of the Graduate School of Arts and Sciences

COLUMBIA UNIVERSITY

2016

ABSTRACT

Neural circuits mediating innate and learned behavior

Felicity Gore

For many organisms the sense of smell is critical to survival. Some olfactory stimuli elicit innate responses that are mediated through hardwired circuits that have developed over long periods of evolutionary time. Most olfactory stimuli, however, have no inherent meaning. Instead, meaning must be imposed by learning during the lifetime of an organism. Despite the dominance of olfactory stimuli on animal behavior, the mechanisms by which odorants elicit learned behavioral responses remain poorly understood.

All odor-evoked behaviors are initiated by the binding of an odorant to olfactory receptors located on sensory neurons in the nasal epithelium. Olfactory sensory neurons transmit this information to the olfactory bulb via spatially organized axonal projections such that individual odorants evoke a stereotyped map of bulbar activity. A subset of bulbar neurons, the mitral and tufted cells, relay olfactory information to higher brain structures that have been implicated in the generation of innate and learned behavioral responses, including the cortical amygdala and piriform cortex.

Anatomical studies have demonstrated that the spatial stereotypy of the olfactory bulb is maintained in projections to the posterolateral cortical amygdala, a structure that is involved in the generation of innate odor-evoked responses. The projections of mitral and tufted cells to piriform cortex however appear to discard the spatial order of the olfactory bulb: each glomerulus sends spatially diffuse, apparently random projections across the entire cortex. This anatomy appears to constrain odor-evoked responses in

piriform cortex: electrophysiological and imaging studies demonstrate that individual odorants activate sparse ensembles that are distributed across the extent of cortex, and individual piriform neurons exhibit discontinuous receptive fields such that they respond to structurally and perceptually similar and dissimilar odorants. It is therefore unlikely that olfactory representations in piriform have inherent meaning. Instead, these representations have been proposed to mediate olfactory learning. In accord with this, lesions of posterior piriform cortex prevent the expression of a previously acquired olfactory fear memory and photoactivation of a random ensemble of piriform neurons can become entrained to both appetitive and aversive outcomes. Piriform cortex therefore plays a central role in olfactory fear learning. However, how meaning is imparted on olfactory representations in piriform remains largely unknown.

We developed a strategy to manipulate the neural activity of representations of conditioned and unconditioned stimuli in the basolateral amygdala (BLA), a downstream target of piriform cortex that has been implicated in the generation of learned responses. This strategy allowed us to demonstrate that distinct neural ensembles represent an appetitive and an aversive unconditioned stimulus (US) in the BLA. Moreover, the activity of these representations can elicit innate responses as well as direct Pavlovian and instrumental learning. Finally activity of an aversive US representation in the basolateral amygdala is required for learned olfactory and auditory fear responses. These data suggest that both olfactory and auditory stimuli converge on US representations in the BLA to generate learned behavioral responses. Having identified a US representation in the BLA that receives convergent olfactory information to generate learned fear responses, we were then able to step back into the olfactory system and demonstrate that

the BLA receives olfactory input via the monosynaptic projection from piriform cortex. These data suggest that aversive meaning is imparted on an olfactory representation in piriform cortex via reinforcement of its projections onto a US representation in the BLA.

The work described in this thesis has identified mechanisms by which sensory stimuli generate appropriate behavioral responses. Manipulations of representations of unconditioned stimuli have identified a central role for US representations in the BLA in connecting sensory stimuli to both innate and learned behavioral responses. In addition, these experiments have suggested local mechanisms by which fear learning might be implemented in the BLA. Finally, we have identified a fundamental transformation through which a disordered olfactory representation in piriform cortex acquires meaning. Strikingly this transformation appears to occur within 3 synapses of the periphery. These data, and the techniques we employ, therefore have the potential to significantly impact upon our understanding of the neural origins of motivated behavior.

TABLE OF CONTENTS

LIST OF FIGURES

ACKNOWLEDGEMENTS

The work described in this thesis is the culmination of 5 years of work, none of which would have been possible without the contributions and support of those around me.

First and foremost I would first like to thank my family and my husband, Sam. I would not have achieved all I have without your unconditional love and support. Thank you for the faith you have always had in me.

Thank you to my undergraduate advisers, Barry Everitt and Amy Milton, who first introduced me to Neuroscience. Thank you for giving me the chance to work with you and showing me the importance of carefully designed behavioral paradigms. Thank you Barry for the piece of advice that has fundamentally changed my life – "go to the USA".

I am deeply thankful to my long-term collaborator, Edmund Schwartz. You've been an exceptional colleague, mentor, and friend. I am grateful for all that you have taught me, and the years that we have worked together. I would also like to thank my collaborators Joseph Stujenske, Ekaterina Likhtik, Joshua Gordon, and Marco Russo. Thank you for all your help.

Thanks to Columbia's doctoral program in Neurobiology and Behavior, for providing such a great place to do good science. Thank you especially to Carol Mason for all your help in my early days at Columbia.

Thank you to all members of the Salzman and Axel labs, as well as my friends in the Neurobiology program. Thank you to Baylor Brangers, Stanley Aladi, Samara Miller,

Jessica Freeland, Cynthia Franqui, Martin Vigniovich, Lori Glenwinkel, Patrick Kaifosh, Kevin Franks, Dara Sosulski and Pia Kelsey O'Neill, you have all made Columbia a great place to be.

Thanks to Phyllis Kisloff, Miriam Guiterrez, Adriana Nemes, Monica Mendelsohn and Nataliya Zabello for all your assistance over the years.

Thank you to René Hen, Larry Abbott, and Carlos Brody for serving on my committee - your time and scientific input are greatly appreciated.

Finally, my eternal thanks go to my thesis advisers, Richard Axel and Daniel Salzman, who have both taught me invaluable lessons throughout my time at Columbia. They have shown me the importance of diligence, care and rigor in experimentation, but perhaps more importantly they have taught me to think. I would have achieved none of this without you and I am forever indebted to you both. Thank you.

DEDICATION

For Mum, Dad, Jack, and Sam; thank you for your unconditional love and support.

CHAPTER 1

INTRODUCTION

All organisms must solve the same fundamental problem; they must approach reward and avoid danger in order to survive. Some stimuli possess inherently rewarding or aversive qualities and elicit innate behavioral responses. Most stimuli, however, have no inherent meaning. Instead meaning must be imparted by learning. This is advantageous, allowing an animal to maximize its chances of obtaining reward and avoiding punishment in a constantly changing environment. Understanding how animals detect and respond to motivationally salient sensory stimuli is therefore critical to understanding how animals survive in a dynamic and often unpredictable sensory world.

Over the past century, tremendous advances in our understanding of the development and function of the nervous system have come from a diverse array of model organisms. The mouse has provided a particularly powerful model organism with which to study how sensory stimuli generate behavioral responses owing to its substantial homology with human neurobiology, the plethora of molecular and physiological techniques available for its study, and the diversity of behavioral responses it exhibits. Many of these behavioral responses are mediated by the sense of smell, ranging from innate responses such as the selection of mates, to learned behaviors such as remembering a previously treacherous location. The mouse olfactory system therefore provides a potentially insightful model with which to study the neurobiological origins of motivated behavior.

The Mouse Olfactory System

Olfactory stimuli, like stimuli from each of the five sensory modalities, elicit innate responses that are mediated through hardwired circuits that have developed over long periods of evolutionary time. Most olfactory stimuli however have no inherent meaning. Instead, meaning must be imparted by learning during the lifetime of an organism. The mouse olfactory system must therefore generate a diverse array of odor-evoked innate and learned behavioral responses to facilitate survival in a constantly changing sensory world.

Odor-evoked behavioral responses are initiated via the binding of odorants in the environment to olfactory receptors in the nasal epithelium. Olfactory receptors comprise a large, multigene family of 7-transmembrane receptors that are selectively expressed on dendrites of primary sensory neurons in the nasal epithelium (Buck and Axel, 1991, DeMaria and Ngai, 2010, Hayden and Teeling, 2014). The binding of odorants to olfactory receptors therefore provides a means by which sensory neurons can convert a chemical odorant stimulus to an electrical stimulus that can be transmitted into the brain.

Each olfactory receptor neuron expresses only 1 of over 1000 olfactory receptors, a choice that is stabilized throughout the life of a sensory neuron via a negative feedback loop (Chess et al., 1994, Clowney et al., 2011, Dalton and Lomvardas, 2015, Feinstein et al., 2004, Lewcock and Reed, 2004, Markenscoff-Papdimitriou et al., 2014, Mombaerts, 2006, Nguyen et al., 2007, Rodriguez, 2014, Serizawa et al., 2004, Shykind et al., 2004, Vassalli et al., 2002). Sensory neurons expressing a given receptor are distributed in an apparently random manner within 1 of 4 zones in the nasal epithelium (Ressler et al., 1993, Vassar et al., 1993) (Figure 1). Each olfactory receptor can bind multiple

structurally and perceptually distinct odorants and each odorant binds multiple olfactory receptors. As such a single odorant is detected by a unique combination of olfactory receptors (Malnic et al., 1999). Individual odorants therefore evoke activity in a spatially diffuse subset of neurons, and different odorants activate distinct but partially overlapping neuronal ensembles in the epithelium. This combinatorial coding, in addition to the large number of olfactory receptors, underlies the mouse's ability to detect and discriminate a very large number of odorants (Malnic et al., 1999, Touhara and Vosshall, 2009).

Olfactory sensory neurons project their axons out of the nasal epithelium to the olfactory bulb. Here, axons of sensory neurons expressing the same receptor converge on 2 spatially invariant points, termed glomeruli (Mombaerts et al., 1996, Ressler et al., 1994, Vassar et al., 1994) (Figure 2). This convergence is genetically hardwired such that axons expressing the same receptor converge on the same spatially localized glomeruli in all mice.

This topography of sensory neuron input directly shapes odor-evoked activity. Functional imaging experiments reveal that natural odorants delivered at physiological concentrations induce activity in approximately 5% of glomeruli (Lin et al., 2006). Moreover, this activity is spatially stereotyped with individual odorants inducing the same pattern of glomerular activity across animals (Belluscio and Katz, 2001, Bozza et al., 2004, Soucy et al., 2009) (Figure 3). The diffuse, spatially stochastic representation of odorants in the nasal epithelium is therefore transformed into a convergent, spatially organized representation in the olfactory bulb.

Notably the stereotyped pattern of odor-evoked activity in the olfactory bulb does not appear to reflect a chemotopic map, as adjacent glomeruli are equally likely to respond to structurally similar odorants as they are to structurally dissimilar odorants (Soucy et al., 2009). Instead, the generation of a spatially ordered representation in the olfactory bulb may facilitate the segregation of innate and learned behavioral responses. Genetic ablation of glomeruli that respond to an innately aversive predator odor in the dorsal olfactory bulb abolishes innate behavioral responses while leaving learned responses to the same odorant intact (Kobayakawa et al., 2007). Thus the spatially stereotyped organization of the olfactory bulb might establish divergent circuits that mediate hardwired, innate odor-evoked behaviors and more flexible learned olfactory responses.

The stereotyped nature of olfactory sensory neuron input to the bulb suggests that the position of individual glomeruli has an inherent meaning for olfactory perception that is likely implemented through downstream connectivity. Glomeruli themselves are heterogeneous structures that consist of the terminals of olfactory sensory neurons, the apical dendrites of the olfactory bulb projection neurons (mitral and tufted cells), and the processes of local interneurons (Shepherd, 1994). The mitral and tufted cells project their axons out of the olfactory bulb to several higher order brain structures, including the piriform cortex and the cortical amygdala (Figure 4). While the gain and sharpness of mitral and tufted cell responses can be modulated by local interneuron interactions (Yokoi et al., 1995), the primary determinant of mitral and tufted cell tuning is the tuning of the olfactory sensory neurons that innervate them (Tan et al., 2010). Thus, much like the olfactory sensory neurons, each mitral and tufted cell responds to a subset of odorants

that can be perceptually and structurally distinct (Kikuta et al., 2013, Nagayama et al., 2004, Rinberg et al., 2006). Interestingly, associative learning can facilitate pattern separation in mitral and tufted cell assemblies, however the mechanisms underlying this effect are poorly understood (Gschwend et al., 2015).

Mitral and tufted cells innervate multiple higher brain structures. Notably, their innervation patterns appear to constrain the function of downstream structures. For example mitral and tufted cells arising from different glomeruli project axons to broad but anatomically distinct regions of the posterolateral cortical amygdala and this is stereotyped across animals (Sosulski et al., 2011) (Figure 4). This anatomical connectivity directly shapes odor-evoked responses in posterolateral cortical amygdala: innately appetitive and aversive odorants evoke activity in different regions of the cortical amygdala (Root et al., 2014). This anatomical stereotypy has implicated the mitral and tufted cell projections to the posterolateral cortical amygdala in the generation of innate olfactory behaviors. In accord with this, optogenetic inhibition of this projection abolishes innate, odor-evoked responses, but leaves learned olfactory behaviors intact (Root et al., 2014).

In contrast to the anatomically stereotyped projections of mitral and tufted cells to cortical amygdala, mitral and tufted cell projections to the piriform cortex appear to discard the spatial order of the olfactory bulb. Axons from single glomeruli in the olfactory bulb project diffusely across the piriform cortex without spatial bias and individual neurons in piriform cortex receive convergent input from multiple glomeruli (Apicella et al., 2010, Davison and Ehlers, 2011, Ghosh et al., 2011, Miyamichi et al., 2011, Sosulski et al., 2011) (Figure 5). This anatomical connectivity is reflected in the

response properties of neurons in piriform cortex to odorants. Individual odorants evoke activity in diffuse, spatially distributed ensembles of neurons and single piriform neurons can respond to structurally and perceptually similar and dissimilar odorants (Illig and Haberly, 2003, Poo and Isaacson, 2009, Rennaker at al., 2007, Stettler and Axel, 2009) (Figure 6).

The representation of an odorant in piriform cortex is further transformed via local inhibitory and long-range excitatory connectivity. These interactions are believed to further sparsen and distribute the olfactory representation in piriform (Franks et al., 2011, Poo and Isaacson, 2009). Thus individual odorants are represented by the activity of a unique ensemble of neurons in piriform cortex, and this ensemble extends across the extent of piriform with no evident spatial bias. The representation of odorants in piriform cortex is therefore fundamentally different from other sensory cortices where neurons that respond to a specific stimulus feature are likely to respond to stimuli with similar features and neurons with specific response properties are anatomically clustered (Hubel and Weisel, 1959, Mountcastle, 1957, Peron et al., 2015, Rothschild et al., 2010).

The nature of the olfactory representation in piriform cortex suggests a role in associative learning. Indeed, the existence of sparse representations across a large number of neurons has been proposed to facilitate associative learning through Hebbian processes (Marr, 1971). In accord with a role for piriform cortex in associative learning, training can modulate the response properties of piriform neurons (Calu et al., 2007, Chen et al., 2011, Li et al., 2008, Roesch et al., 2007, Sevelinges et al., 2004), and lesions of posterior piriform cortex impair the retrieval of a remote olfactory fear memory (Sacco and Sacchetti, 2010). In addition, it has been demonstrated that photoactivation of a random

subset of piriform neurons can become entrained to elicit either appetitive or aversive behavioral responses through temporal pairing with rewards or punishments, respectively (Choi et al., 2011). These data suggest that the distributed representation of an odorant in piriform cortex might play a critical role in olfactory learning.

One model consistent with the anatomical, physiological and behavioral studies invokes the random convergence of mitral and tufted cell inputs onto piriform neurons such that each neuron in piriform cortex samples from a random combination of glomeruli (Davison and Ehlers, 2011, Miyamichi et al., 2011, Sosulski et al., 2011). In this model, each odorant would evoke activity in an apparently random subset of piriform neurons such that each odorant representation in piriform would have no inherent meaning. Instead, meaning would be imposed by experience, potentially via the reinforcement of projections to valence-specific outputs.

Principal neurons of piriform cortex project axons to numerous cortical and subcortical regions that have been implicated in learned olfactory behaviors, including the striatum, amygdala, and neocortex (Cajal, 1909, Haberly and Price, 1997, McDonald, 1998, Miyamichi et al., 2011, Sah et al., 2003, Shepherd, 1994, Sosulski et al., 2011). Potentiation of subsets of these projections might therefore provide a mechanism by which meaning can be imposed on representations of odor in piriform cortex. However the neural circuitry through which valence is imposed on an odor representation in piriform cortex has not been identified.

The Basolateral Amygdala

Piriform cortex sends direct and indirect projections to the basolateral amygdala, a structure in the medial temporal lobe that is critically required for the acquisition and expression of learned fear. Animals with BLA lesions are unable to associate auditory, visual, gustatory, or olfactory conditioned stimuli with aversive outcomes (Campeau and Davis, 1995, Cousens and Otto, 1998, Yamamoto et al., 1995). In addition inactivation of the BLA abolishes behavioral responses to previously learned cues of all sensory modalities (Campeau and Davis, 1995, Cousens and Otto, 1998, Nachman and Ashe, 1974). Activity within the BLA is therefore required for both the acquisition and expression of learned fear to stimuli of multiple sensory modalities. These data suggest that circuitry in the BLA exists that mediates the association of neutral stimuli with aversive outcomes; however this circuitry has not been identified.

The BLA receives extensive sensory input from all modalities via both cortical and subcortical routes. This provides the BLA with sensory information about both neutral conditioned stimuli and emotionally salient unconditioned stimuli (Amaral et al., 1992, Cruikshank et al., 1992, Lanuza et al., 2004, Lanuza et al., 2008, McDonald, 1998, Romanski and LeDoux, 1992, Sah et al., 2003, Shi and Davis, 2001) (Figure 7). Studies in animals with lesions of auditory thalamus or cortex demonstrate that thalamic input to the BLA is adequate for fear conditioning using simple stimuli, whereas cortical input is required for discrimination tasks involving more complex cues (Jarrel et al., 1987). Thalamic input might therefore provide rapid access to a crude representation of a stimulus while cortical pathways convey information about the more discriminative features of a cue.

In addition to purely sensory inputs, the BLA is also innervated by structures implicated in cognitive processes. For example, the BLA receives dense innervation from the prefrontal cortex, which may afford the amygdala access to information about complex, multimodal cues. Extensive input to the BLA from the medial temporal lobe memory system might facilitate the integration of declarative memories with affective information (McDonald, 1998), and input from neuromodulatory systems has been proposed to convey additional information about unconditioned stimuli (Schultz, 2001).

For all sensory modalities, subcortical projections primarily target the dorsal portion of the lateral amygdala. This information is then transmitted to the ventral division of the lateral amygdala before being transmitted to the basal nucleus, where it is integrated with neuromodulatory input, additional thalamic and cortical input from the same modalities, as well as polymodal sensory input (Amaral et al., 1992, Sah et al., 2003). The termination of diverse sensory inputs in the restricted space of the amygdala might permit their integration and association via amygdala circuits.

The basolateral amygdala sends projections to both cortical and subcortical structures that mediate the cognitive, behavioral and physiologic output that are integral to an emotional response (Amaral et al., 1992, Sah et al., 2003) (Figure 7). Efferent projections to cortex have been implicated in numerous cognitive processes, such as the allocation of attention and memory consolidation (Quirk et al, 1997), projections to the striatum can support instrumental learning (Stuber et al., 2010), and projections to the extended amygdala can elicit valence-specific changes in autonomic reactivity (Kim et al., 2013). These data suggest the existence of potentially hardwired circuitry with

differential connectivity in the BLA that may be engaged by emotionally salient stimuli to generate appropriate responses.

The amygdala therefore receives convergent input from all sensory modalities and projects to downstream structures that mediate different components of an emotional response. This might afford the amygdala the ability to associate sensory stimuli and generate appropriate responses.

Electrophysiological recordings have identified neurons in the BLA that respond to novel, neutral conditioned stimuli of all modalities (Herry et al., 2008, Livneh and Paz, 2012, Paton et al., 2006, Schoenbaum et al., 1998, Shabel and Janak, 2009 and Uwano et al., 1995). These responses appear to be quite broadly tuned (Cain and Bindra, 1972), and can often be complex and non-linear (Saez et al., 2015).

Responses of neurons in the BLA to conditioned stimuli rapidly habituate to repeated presentations of the conditioned stimulus if it is not paired with a biologically significant outcome, an unconditioned stimulus (Balderston et al., 2011, Rosenkranz and Grace, 2002, Rosenkranz et al., 2003). However pairing of a conditioned stimulus with an unconditioned stimulus increases the size and number of CS-evoked responses in the BLA, in a dopamine dependent manner (Quirk et al., 1995, Rogan et al., 1997, Rosenkranz and Grace, 2002, Tye et al., 2008). This plasticity precedes the development of conditioned behavioral responses to the CS and is therefore believed to underlie fear learning (Quirk 1997, Repa 2001). This is supported by the demonstration that depression of synaptic inputs into the BLA conveying auditory information can abolish a previously acquired auditory fear memory, while subsequent potentiation of the same inputs can restore the memory (Nabavi et al., 2014).

Interestingly, while learning often potentiates CS-evoked responses, responses to the unconditioned stimulus are often diminished. For example, in auditory fear conditioning a neutral tone (CS) is temporally paired with an aversive footshock (US). As trials progress, the tone comes to predict the delivery of the footshock. Behaviorally, the degree of learning that occurs on each trial is inversely proportional to the expectation of the unconditioned stimulus. As such, the degree of learning decreases as trial progress (Rescorla and Wagner, 1972). This is reflected in US-evoked responses in the BLA: as trials progress US-evoked responses are diminished (Johansen et al., 2010). In addition, responses to USs are greater when USs are presented alone than when proceeded by the learned CS (Belova et al., 2007, Johansen et al., 2010). Taken together, these data suggest that US-evoked activity in the BLA is suppressed by expectation. It has therefore been suggested that US-evoked activity in the BLA reflects a prediction error signal and this instructs plasticity in CS responsive-neurons based on expectation (McNally et al., 2011).

The activity of a US representation in the BLA might therefore directly reinforce a CS representation to connect it to appropriate output and thus drive associative learning. Indeed, neurons have been identified in the BLA that respond to both conditioned and unconditioned stimuli (Barot et al., 2008, Belova et al., 2008, Paton et al., 2006 and Romanski et al., 1993). In addition, recent electrophysiological recordings have identified local inhibitory microcircuits that might regulate the association of conditioned and unconditioned stimuli in the BLA (Wolff et al., 2014). However, relatively little is known about how the neural representations of conditioned and unconditioned stimuli in the amygdala interact to mediate fear learning. Progress has been limited by the fact that the representations of unconditioned and conditioned stimuli in the BLA are anatomically

intermingled and do not appear to be molecularly defined. As such we have lacked techniques to fully characterize these representations or manipulate their activity during controlled behavioral tasks.

Novel Techniques For The Manipulation Of Physiologically Classified Populations Of Neurons

Our understanding of brain function has been greatly advanced by the development and application of methods for manipulating the activity of neurons in awake experimental subjects. The suppression of neural activity through lesions, pharmacological inactivation, or genetic manipulations can powerfully demonstrate the necessity of targeted neural elements in mediating specific functions. However, a detailed understanding of the neural mechanisms underlying different cognitive, emotional and behavioral processes requires knowing more than the identity of the critical neural elements. A full understanding demands characterization of the information encoded by the activity of neurons, and of how this information produces meaningful behavioral output. The ability to manipulate neural activity in populations of neurons targeted by virtue of their physiological response properties is therefore a vital tool for identifying neural circuits that mediate behavioral responses.

Perhaps the most influential method for activating physiologically defined neurons in experimental subjects has been the application of electrical microstimulation to targeted neuronal elements (Cohen and Newsome, 2004, Clark et al., 2011, Doron et al., 2015, Histed et al., 2013, Cicmil et al., 2015, Wurtz, 2015, Yau et al., 2015). The earliest studies using electrical stimulation focused on stimulating motor systems to elicit

movements (Berlucchi, 2010 and Graziano, 2006). Penfield then established that applying stimulation to many brain areas outside of the motor system could produce sensory and cognitive effects (Penfield and Jasper, 1954, Penfield and Rasmussen, 1950). Indeed, this approach was used to verify the presence of topographic maps in sensory cortices; for example, stimulation of primary visual cortex produces phosphenes at the location of the receptive field of the stimulated neurons (Brindley and Lewin, 1968, Lee et al., 2000, Penfield and Perot, 1963, Tehovnik and Slocum, 2006).

The discovery that electrical microstimulation could produce sensory effects led to approaches that utilized the power of electrophysiological recordings in combination with carefully designed psychophysical tasks to test causal hypotheses about the role of physiologically classified neurons. These studies typically exploit the fact that many sensory areas exhibit functional organization whereby neurons with similar physiological properties are clustered together anatomically (e.g. in cortical columns). This organization permits the positioning of microelectrodes in the middle of a cluster of neurons that encode a similar sensory parameter. The goal is to preferentially activate neurons that encode this feature. In a series of experiments, Salzman, Newsome and colleagues provided causal evidence that the activity of direction selective neurons in visual area MT is related to perceptual judgments of motion direction (Krug et al., 2015, Histed et al., 2013, Murasugi et al., 1993a, Murasugi et al., 1993b, Salzman et al, 1990, Salzman et al., 1992, Salzman and Newsome, 1994). The effects of stimulation were closely tied to the physiological properties of neurons at the stimulation site, as moving the electrode very small distances (100-300μm) could alter the effect of stimulation dramatically (Salzman et al., 1992, Murasugi et al., 1993a). Further, increasing

stimulating current to levels that would directly activate neurons well beyond the targeted cortical column resulted in a loss of directional influence on perceptual judgments (Murasugi et al., 1993a). Instead, performance deteriorated, as if noise had been injected into the sensory representation. Taken together, these experiments illustrate that when neurons sharing physiological response properties are anatomically clustered, electrical microstimulation provides a powerful approach for establishing a predictable and causal link between neural activity and behavior.

Similar approaches have also been utilized to study causal mechanisms mediating different aspects of perceptual decision-making and attention. Stimulation has been applied to physiologically classified neurons in somatosensory cortex (London et al., 2008, Romo et al., 2000), inferotemporal cortex (Afraz at al., 2006), the frontal eye fields (Moore and Armstrong, 2003, Moore and Fallah, 2004), the lateral and ventral intraparietal areas (Zhang and Britten, 2011, Hanks et al, 2006), and visual area MST (Britten and van Wezel, 1998, Celebrini and Newsome, 1995, Gu et al., 2012), among other areas. These experiments all took advantage of the physiological response properties recorded at a stimulation site to test whether activity predicts behavioral effects according to the stimulated neurons' response preference.

The success of the microstimulation experiments outlined above is critically dependent on the anatomical clustering of neurons that share response properties. However, in many brain areas, including the BLA, neurons with different and even opposing physiological response properties are anatomically intermingled (Gore et al., 2015a, Paton et al., 2006). Thus the application of microstimulation cannot selectively activate neurons that share a particular physiological response feature. Establishing

causal mechanisms for physiologically classified neurons in these brain systems therefore requires new experimental approaches.

Our current understanding of the molecular, morphological, and anatomical features of neurons is often insufficient to deduce the specific physiological response properties encoded by neurons. The development of novel genetic strategies that permit the labeling and manipulation of populations of neurons based upon their responses to individual stimuli is therefore critical to furthering the understanding of neural circuits that mediate complex behaviors (Cruz et al., 2013, Gore et al., 2015b, Kawashima et al., 2014, Liu et al., 2013, Mayford, 2013, Ramirez et al., 2013).

Immediate early genes (IEGs), including *Arc*, *c-fos*, and *zif268*, are transiently expressed in response to cellular depolarization (Bito et al., 1996, Greenberg and Ziff, 1984, Link et al., 1995, Morgan et al., 1987). IEGs therefore provide a potential tool for identifying neurons that respond to a specific stimulus. Indeed, immunostaining for the protein products of IEGs has identified circuits activated by numerous sensory stimuli and events (Knapska et al., 2011). In addition, exploitation of the temporal dynamics of *c-fos* and *Arc* RNA migration from the nucleus to the cytoplasm has permitted the identification of cells that respond to different stimuli in the same animal (Guzowski et al., 1999). These studies have revealed distinct ensembles that are activated by mating and fighting in the ventromedial hypothalamus (Lin et al., 2011), and distinct populations of neurons that are activated by an appetitive and aversive unconditioned stimulus in the basolateral amygdala (Gore et al., 2015a). IEG immunostaining therefore provides a powerful genetic means to identify neurons activated by specific stimuli or events. However, the transient nature of expression limits its use over prolonged time periods.

Moreover, the visualization of stimulus representations using IEGs offers no indication as to the causal role of these representations in behavior.

Recently developed strategies have exploited IEG promoters to drive the expression of reporters. These approaches facilitate the prolonged labeling and manipulation of intermingled cells that respond to specific stimuli or events. These emerging technologies have afforded novel insight into the neural circuits that mediate a range of behavioral responses to complex sensory stimuli including innate olfactory behaviors, contextual drug conditioning and contextual fear conditioning (Cruz et al., 2013, Gore et al., 2015b, Kawashima et al., 2014, Liu et al., 2013, Mayford, 2013, Ramirez et al., 2013, Root et al., 2014).

To further our understanding of how sensory stimuli generate appropriate behavioral responses, we have developed a novel genetic strategy to mark and manipulate neurons in the BLA that respond to conditioned and unconditioned stimuli. This strategy enables us to ask specific questions about the role of these targeted representations in the generation of innate and learned behaviors: are the representations of unconditioned stimuli of opposing valence in the BLA distinct or overlapping? What role do these representations play in the generation of behaviors? How do CS and US representations in the BLA interact to generate learned olfactory behavioral responses? Finally, what can the interaction of these representations tell us about the mechanisms underlying fear learning? Having explored the mechanisms underlying fear learning in the BLA, we can then step back into the mouse olfactory system and use optogenetic techniques to ask how meaning is imparted on the disordered odorant representation in piriform cortex to generate appropriate behavioral responses.

The work described in this thesis has identified mechanisms by which sensory stimuli generate appropriate behavioral responses. Manipulations of representations of unconditioned stimuli have identified a central role for US representations in the BLA in connecting sensory stimuli to both innate and learned behavioral responses. In addition, these experiments have suggested local mechanisms by which fear learning might be implemented in the BLA. Finally, we have identified a fundamental transformation through which a disordered olfactory representation in piriform cortex acquires meaning. Strikingly this transformation appears to occur within 3 synapses of the periphery. These data, and the techniques we employ, therefore have the potential to significantly impact upon our understanding of the neural origins of perception and behavior.

Figure 1.

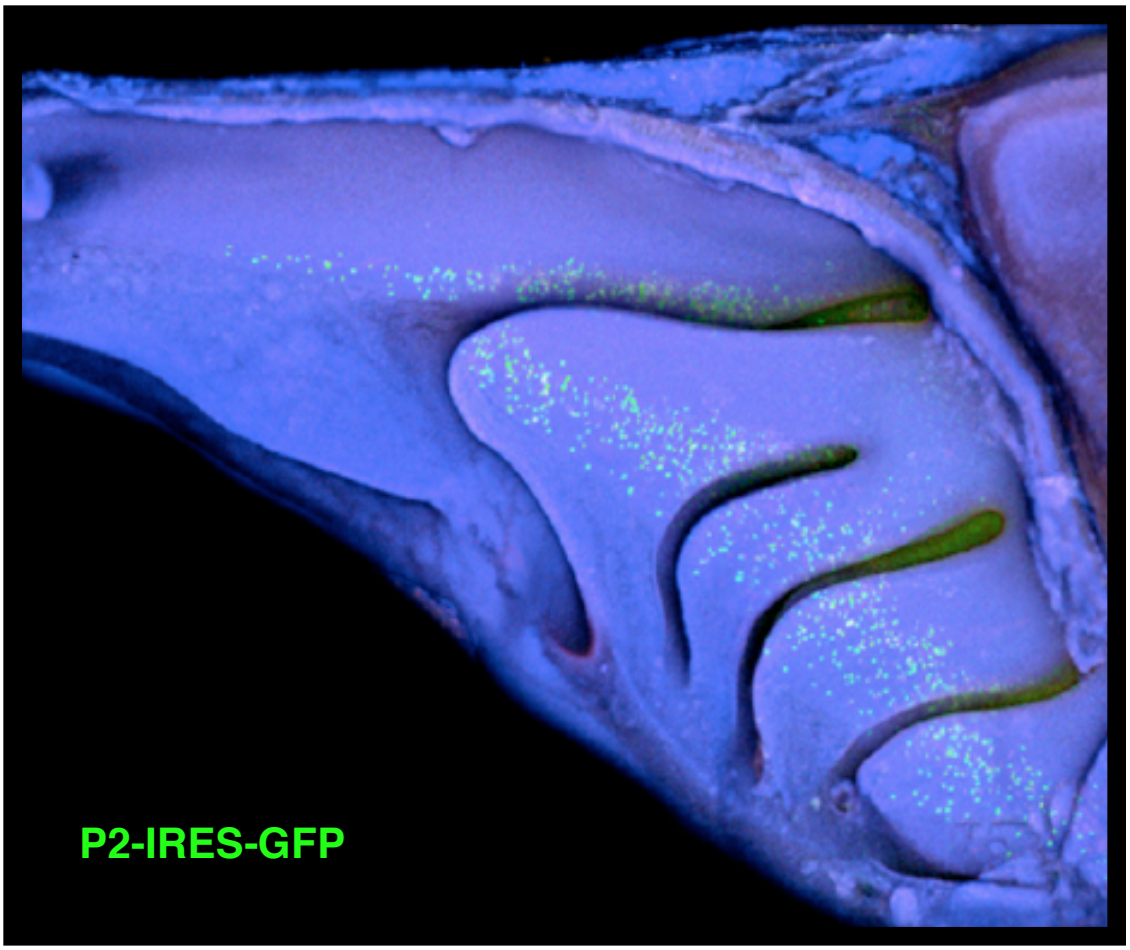

Figure 1. Sensory neurons expressing a single olfactory receptor are distributed without spatial bias in the nasal epithelium. A whole-mount preparation of the olfactory epithelium from a mouse expressing GFP under the control of the promoter for the P2 olfactory receptor. Adapted from an image by Ben Shykind.

Figure 2.

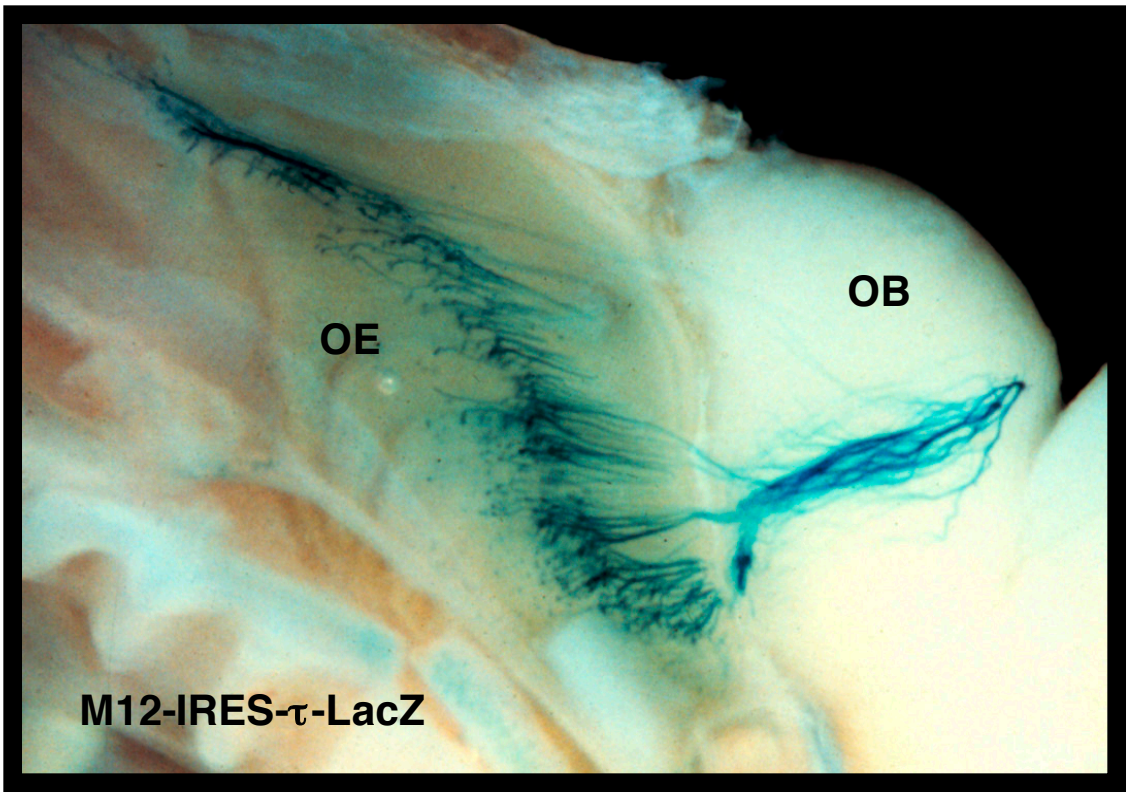

Figure 2. Axons of olfactory sensory neurons project to the olfactory bulb in a spatially stereotyped manner. Medial view of the olfactory epithelium (OE) and olfactory bulb (OB) in a mouse expressing LacZ under the control of the promoter for the M12 olfactory receptor (M12-IRES-τ-LacZ. LacZ visualized using X-gal staining (blue)). Sensory neurons expressing the same receptor all terminate on the same 2 glomeruli in the olfactory bulb. Note that only 1 M12 glomerulus is visible in this preparation. Adapted from an image by Peter Mombaerts.

Figure 3.

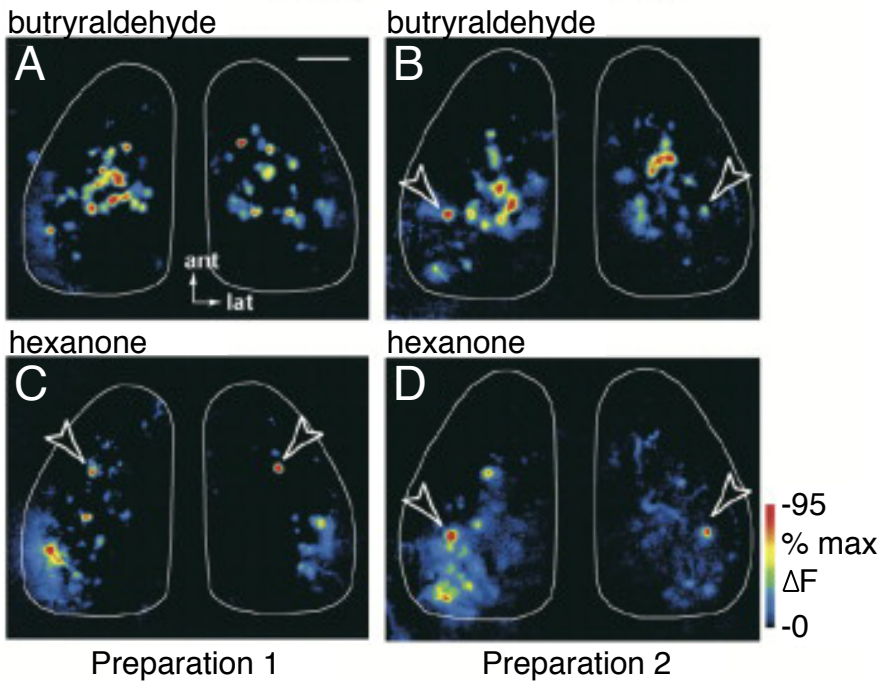
butryraldehyde
A
ant
lat
butryraldehyde
B
hexanone
C
hexanone
D
-95
% max
ΔF
-0
Preparation 1
Preparation 2

Figure 3. Spatial stereotypy of odor-evoked responses in the olfactory bulb across animals. A-D. Pseudocolored maps of odor-evoked activity (ΔF/F) in the olfactory bulb in mice expressing synapto-pHluorin, an indicator of synaptic release, in all olfactory sensory neurons. **A-B**. Pattern of activity evoked by butyraldehyde in mouse 1 (**A**) and mouse 2 (**B**). **C-D**. Pattern of activity evoked by hexanone in mouse 1 (**C**) and mouse 2 (**D**). Odorant concentrations were 1% for A and D, 0.5% for E, and 1.8% for C. Adapted from Bozza et al., 2004.

Figure 4.

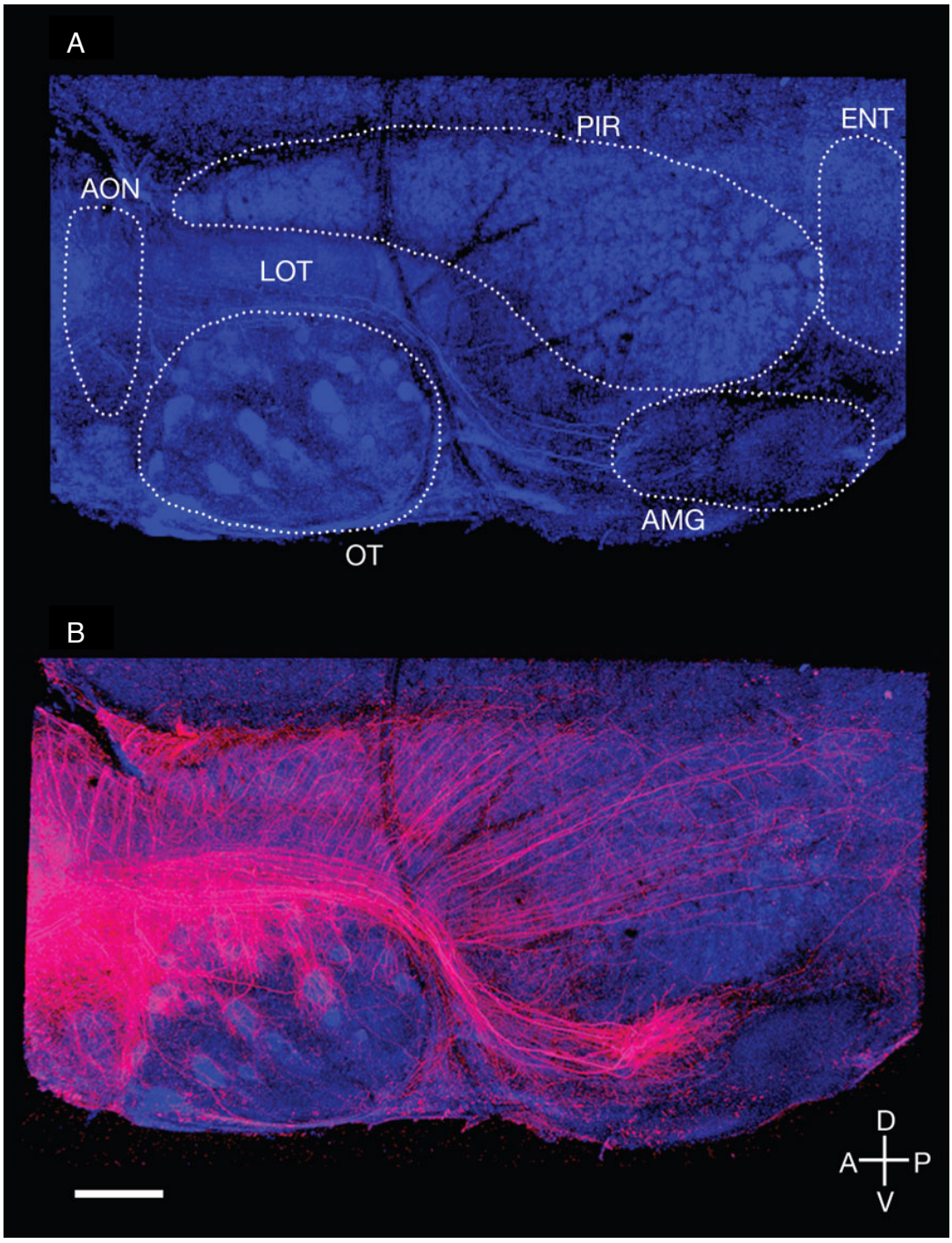

Figure 4. Mitral and tufted cells from a single glomerulus show distinct projection patterns to higher olfactory structures. A. Flattened hemibrain preparation with targets of the olfactory bulb outlines in white (AON, anterior olfactory nucleus; AMG, cortical amygdala; ENT, lateral entorhinal cortex; LOT, lateral olfactory tract; OT, olfactory tubercle; PIR, piriform cortex). **B**. Hemibrain of a mouse in which a single glomerulus was electroporated with TMR-dextran (red) to label axonal projections. Adapted from Sosulski et al., 2011.

Figure 5.

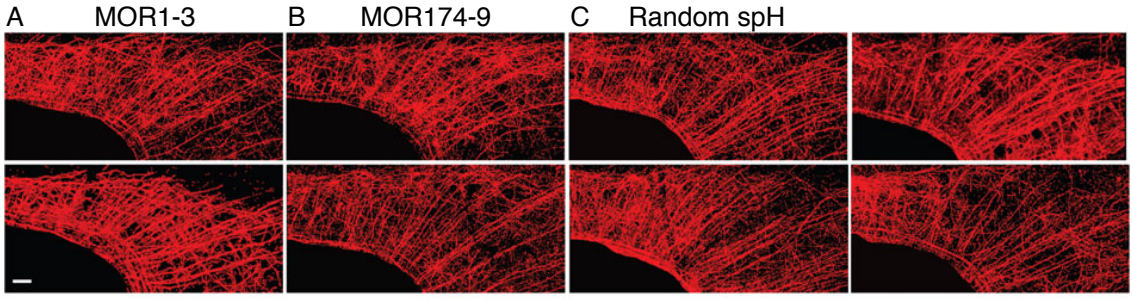

Figure 5. Projections from a single glomerulus have no apparent spatial order. A-C. Mitral and tufted cell axonal projections to piriform cortex from 2 mice in which the MOR1-3 glomerulus (**A**), the MOR174-9 glomerulus (**B**), or a randomly selected glomerulus (**C**) was electroporated with TMR-dextran (red). Adapted from Sosulski et al., 2011.

Figure 6.

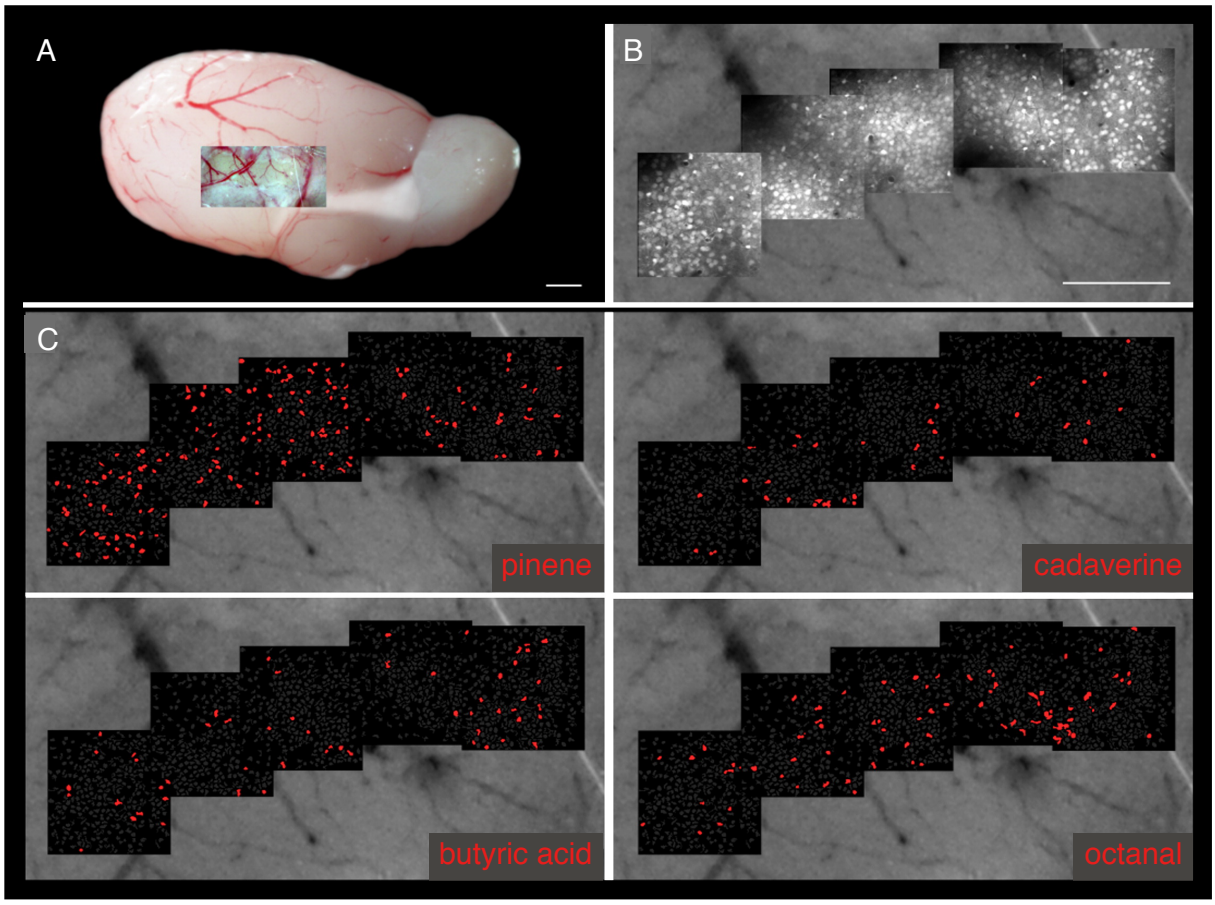

Figure 6. Different odorants evoke activity in sparse ensembles of neurons that are distributed across the extent of piriform cortex with no apparent spatial order. A. Ventral lateral view of the mouse cerebral hemisphere superimposed with the imaging craniotomy. **B.** Montage of images showing the baseline fluorescence of labeled cells in five contiguous imaging sites in piriform cortex. **C.** Cells responsive to 4 odorants across the region of piriform cortex shown in B.

Figure 7.

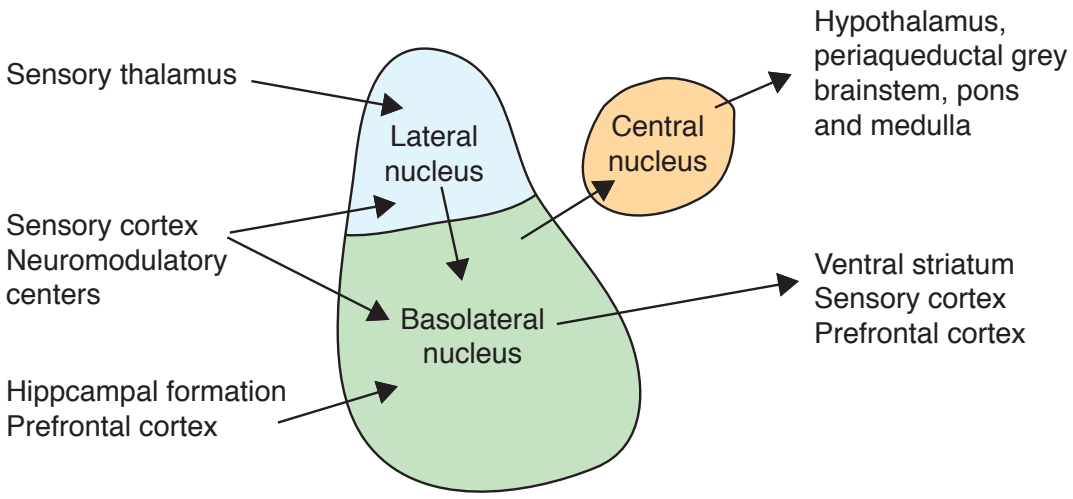
Sensory thalamus
Lateral nucleus
Central nucleus
Hypothalamus, periaqueductal grey brainstem, pons and medulla
Sensory cortex
Neuromodulatory centers
Basolateral nucleus
Ventral striatum
Sensory cortex
Prefrontal cortex
Hippcampal formation
Prefrontal cortex

Figure 7. Major anatomical connections of the basolateral amygdala. The basolateral complex receives sensory input from all sensory systems as well as higher cortical centers and neuromodulatory systems. The amygdala sends projections to both cortical and subcortical structures that mediate the cognitive, physiologic and behavioral output that are integral to an emotional response.

CHAPTER 2

NEURAL REPRESENATIONS OF UNCONDITIONED STIMULI IN THE BASOLATERAL AMYGDALA MEDIATE IN INNATE AND LEARNED BEHAVIOR

Emotions may arise in response to unconditioned and conditioned stimuli from each of the sensory modalities (Cardinal et al., 2002, Davis, 1998, LeDoux, 2000, Rosen, 2004 and Schultz, 2001). Unconditioned stimuli (USs) possess inherently rewarding or aversive qualities and elicit innate emotional responses. However, the responses to most stimuli are not innate but learned, allowing an organism to respond appropriately to a variable and often unpredictable world. Stimuli that drive innate responses also contribute to learning by imparting meaning on neutral sensory cues. An animal can therefore predict the consequence of a conditioned stimulus (CS) after learning and respond with appropriate behavioral output (Lang and Davis, 2006, LeDoux, 2000, Pavlov, 1927 and Schultz, 2006). Thus an unconditioned stimulus may participate in both innate and learned responses.

Representations of unconditioned stimuli are generated at the earliest stages of sensory processing. These representations must connect with neural circuits that elicit both innate and learned emotional responses. Anatomical, electrophysiological and behavioral experiments provide evidence that the basolateral amygdala (BLA) may connect sensory representations and behavioral output (Amaral et al., 1992, Everitt et al., 2003, Fendt and Fanselow, 1999, Gallagher and Holland, 1994, Janak and Tye, 2015, Lang and Davis, 2006, McDonald, 1998, Russchen et al., 1985, Sah et al., 2003, Salzman

and Fusi, 2010 and Sarter and Markowitsch, 1985). Neural representations of appetitive and aversive USs have been identified in the BLA (Belova et al., 2007, Bermudez and Schultz, 2010, Knapska et al., 2007, Livneh and Paz, 2012, Muramoto et al., 1993, Paton et al., 2006, Romanski et al., 1993, Uwano et al., 1995 and Wolff et al., 2014). Pharmacologic silencing and lesions of the BLA impair aversive conditioning and some forms of appetitive conditioning (Amano et al., 2011, Ambroggi et al., 2008, Anglada and Quirk, 2005, Balleine and Killcross, 2006, Hatfield et al., 1996 and Maren et al., 2001). Optogenetic activation of random populations of neurons in the lateral amygdala can entrain a neutral tone to elicit freezing behavior (Johansen et al., 2010, Yiu et al., 2014), and activation of different populations of BLA neurons or their distinct projections can elicit either anxiety-related or self-stimulation behaviors (Felix-Ortiz et al., 2013, Kim et al., 2013, Namburi et al., 2015, Stuber et al., 2011 and Tye et al., 2011). Finally, photoactivation of BLA cells activated by an appetitive or aversive conditioning paradigm can generate valence-specific responses (Redondo et al., 2014). These studies indicate that the BLA is involved in linking sensory representations to behavioral output, but the nature of the neural representations of different USs in the BLA and their causal role in the generation of innate responses and emotional learning has remained elusive.

We have developed a genetic strategy to examine the functional role of US representations in the BLA. This approach permits the identification and optogenetic manipulation of the activity of BLA neurons responsive to an appetitive or aversive US. We demonstrate that photoactivation of an ensemble of US-responsive cells in the BLA elicits valence-specific innate responses. These US ensembles can also drive appetitive and aversive learning. Moreover, activation of US-responsive cells in the BLA is

necessary for the expression of a conditioned response. Thus, representations of sensory stimuli ultimately connect to a US representation in the BLA to elicit both innate and learned responses.

Results

An appetitive and an aversive unconditioned stimulus are represented by distinct but intermingled subpopulations in the BLA

In initial experiments, we examined the neural representations of two opposing USs in the BLA. Footshock, which elicits defensive behaviors, was used as an aversive US (LeDoux, 2000). Intraperitoneal injection (i.p.) of nicotine at a dose that elicits a conditioned place preference (Figure 1) was used as an appetitive US (Merritt et al., 2008). Footshock or i.p. injection of nicotine resulted in the expression of c-Fos, an activity-dependent gene, in ~6% of neurons in the BLA (shock treated 5.94±0.43%, n=6; nicotine treated 6.13±0.46%, n=6). Spatial segregation of neurons responsive to footshock or nicotine was not observed. Control experiments with untreated animals or animals treated with an i.p. injection of saline revealed that less than 1% of neurons stained for c-Fos (untreated 0.88±0.14%, n=6; i.p. saline 0.83±0.13% n=8). The observation that appetitive and aversive USs result in significant increases in c-Fos-expressing cells with little background c-Fos staining suggested the use of the *c-fos* promoter to drive the expression of the photoactivatable cation channel channelrhodopsin after US exposure. This genetic strategy allowed us to mark and manipulate the activity of neurons that respond to either an appetitive or aversive US.

We next asked whether footshock and nicotine administration activated different neurons in the BLA. We injected a bicistronic lentiviral vector encoding channelrhodopsin2 fused to enhanced yellow fluorescent protein (ChR2-EYFP) and nuclear-targeted mCherry under the control of the *c-fos* promoter into the BLA (c-fos:ChR2-EYFP-2A-mCherry). Nine days later animals were exposed to footshock or nicotine. Endogenous c-Fos expression was observed 1 hour after footshock or nicotine exposure, whereas mCherry expression was not detected at this time. Conversely, animals sampled 19 hours after footshock or nicotine exhibit mCherry expression in the BLA but endogenous c-Fos expression is not observed (Figure 2).

This temporal separation in the expression of lentiviral mCherry and endogenous c-Fos allowed us to identify the populations of neurons activated by sequential stimuli in the same animal and to ask whether the expression of mCherry is a faithful reporter of endogenous c-Fos activity. Animals were injected with virus, treated with 2 sessions of 20 footshocks separated by 18 hours, and sacrificed 1 hour later allowing us to determine the overlap of cells expressing mCherry and c-Fos. Staining for endogenous c-Fos and mCherry revealed that 84.07±4.46% of mCherry$^+$ cells also expressed c-Fos (n=6, Figure 3A-C, M). Mice were also injected with virus and treated with 2 sessions of i.p. nicotine administration separated by 18 hours and sacrificed 1 hour later. 76.02±4.90% of the mCherry$^+$ cells also expressed c-Fos (n=5, Figure 3D-F, M). Moreover, the expression of mCherry and ChR2 was observed in 47.73±4.48% of the cells expressing endogenous c-Fos. Therefore, expression of mCherry faithfully identifies a population of neurons responsive to the different USs: 80% of mCherry expressing cells after US exposure are c-Fos$^+$, and 50% of c-Fos$^+$ cells also express mCherry.

We next examined whether USs of distinct valence activated different populations of BLA neurons. Animals were injected with c-fos:ChR2-EYFP-2A-mCherry, and exposed to footshock. Eighteen hours later nicotine was injected and animals were sampled 1 hour later. This protocol results in only 8.22±1.40% overlap of neurons expressing mCherry (presumably representing shock) and c-Fos expressing neurons (presumably representing nicotine administration, n= 6, Figure 3G-I, M). Similarly, animals were injected with virus and exposed to nicotine. Eighteen hours later animals were treated with footshock and sampled 1 hour later. In these animals we observed 9.28±2.94% overlap of neurons expressing mCherry and c-Fos expressing neurons (n=5, Figure 3J-L, M). Similar levels of overlap were observed in animals where the populations of cells activated by footshock and nicotine were examined using cellular compartment analysis of temporal activity by fluorescence in situ hybridization (catFISH, Guzowski and Worley, 2001) (shock-nicotine 8.63±2.67%, n=4; nicotine-shock 11.62±1.75%, n=6; Figure 3N-R). These data demonstrate that distinct but intermingled subpopulations of BLA neurons are activated by exposure to an aversive and appetitive US. We cannot distinguish whether these 2 neural representations reflect valence or simply different sensory qualities of the USs independent of valence. Nonetheless, we can define the valence of these representations by virtue of the behaviors they elicit upon activation. We therefore employed this lentiviral strategy to manipulate the activity of neurons responsive to specific unconditioned stimuli.

Photoactivation of US representations in the BLA elicits innate responses

We asked whether BLA neurons that express ChR2 in response to a US could elicit valence-specific physiological and behavioral responses upon stimulation with light. Mice injected with the c-fos:ChR2-EYFP-2A-mCherry lentivirus were implanted with a guide cannula 250μm above the injection site. Nine days following surgery, animals were exposed to either footshock (shock-induced animals), or received an i.p. nicotine injection (nicotine-induced animals) to induce ChR2 and mCherry expression. This resulted in mCherry expression in ~3% neurons (shock-induced animals 3.01±0.44%, n=7; nicotine-induced animals 3.29±0.54%, n=6). This was significantly greater than the number of neurons expressing mCherry in animals not exposed to a US (0.82±0.13%, n=5. One way ANOVA $F_{2,15}$=8.52, P<0.01). After 18 hours to allow ChR2 expression, a fiber-optic cable connected to a 473nm laser was positioned above the BLA for optical stimulation. *In vivo* electrophysiological experiments as well as recordings in slice demonstrated that photostimulation of cells induced to express ChR2 by footshock or nicotine exposure elicits photocurrents and spiking (Figure 4). Excitation of footshock-responsive neurons decreased both heart and respiration rate (n=5, Figure 5A, B) (Belkin, 1968 and Lang and Davis, 2006). Conversely, excitation of nicotine-responsive neurons increased heart and respiration rate (n=5, Figure 5A, B). In control experiments, we measured the effects on heart and respiratory rate upon photoactivation of a random population of BLA neurons. Mice were injected with a lentivirus expressing ChR2-EYFP-2A-mCherry under the control of the *synapsin* promoter to achieve a frequency of ChR2 expression similar to that observed in shock or nicotine treated mice infected with the c-fos:ChR2-EYFP-2A-mCherry lentivirus (3.48±0.64% of neurons expressing

mCherry, n=7). Photoactivation of this random population of neurons did not elicit a change in heart or respiratory rate (n=6, Figure 5A, B).

Shock-induced animals also exhibited significantly elevated levels of freezing upon photostimulation, compared with either nicotine-induced animals, or with animals expressing ChR2 in a random population of neurons (shock 26.05±2.83%, n=7; nicotine 6.93±1.58%, n=6; synapsin 7.43±2.19%, n=5; Figure 5C). Animals that were injected but not exposed to a US failed to show freezing behavior to optical stimulation (No US 8.96±1.42%, n=5, Figure 5C). In addition, mice injected with a lentivirus encoding c-fos:GFP and treated with footshock or nicotine did not freeze in response to optical stimulation (shock GFP 7.70±1.37%, n=6; nicotine GFP 11.07±2.42%, n=6; Figure 5C). Control experiments demonstrate that the freezing behavior we observe results from activation of neurons responsive to footshock rather than activation of neurons that represent a rapidly formed contextual association (Fanselow, 1980, Figure 6). Thus, photoactivation of US-responsive cells in the BLA elicits innate behavioral and physiological responses of different valence. We are unable to provide evidence of an innate behavioral response to the photoactivation of an appetitive US representation because it is difficult to conceive of a behavioral assay that reports an innate, as opposed to an instrumental, appetitive response.

Photoactivation of US representations in the BLA drives learning

Rewarding and aversive USs can drive associative learning when paired with a CS. We therefore tested whether the activation of an ensemble of cells responsive to a US in the BLA, when temporally paired with a CS, results in valence-specific learning. We

subjected mice to a modified fear-conditioning paradigm in which a tone served as the CS and tested whether optical stimulation of neurons responsive to footshock could serve as a US (Figure 7A). Animals were injected with lentivirus and treated with footshock or nicotine to induce ChR2 expression. The following day, shock-induced and nicotine-induced animals were placed into a behavioral testing chamber where they received 20 10-second tone presentations (CS), co-terminating with 2 seconds of optical stimulation of the BLA (US). A second group of shock-induced animals (shock unpaired) received 20 randomly timed presentations of the CS and US. Freezing behavior was then assessed during 5 presentations of the CS. Shock paired animals showed significantly more freezing in response to the CS compared to both shock unpaired and nicotine paired control animals (shock paired 20.46±3.59%, n=10; shock unpaired 8.19±1.51%, n=8; nicotine paired 4.62±1.38%, n=8, Figure 7B). Activation of a random population of BLA neurons did not drive aversive learning in animals trained with this fear conditioning protocol (synapsin 5.26±0.80% freezing, n=6, Figure 7B). Furthermore, shock unpaired animals that received random presentations of tone and optical stimulation showed freezing behavior that was significantly correlated with the number of chance paired presentations of the CS and optical stimulation ($r=0.80$, $P<0.05$, n=8, Figure 7C). Thus, selective optical reactivation of footshock-responsive cells in the BLA, when temporally paired with a neutral tone, can induce aversive learning. The levels of freezing observed using optical stimulation are, however, lower than those exhibited by animals exposed to a similar training protocol using footshock as the US (classical shock paired 55.53±6.14%, n=8; classical shock unpaired 19.85±3.11%, n=8).

We next employed an odor-learning task to determine whether the photoactivation of an ensemble of nicotine-responsive cells could induce appetitive learning (Figure 8A). This experimental design also tested whether photoactivation of footshock-responsive cells could impart an aversive valence upon a neutral odor. Animals were injected with lentivirus and treated with either nicotine or footshock to induce ChR2 expression. Shock-induced and nicotine-induced animals were placed into a chamber where they received 20 presentations of 1% acetephenone (CS+) that co-terminated with optical stimulation of the BLA. As a control, animals also received 20 randomly interleaved presentations of 2% octanol (CS-). Mice were then placed in the center of a 3-compartment chamber. CS+ and CS- odors were infused from opposite ends of the apparatus. In the absence of odor, nicotine- and shock-induced animals, as well as untreated controls, spent equal amounts of time in the CS+ and CS- compartments (Figure 8B). Following odor delivery, shock-induced animals avoided of the CS+ compartment, while nicotine-induced animals approached the CS+ compartment. Animals not exposed to a US showed no compartment preference (Approach-avoid index: shock without odor 0.13±0.12, with odor -0.47±0.14, n=6; untreated without odor 0.08±0.03, with odor 0.02±0.07, n=6; nicotine without odor -0.09±0.05, with odor 0.57±0.13, n=6, Figure 8B). Animals injected with lentivirus expressing ChR2 under the control of the *synapsin* promoter to generate a random ensemble of ChR2 expressing neurons showed no compartment preference when trained and tested in the same manner (synapsin without odor 0.01±0.12, with odor 0.00±0.14, n=5, Figure 8B). The selective reactivation of BLA neurons responsive to footshock can therefore induce aversive learning across two sensory modalities, auditory and olfactory. Each modality can evoke

behaviorally distinct defensive behaviors, freezing and avoidance. Moreover, reactivation of BLA neurons responsive to nicotine can drive appetitive learning about olfactory stimuli.

In addition to Pavlovian learning, unconditioned stimuli can reinforce operant behavior. We therefore asked whether US-responsive cells in the BLA could direct instrumental conditioning. Animals injected with lentivirus were exposed to either footshock or nicotine to induce ChR2 expression in BLA neurons. Shock-induced and nicotine-induced animals were placed into a chamber equipped with an active and an inactive portal for 1 hour. Nosepoke entry into the active portal, but not the inactive portal, resulted in 5 seconds of optical stimulation of the BLA (Figure 9A). On the second day of testing, nicotine-induced mice performed significantly more nosepokes into the active portal than the inactive portal (nicotine-ChR2 active 24.83±5.02, inactive 9.00±1.57, n=6). Footshock-induced mice and control animals injected with a virus encoding c-fos:GFP and exposed to footshock or nicotine showed a small, but statistically insignificant, bias towards the active portal (shock-ChR2 active 9.30±2.54, inactive 5.60±1.81, n=10; shock-GFP active 8.71±3.11, inactive 6.71±3.58, n=7; nicotine-GFP active 8.29±2.92, inactive 5.14±0.91, n=7; Figure 9B, C). Overall, the total number of nosepokes was 2.5 times greater in the nicotine-induced mice expressing ChR2 than in all other groups. These observations demonstrate that selective reactivation of neurons responsive to nicotine in the BLA can reinforce instrumental behavior. Thus BLA neurons encode behaviorally relevant information about the valence of unconditioned stimuli and the exogenous activation of these ensembles is sufficient to drive both Pavlovian and instrumental learning.

Learning connects CS and US representations in the BLA

These data suggest a concise circuit in which CS-responsive cells connect with US-responsive neurons in the BLA such that this connection is only capable of driving behavior after learning. We therefore devised a strategy to express ChR2 in CS-responsive neurons in the BLA to test whether these neurons can elicit behavior after conditioning (Figure 10A). One group of animals, CS paired, received 20 presentations of a tone (CS) that co-terminated with footshock. A second group of animals, CS unpaired, received random presentations of the CS and footshock. Both groups were then injected with lentivirus expressing c-fos:ChR2-EYFP-2A-mCherry; 9 days later, animals received 5 presentations of the CS. Expression of ChR2 in the BLA was significantly elevated in CS paired compared to CS unpaired animals (% neurons expressing mCherry: CS paired 4.85±0.52%, n=9; CS unpaired 2.19±0.28%, n=10. Unpaired *t*-test, $P<0.001$). As expected, CS paired animals showed significantly elevated freezing in response to the CS compared to CS unpaired animals (CS paired 59.84±8.58%, n=9; CS unpaired 14.92±1.86%, n=10. Unpaired *t*-test, $P<0.001$). CS paired animals showed significantly elevated freezing levels in response to optical stimulation compared to CS unpaired controls (CS paired 25.22±2.25%, n=9; CS unpaired 9.93±1.40%, n=10, Figure 10B). Animals injected with a lentivirus expressing c-fos:GFP after training did not freeze upon optical stimulation of the CS representation (CS paired GFP 9.98±1.36%, n=6; CS unpaired GFP 9.59±1.50%, n=6; Figure 10B). Thus, a population of CS-responsive cells exists in the BLA after learning, and activation of this population can elicit learned behavior.

We next asked whether CS-responsive cells mediate learned behavior through the activation of US-responsive cells in the BLA. Animals were trained to associate a tone with footshock and the following day mice were injected with c-fos:ChR2-EYFP-2A-mCherry. Nine days later animals were exposed to footshock to induce mCherry expression and the following day they received 5 presentations of the auditory CS to induce endogenous c-Fos expression. Animals were sacrificed 1 hour later and the overlap of endogenous c-Fos and mCherry was calculated (($mCherry^+$ + $c\text{-}Fos^+$)/$mCherry^+$). Mice that received paired training demonstrated higher levels of overlap than unpaired controls (CS paired 34.76±2.75%, n=6; CS unpaired 16.23±3.33%, n=6. Unpaired *t*-test, $P<0.05$). Thus, CS-activated neurons (expressing endogenous c-Fos) overlap with shock-responsive neurons (expressing mCherry) and this overlap is 2 fold greater after learning.

These data suggest that a CS ensemble connects with a US representation in the BLA and this US representation may be necessary for the expression of a conditioned response. Mice were therefore trained with 20 presentations of a 10 second tone that co-terminated with 2 seconds of footshock (Figure 11A). The following day, a lentivirus expressing the neural silencer halorhodopsin (NpHR) fused to EYFP under the control of the *c-fos* promoter (c-fos:NpHR-EYFP) was injected into the BLA of both brain hemispheres. Nine days later, animals were treated with either footshock or nicotine to induce NpHR in US-responsive cells (Figure 12). The next day a fiber optic cable connected to a 593nm laser was positioned above each BLA. Animals then received 5 presentations of the auditory CS with photostimulation of NpHR, followed by 5 presentations of the auditory CS without photostimulation. In the absence of optical

silencing, footshock-treated animals demonstrated comparable levels of freezing to classically fear conditioned animals (shock NpHR without light 59.84±8.72%, n=6; CS paired 59.84±8.58%, n=10). However, optical inhibition of footshock-responsive cells attenuated freezing in response to the CS (shock NpHR with light 31.70±5.62%, n=6, Figure 11B). Freezing was not completely abolished, which may be due to incomplete optical silencing or the existence of parallel pathways for fear conditioning.

In control experiments, nicotine-treated animals showed equal levels of freezing in response to the CS in the presence or absence of optical inhibition (nicotine NpHR with light 51.70±6.54%, without light 44.73±4.45%, n=9, Figure 11B). Similarly, animals injected with a lentivirus expressing c-fos:GFP and treated with either footshock or nicotine showed equal levels of freezing in response to the CS with or without optical inhibition (shock GFP with light 61.92±6.06%, without light 57.59±6.55%, n=6; nicotine GFP with light 58.59±5.84%, without light 52.64±8.19%, n=6; Figure 11B). Whole cell electrophysiological recordings in slice preparations confirmed that photostimulation of cells induced to express NpHR by footshock or nicotine exposure can inhibit spiking elicited by current injection (Figure 13). These experiments demonstrate that an auditory CS activates a US representation in the BLA to generate learned behavior.

We next asked whether cells responsive to an olfactory CS also mediate learned behavior through the activation of US-responsive neurons. Animals were placed into a chamber where they received 20 presentations of 10 seconds of 1% acetephenone (CS+) that coterminated with 2 seconds of footshock. Animals also received 20 randomly interleaved presentations of 2% octanol (CS-). The following day, lentivirus expressing c-fos:NpHR-EYFP was injected into the BLA of both brain hemispheres. Nine days later

animals were treated with footshock or nicotine to induce NpHR expression in US-responsive neurons. The next day animals were placed in the center of a 3-compartment chamber. CS+ and CS- odors were infused from opposite ends of the apparatus. Animals explored the chamber for 5 minutes with optical stimulation of NpHR, followed by 5 minutes without optical stimulation (Figure 11C). In the absence of optical silencing, animals expressing NpHR in footshock-responsive neurons avoided the CS+ odor. However, in the presence of optical silencing, avoidance of the CS+ was abolished (approach avoid index: shock NpHR with light 0.16±0.28, without light -0.51±0.15, n=6, Figure 11D). In control experiments, nicotine-treated animals showed no reduction in avoidance of the CS+ upon optical inhibition (nicotine NpHR with light -0.83±0.07, without light -0.69±0.15, n=6, Figure 11D). Similarly, animals injected with c-fos:GFP and treated with either footshock or nicotine showed equal levels of avoidance of the CS+ in the presence or absence of yellow light (shock GFP with light -0.78±0.13, without light -0.72±0.17, n=6; nicotine GFP with light -0.76±0.15, without light -0.71±0.22, n=6, Figure 11D). These data indicate that the activity of cells responsive to the entraining US is necessary for the expression of conditioned responses to CSs of two different modalities. Thus the expression of learned behavior requires the projection of CS inputs onto US representations in the BLA.

Discussion

Stimuli that possess inherently rewarding or aversive qualities elicit emotional responses and also induce learning by imparting valence upon neutral sensory cues (Lang and Davis, 2006, Pavlov, 1924, Rosen, 2004, Schultz, 2001 and Seymour and Dolan,

2008). We used a genetic strategy to identify and manipulate the representations of innately rewarding and aversive stimuli in the BLA. Our experiments demonstrate that the activation of these representations can generate innate physiological and behavioral responses and can also reinforce Pavlovian and operant learning. Furthermore, the convergence of a CS representation onto a US ensemble in the BLA is required for the expression of learned behavior. These data suggest that US representations in the amygdala link representations of sensory stimuli to appropriate behavioral output.

The US Representation

Electrophysiological studies have demonstrated that neurons in the BLA respond to appetitive and aversive USs (Belova et al., 2007, Bermudez and Schultz, 2010, Livneh and Paz, 2012, Muramoto et al., 1993, Paton et al., 2006, Romanski et al., 1993, Uwano et al., 1995 and Wolff et al., 2014). Our data demonstrate that an appetitive and an aversive US activate distinct representations in the BLA. Photoactivation of the aversive US ensemble elicits innate responses and also reinforces aversive learning. Activation of this US representation is also necessary for the expression of a conditioned response. Representations of USs are likely to reside in multiple brain structures. Our data imply that the representation in the BLA participates in the innate responses to a US and the same representation is an essential component of the neural circuit that mediates learned responses. We emphasize, however, that we have not demonstrated the necessity of the US representation in the BLA for the generation of innate behaviors.

The observation that the activation of valence-specific representations elicits different behavioral responses poses the question as to whether different USs of the same

valence activate the same or different representations in the BLA. Innate behaviors are complex and consist of multiple components (Lang and Davis, 2006 and Rosen, 2004). The response to different aversive USs may therefore result from the activation of different representations that elicit subtly different behaviors. Consistent with this idea, lesion experiments suggest that the BLA encodes information about the sensory quality of USs (Blundell et al., 2001, Corbit and Balleine, 2005 and Balleine and Killcross, 2006). This would imply that the BLA contains multiple, distinct representations encoding different USs of each valence, and each of these representations connects to US-specific output circuitry.

We have identified distinct representations of unconditioned stimuli in the BLA that can generate behaviors of opposing valence. In one model of BLA circuitry, these distinct subpopulations of neurons are determined to receive inputs of specific valence and project to different downstream targets that elicit appropriate behavioral responses. Consistent with this model, activation of different populations of BLA neurons or their distinct projections can elicit valence-specific responses in the absence of US presentation (Felix-Ortiz et al., 2013, Kim et al., 2013, Namburi et al., 2015, Stuber et al., 2011 and Tye et al., 2011). An alternative model proposes that cells in the BLA do not possess an inherent valence and only acquire valence after experience. In this model, each BLA neuron would be connected to both appetitive and aversive outputs. US exposure activates an arbitrary subset of these neurons and potentiates valence-specific outputs appropriate for a given US. At present, we cannot distinguish among these alternative models for the origin of the valence-specific neuronal populations we have identified.

Extensive evidence has established the importance of the BLA in aversive learning whereas the role of the BLA in appetitive learning and behavior is more nuanced (Balleine and Killcross, 2006, Everitt et al., 2003 and LeDoux, 2000). Our results demonstrate that activation of the representation of an appetitive US in the BLA can elicit innate responses and can drive both instrumental and Pavlovian conditioning. Consistent with this finding, instrumental responses to appetitive conditioned stimuli require the BLA (Ambroggi et al., 2008 and Stuber et al., 2011). However, lesion and pharmacological inactivation studies indicate that the BLA is not necessary for the formation of simple CS-appetitive US associations (Hatfield et al., 1996 and Holland, 1997). These data suggest the presence of multiple representations of an appetitive US in the brain capable of eliciting multiple forms of appetitive behavior.

The CS Representation

We have shown that the activation of US-responsive neurons in the BLA can drive conditioning of auditory and olfactory CSs. Electrophysiological studies have identified neurons in the BLA responsive to CSs of all sensory modalities (Herry et al., 2008, Livneh and Paz, 2012, Paton et al., 2006, Schoenbaum et al., 1998, Shabel and Janak, 2009 and Uwano et al., 1995), and neurons have been observed that respond to both CSs and USs (Barot et al., 2008, Belova et al., 2008, Paton et al., 2006 and Romanski et al., 1993). Moreover, appetitive and aversive learning modulates the activity of CS-responsive cells in the amygdala (Morrison et al., 2011, Paton et al., 2006, Quirk et al., 1995, Rogan et al., 1997, Rosenkranz and Grace, 2002 and Tye et al., 2008) and this activity correlates with behavioral output (Belova et al., 2008, Repa et al., 2001). We

have shown that optogenetic activation of an auditory CS representation generated after learning can elicit an appropriate behavioral response. In addition, we demonstrate that the projection of a CS representation onto a US ensemble in the BLA is required for the expression of learned behavior. These findings are in accord with models in which CS-US pairing results in the Hebbian potentiation of CS inputs onto US representations in the BLA (Holland, 1990, Johansen et al., 2011, Maren and Quirk, 2004, Pape and Paré, 2010 Pickens and Holland, 2004, Rescorla, 1988 and Sah et al., 2008).

We have also shown that an olfactory CS connects to US representations in the BLA to generate learned behavior, indicating that olfactory conditioning may utilize the same circuit mechanisms as those proposed for auditory fear conditioning. In olfaction each odor activates a distinct ensemble of neurons in piriform cortex and each unique ensemble is capable of serving as a CS (Choi et al., 2011, Illig and Haberly, 2003, Rennaker et al., 2007 and Stettler and Axel, 2009). Piriform cortex projects directly to the BLA (Luskin and Price, 1983 and Schwabe et al., 2004) and we demonstrate that an US representation in the BLA is essential for the expression of learned olfactory behavior. These experiments suggest that an odor representation in piriform cortex must ultimately connect with US representations in the BLA, extending an olfactory circuit responsible for odor conditioning from the nose to the BLA.

Unconditioned stimuli are likely to elicit innate behavioral and physiological responses through determined neural circuits that have emerged over long periods of evolutionary time. Most sensory stimuli, however, have no inherent meaning and only generate responses upon learning during the life of an organism. An unconditioned stimulus can therefore elicit innate responses and also drive learning about neutral

stimuli. In all sensory modalities, brain areas proximal to the amygdala, such as sensory cortices and thalamic nuclei, provide the initial representation of both conditioned and unconditioned stimuli. These sensory representations must ultimately engage neural circuits that produce valence-specific innate and learned responses. We have identified populations in the BLA that are both responsive to conditioned and unconditioned stimuli and are able to elicit valence-specific responses. These populations therefore serve to link earlier stage sensory representations to neural circuits that generate appropriate emotional responses.

Figure 1.

A

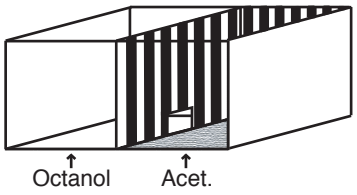

B

	Group	
	Saline	Nicotine
Day 1	Pre-test	Pre-test
Day 2 AM	I.p. saline in initally non-prefered chamber	I.p. nicotine in initally non-prefered chamber
Day 2 PM	I.p. saline in initally prefered chamber	I.p. saline in initally prefered chamber
Day 3	Test	Test

C

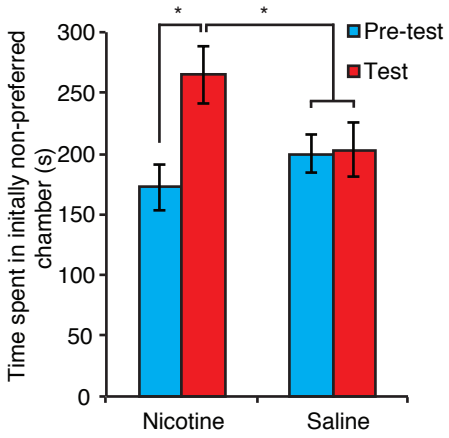

Figure 1: Nicotine (0.7mg/kg) elicits conditioned place preference. A. Conditioned place preference (CPP) apparatus. **B.** Schematic of training protocol for CPP. **C.** Percent time spent in initially non-preferred chamber before and after conditioning (nicotine pre conditioning 172.53±19.21s, post conditioning 264.86±25.55s, n=6; saline pre conditioning 199.61±15.89s, post conditioning 203.33±22.40s, n=6. Two-way ANOVA, group × conditioning interaction, $F_{1,20}$=4.68, P<0.05). All error bars represent ± s.e.m.

Figure 2.

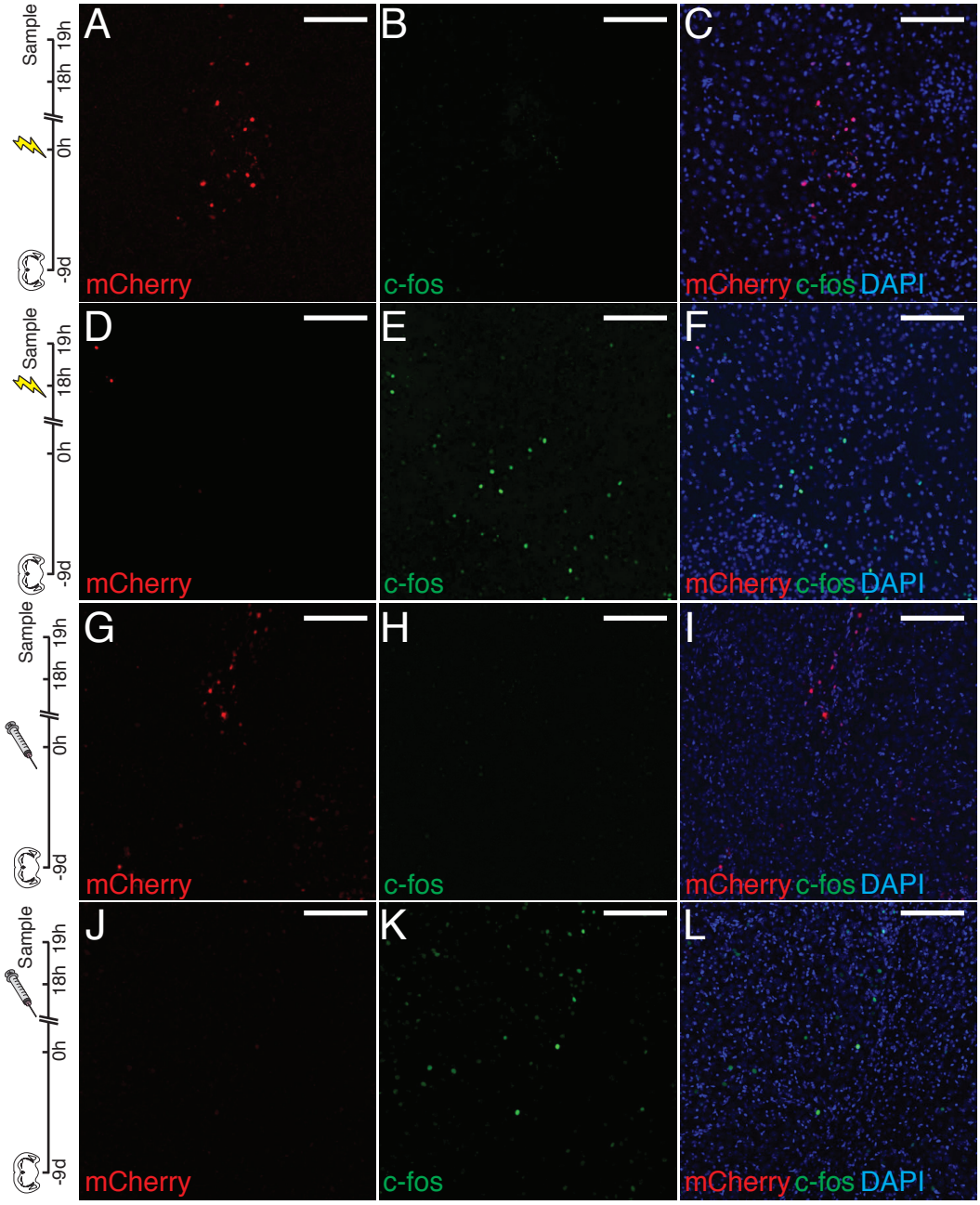
A
B
C
D
E
F
G
H
I
J
K
L
Sample
19h
18h
0h
-9d
mCherry
c-fos
mCherry c-fos DAPI

Figure 2. Time course of mCherry and c-Fos expression. A-C: Animals injected with lentivirus expressing c-fos:ChR2-EYFP-2A-mCherry were treated with footshock 19 hours prior to sacrifice and stained for mCherry (**A**), c-Fos (**B**) and merged (**C**). **D-F:** Animals injected with lentivirus expressing c-fos:ChR2-EYFP-2A-mCherry were treated with footshock 1 hour prior to sacrifice and stained for mCherry (**D**), c-Fos (**E**) and merged (**F**). **G-I:** Animals injected with lentivirus expressing c-fos:ChR2-EYFP-2A-mCherry were treated with nicotine 19 hours prior to sacrifice and stained for mCherry (**G**), c-Fos (**H**) and merged (**I**). **J-L:** Animals injected with lentivirus expressing c-fos:ChR2-EYFP-2A-mCherry were treated with nicotine 1 hour prior to sacrifice and stained for mCherry (**J**), c-Fos (**K**) and merged (**L**). Scale bars, 100μm.

Figure 3.

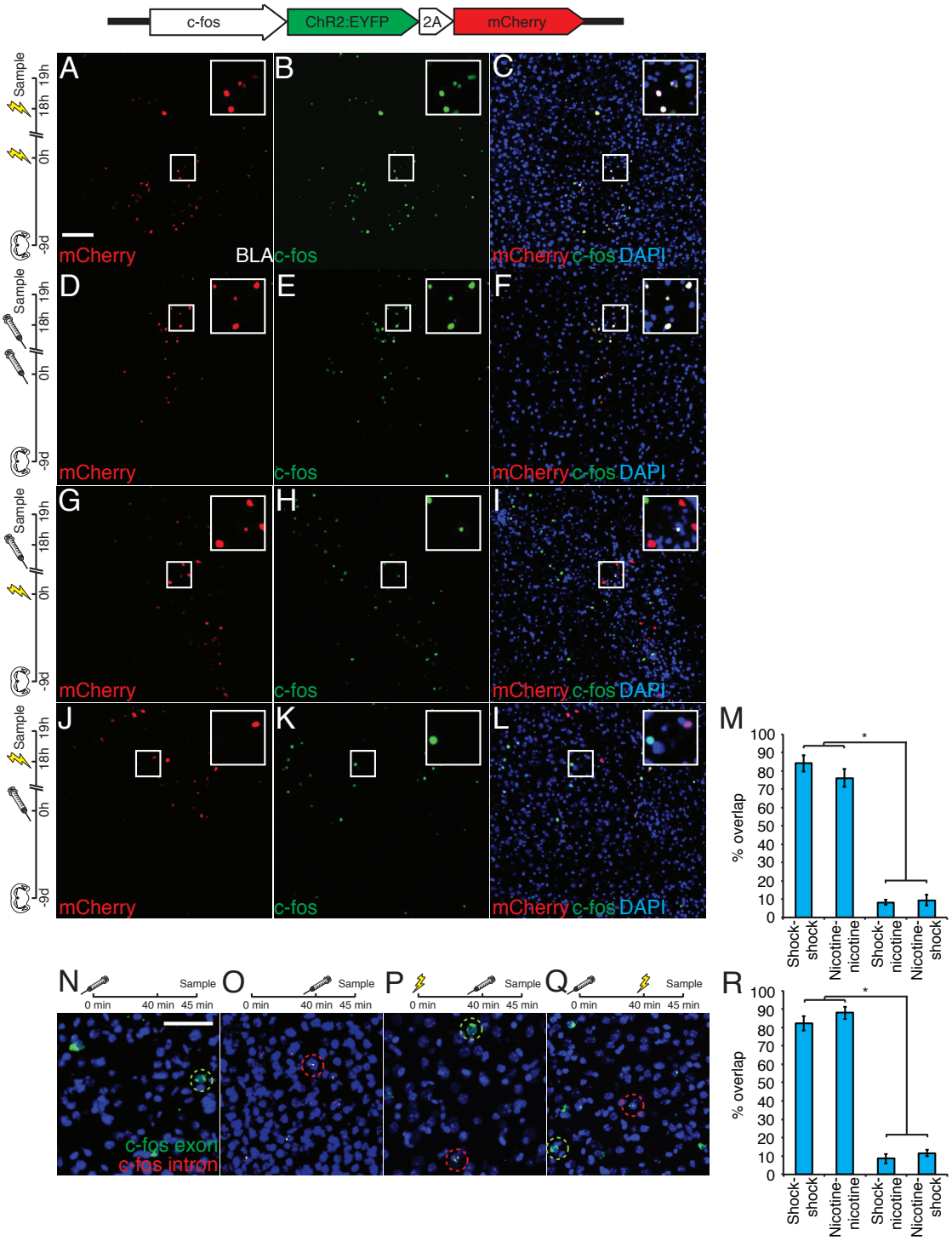
c-fos
ChR2:EYFP
2A
mCherry
A
B
C
D
E
F
G
H
I
J
K
L
Sample
19h
18h
0h
-9d
mCherry
BLA c-fos
mCherry c-fos DAPI
c-fos
M
% overlap
Shock-shock
Nicotine-nicotine
Shock-nicotine
Nicotine-shock
N
O
P
Q
0 min
40 min
45 min
c-fos exon
c-fos intron
R

Figure 3. Anatomically distinct, yet intermingled populations of cells in the BLA respond to appetitive and aversive unconditioned stimuli. A-C: Animals injected with lentivirus expressing c-fos:ChR2-EYFP-2A-mCherry were exposed to 2 footshock treatments separated by 18 hours and stained for mCherry (**A**), c-Fos (**B**), and merged (**C**). **D-F:** Animals injected with lentivirus expressing c-fos:ChR2-EYFP-2A-mCherry were treated with 2 i.p. nicotine injections separated by 18 hours and stained for mCherry (**D**), c-Fos (**E**), and merged (**F**). **G-I:** Animals injected with lentivirus expressing c-fos:ChR2-EYFP-2A-mCherry were treated with footshock followed by nicotine 18 hours later and stained for mCherry (**G**), c-Fos (**H**), and merged (**I**). **J-L:** Animals injected with lentivirus expressing c-fos:ChR2-EYFP-2A-mCherry were treated with nicotine followed by footshock 18 hours later and stained for mCherry (**J**), and c-Fos (**K**), and merged (**L**). **M.** Percent overlap ((mCherry+ + c-fos+)/mCherry+) of c-Fos positive and mCherry positive neurons in the BLA (shock-shock 84.07±4.46, n=6; nicotine-nicotine 76.02±4.90, n=5; shock-nicotine 8.22±1.40, n=6; nicotine-shock 9.28±2.94, n=5. One-way ANOVA, $F_{3,18}$=130.43, P<0.0001). **N-Q: N.** Animals exposed to nicotine treatment 45 minutes prior to sacrifice and stained for intronic *c-fos* RNA (nuclear, red) and exonic *c-fos* RNA (cytoplasmic, green). **O.** Animals exposed to nicotine treatment 5 minutes prior to sacrifice and stained for intronic *c-fos* RNA and exonic *c-fos* RNA. **P.** Animals exposed to footshock treatment 45 minutes prior to sacrifice and nicotine treatment 5 minutes prior to sacrifice and stained for intronic *c-fos* RNA and exonic *c-fos* RNA. **Q.** Animals exposed to nicotine treatment 45 minutes prior to sacrifice and footshock treatment 5 minutes prior to sacrifice and stained for intronic *c-fos* RNA and exonic *c-fos* RNA. **R.** Percent overlap (yellow/green) of *c-fos* intronic RNA positive neurons (nuclear

red) with *c-fos* exonic RNA positive neurons (cytoplasmic green) (shock-shock 82.19±3.86%, n=3; nicotine-nicotine 87.93±3.29%, n=4; shock-nicotine 8.63±2.67%, n=4; nicotine-shock 11.62±1.75%, n=6. One-way ANOVA, $F_{3,13}$=254.29, P<0.0001). Scale bars, 100μm. All error bars for all figures represent ± s.e.m.

Figure 4.

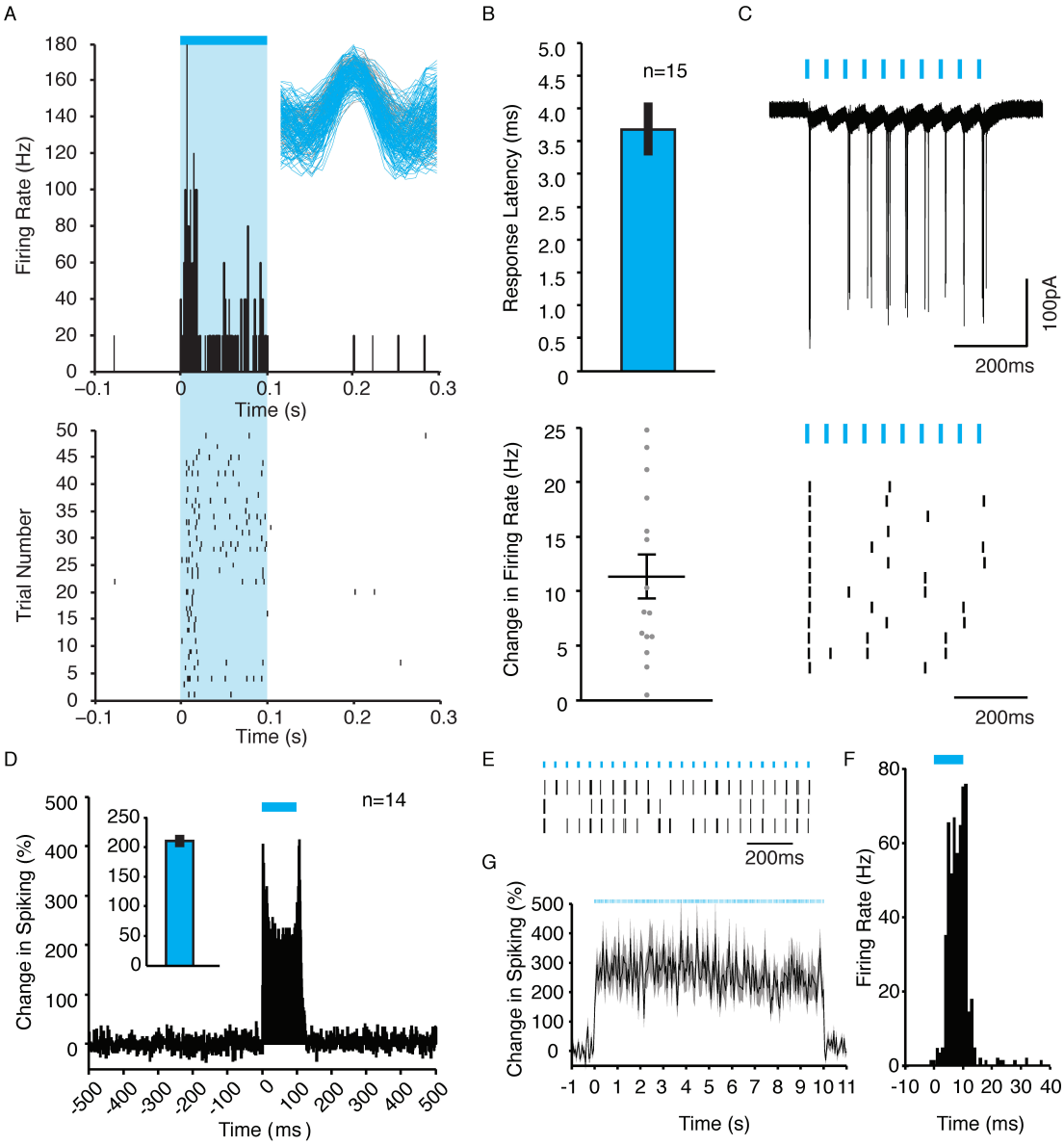
A
Firing Rate (Hz)
Time (s)
Trial Number
Time (s)
B
n=15
Response Latency (ms)
Change in Firing Rate (Hz)
C
100pA
200ms
200ms
D
n=14
Change in Spiking (%)
Time (ms)
E
200ms
F
Firing Rate (Hz)
Time (ms)
G
Change in Spiking (%)
Time (s)

Figure 4. Blue light increases activity in BLA cells of mice that received shock or nicotine exposure the previous day. A. Example single unit response recorded *in vivo* 18 hours after nicotine exposure. Blue shading represents 100ms light stimulus. Top: Peri-stimulus time histogram (PSTH) of firing rate averaged over 50 trials. *Inset*, blue lines; light-evoked waveforms; grey lines, spontaneous waveforms. Bottom: Raster plot of single unit activity over 50 trials. **B.** Top: Mean response latency of all isolated single units (3.68±0.40ms, n=15). Bottom: Change in firing rate (Hz) for all isolated single units from a 500ms baseline before light-onset (11.3±2.0 Hz, n=15). **C.** *Ex vivo* recordings from acute brain slices. Top: Cell attached recording of example BLA cell expressing EYFP 18 hours after shock exposure. Overlay of 20 trials (stimulus train 10 x 2ms pulses, 20Hz). Bottom: Raster plot showing individual trials. Light-evoked photocurrents: shock 106.90±30.63pA, n=9; nicotine 68.48±22.83pA, n=9. **D.** PSTH of change in multiunit spiking in response to blue light stimulation (n=14 stereotrodes recorded *in vivo*; blue horizontal line, 100ms pulse, 0.1Hz). *Inset*, mean change in spiking (210.1±10.6%). **E.** Raster of an example single unit response to blue light (10ms pulses, 20Hz. Blue lines, 10ms pulse). 3 trials shown. **F.** PSTH of example cell's firing rate averaged over 1200 10ms pulses (change in firing rate: 35.50Hz). **G.** Mean percent change in multiunit response in response to 20Hz 10ms blue light stimulation (261.27±55.25%, n=14 stereotrodes recorded *in vivo*; blue lines, 10ms pulse). All error bars represent ± s.e.m.

Figure 5.

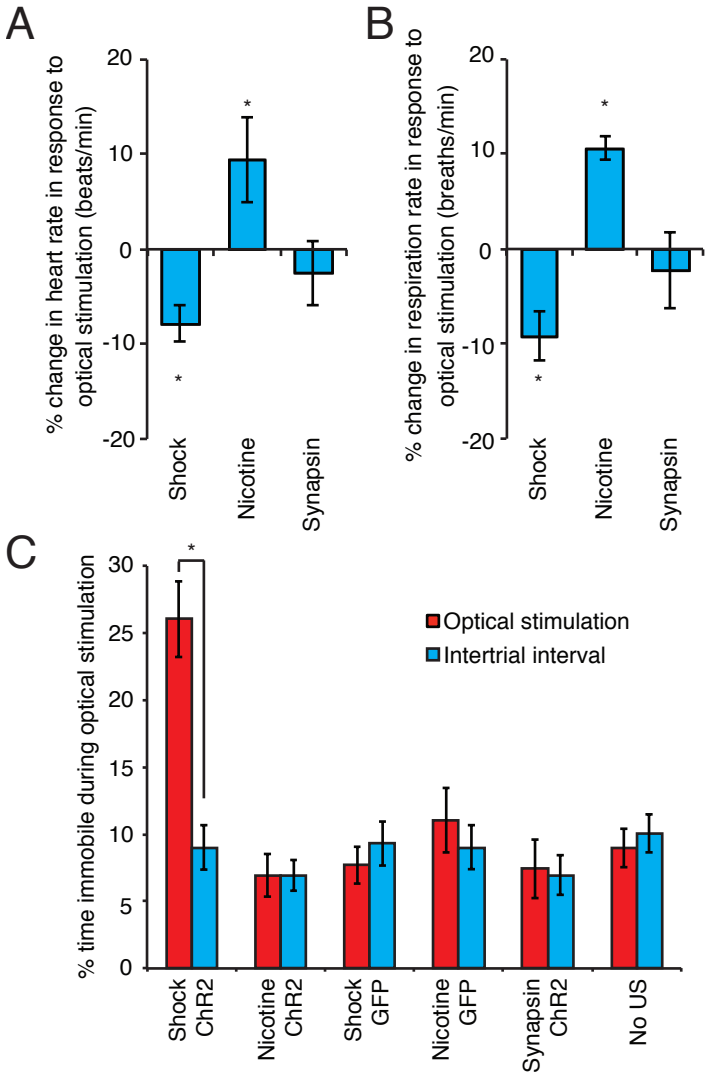
A
% change in heart rate in response to optical stimulation (beats/min)
20
10
0
-10
-20
*
*
Shock
Nicotine
Synapsin
B
% change in respiration rate in response to optical stimulation (breaths/min)
20
10
0
-10
-20
*
*
Shock
Nicotine
Synapsin
C
% time immobile during optical stimulation
30
25
20
15
10
5
0
*
Optical stimulation
Intertrial interval
Shock ChR2
Nicotine ChR2
Shock GFP
Nicotine GFP
Synapsin ChR2
No US

Figure 5. The exogenous activation of cells responsive to footshock and nicotine in the BLA is sufficient to elicit valence-specific physiological and behavioral responses. A. Percent change in heart rate from baseline in response to optical stimulation of footshock- or nicotine-responsive cells, or a random ensemble (shock -7.88±1.93% n=5; nicotine 9.49±4.52% n=5; synapsin -2.55±3.40%, n=6. Two-way ANOVA, group × optical stimulation interaction, $F_{2,26}$=6.24, P<0.01). **B.** Percent change in respiration rate from baseline in response to optical stimulation of footshock- or nicotine-responsive cells, or a random ensemble (shock -9.20±2.55%, n=5; nicotine 10.63±1.21%, n=5; synapsin -2.19±4.05%, n=6. Two-way ANOVA, group × optical stimulation interaction, $F_{2,26}$=10.14, P<0.001). **C.** Percent of time spent freezing in response to optical stimulation compared to the intertrial interval (ITI) (shock ChR2 optical stimulation 26.05±2.83%, ITI 8.99±1.66% n=7; nicotine ChR2 optical stimulation 6.93±1.58%, ITI 6.94±1.44 n=6; shock GFP optical stimulation 7.70±1.37%, ITI 9.32±1.65, n=6; nicotine GFP optical stimulation 11.07±2.42%, ITI 9.02±1.62%, n=6; synapsin ChR2 optical stimulation 7.43±2.19%, ITI 6.95±1.46%, n=5; no US optical stimulation 8.96±1.42%, ITI 10.05±1.40, n=5. Two-way ANOVA, group × optical stimulation interaction, $F_{5,58}$=8.28, P<0.0001). All error bars represent ± s.e.m.

Figure 6.

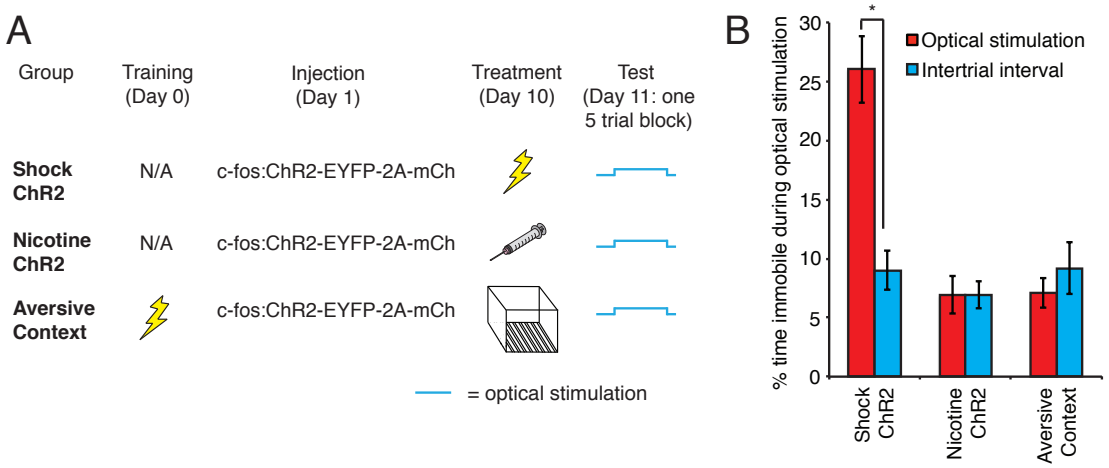
A
Group
Training (Day 0)
Injection (Day 1)
Treatment (Day 10)
Test (Day 11: one 5 trial block)
Shock ChR2
N/A
c-fos:ChR2-EYFP-2A-mCh
Nicotine ChR2
N/A
c-fos:ChR2-EYFP-2A-mCh
Aversive Context
c-fos:ChR2-EYFP-2A-mCh
= optical stimulation
B
% time immobile during optical stimulation
30
25
20
15
10
5
0
*
Optical stimulation
Intertrial interval
Shock ChR2
Nicotine ChR2
Aversive Context

Figure 6. Photoactivation of neurons that respond to an aversive context does not elicit freezing behavior. A. Behavioral training protocol for the reactivation of context-responsive neurons in the BLA. **B.** Percent of time spent freezing in response to optical stimulation compared to the intertrial interval (ITI) (shock ChR2 optical stimulation 26.05±2.83%, ITI 8.99±1.66% n=7; nicotine ChR2 optical stimulation 6.93±1.58%, ITI 6.94±1.44 n=6; aversive context optical stimulation 7.08±1.24%, ITI 9.19±2.22%, n=5. Two-way ANOVA, group × optical stimulation interaction, $F_{2,30}$=15.07, P<0.0001). All error bars represent ± s.e.m.

Figure 7.

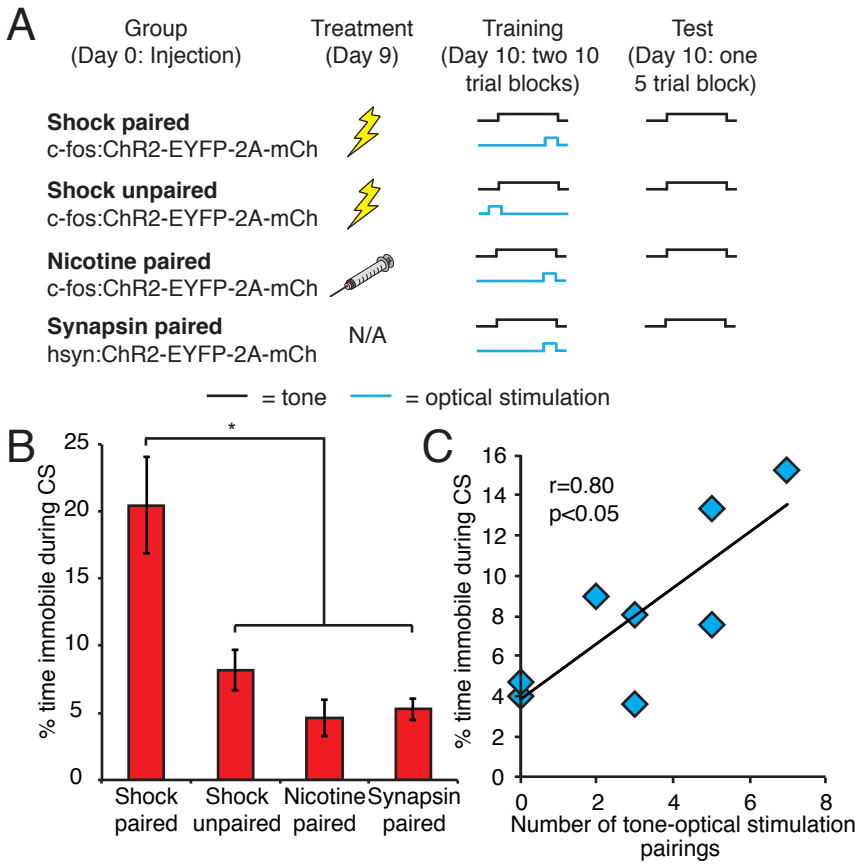
A
Group
(Day 0: Injection)
Treatment
(Day 9)
Training
(Day 10: two 10
trial blocks)
Test
(Day 10: one
5 trial block)
Shock paired
c-fos:ChR2-EYFP-2A-mCh
Shock unpaired
c-fos:ChR2-EYFP-2A-mCh
Nicotine paired
c-fos:ChR2-EYFP-2A-mCh
Synapsin paired
hsyn:ChR2-EYFP-2A-mCh
N/A
= tone
= optical stimulation
B
% time immobile during CS
Shock paired
Shock unpaired
Nicotine paired
Synapsin paired
C
r=0.80
p<0.05
% time immobile during CS
Number of tone-optical stimulation pairings

Figure 7. The exogenous activation of footshock-responsive cells can act as an unconditioned stimulus in an auditory fear conditioning paradigm. A. Modified fear conditioning paradigm. **B.** Percent time spent freezing in response to the auditory CS following fear conditioning using optical stimulation of the BLA as the US (shock paired 20.46±3.59%, n=10; shock unpaired 8.19±1.51%, n=8; nicotine paired 4.62±1.38%, n=8, synapsin paired 5.26±0.80%, n=6. One-way ANOVA, $F_{3,28}$=9.74, P<0.0005). **C.** Correlation between number of tone-optical stimulation pairings and percent immobility to CS in shock unpaired animals. All error bars represent ± s.e.m.

Figure 8.

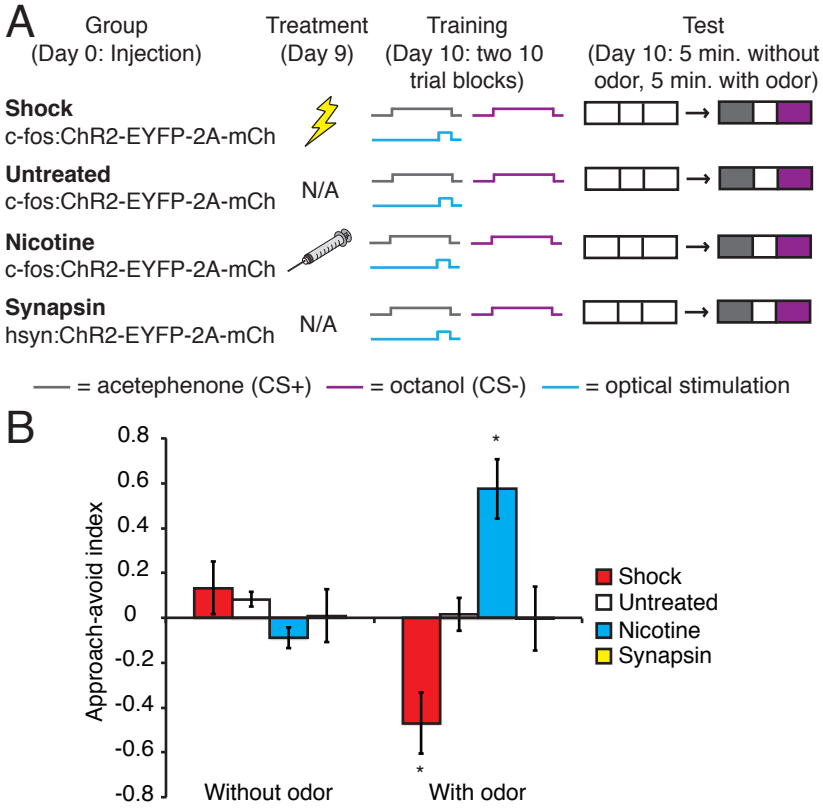
A
Group
(Day 0: Injection)
Treatment
(Day 9)
Training
(Day 10: two 10 trial blocks)
Test
(Day 10: 5 min. without odor, 5 min. with odor)
Shock
c-fos:ChR2-EYFP-2A-mCh
Untreated
c-fos:ChR2-EYFP-2A-mCh
N/A
Nicotine
c-fos:ChR2-EYFP-2A-mCh
Synapsin
hsyn:ChR2-EYFP-2A-mCh
N/A
= acetephenone (CS+)
= octanol (CS-)
= optical stimulation
B
Approach-avoid index
0.8
0.6
0.4
0.2
0
-0.2
-0.4
-0.6
-0.8
Without odor
With odor
Shock
Untreated
Nicotine
Synapsin

Figure 8. The exogenous activation of footshock- and nicotine-responsive cells can reinforce aversive and appetitive olfactory conditioning, respectively. A. Behavioral training protocol for associative olfactory learning. **B.** Approach-avoid index (difference in time spent in CS+ and CS- compartments of a 3 compartment chamber, divided by the time spent in both compartments) of shock-induced, untreated and nicotine-induced animals trained to associate odor with optical stimulation of the BLA, as well as animals expressing ChR2 in a random population of BLA neurons (shock without odor 0.13±0.12, with odor -0.47±0.14, n=6; untreated without odor 0.08±0.03, with odor 0.02±0.07, n=6; nicotine without odor -0.09±0.05, with odor 0.57±0.13, n=6; synapsin without odor 0.01±0.12, with odor 0.00±0.14, n=5. Two-way ANOVA, group × conditioning interaction, $F_{3,38}=12.65$, $P<0.0005$). All error bars represent ± s.e.m.

Figure 9.

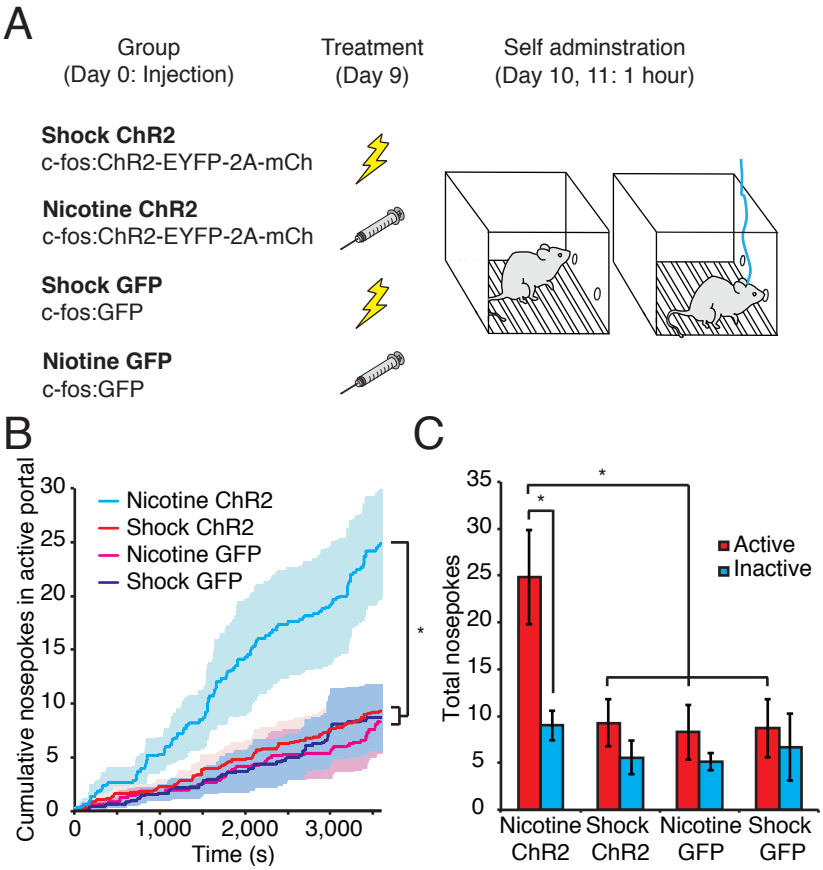
A
Group
(Day 0: Injection)
Treatment
(Day 9)
Self adminstration
(Day 10, 11: 1 hour)
Shock ChR2
c-fos:ChR2-EYFP-2A-mCh
Nicotine ChR2
c-fos:ChR2-EYFP-2A-mCh
Shock GFP
c-fos:GFP
Niotine GFP
c-fos:GFP
B
Cumulative nosepokes in active portal
Nicotine ChR2
Shock ChR2
Nicotine GFP
Shock GFP
Time (s)
C
Total nosepokes
Active
Inactive
Nicotine ChR2
Shock ChR2
Nicotine GFP
Shock GFP

Figure 9. The exogenous activation of nicotine-responsive cells can reinforce instrumental conditioning. A. Behavioral protocol for instrumental conditioning. **B.** Average cumulative nosepokes for the active portal on the second day of testing in animals expressing ChR2 or GFP in footshock or nicotine responsive cells. Shading represents ± s.e.m. (One-way ANOVA, $F_{3,26}$=5.08, P<0.01). **C.** Total nosepokes in the active and inactive portal on the second day of testing (nicotine-ChR2 active 24.83±5.02, inactive 9.00±1.57, n=6; shock-ChR2 active 9.30±2.54, inactive 5.60±1.81, n=10; nicotine-GFP active 8.29±2.92, inactive 5.14±0.91, n=7; shock-GFP active 8.71±3.11, inactive 6.71±3.58, n=7. Two-way ANOVA, group $F_{3,52}$=5.08, P<0.01, portal $F_{1,52}$=8.03, P<0.01). All error bars represent ± s.e.m.

Figure 10.

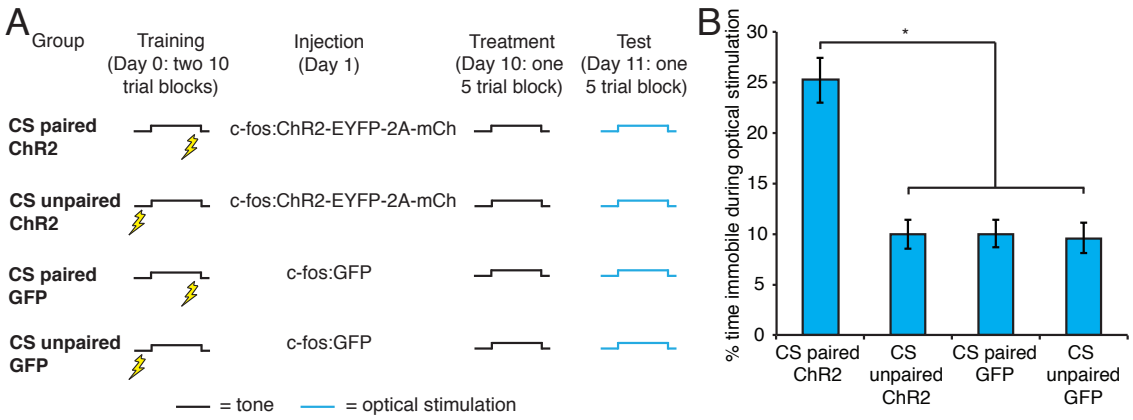
A
Group
Training (Day 0: two 10 trial blocks)
Injection (Day 1)
Treatment (Day 10: one 5 trial block)
Test (Day 11: one 5 trial block)
CS paired ChR2
c-fos:ChR2-EYFP-2A-mCh
CS unpaired ChR2
c-fos:ChR2-EYFP-2A-mCh
CS paired GFP
c-fos:GFP
CS unpaired GFP
c-fos:GFP
= tone
= optical stimulation
B
% time immobile during optical stimulation
30
25
20
15
10
5
0
*
CS paired ChR2
CS unpaired ChR2
CS paired GFP
CS unpaired GFP

Figure 10. The exogenous activation of a learned aversive CS representation can drive freezing behavior, whereas the exogenous activation of an unlearned CS representation cannot. A. Behavioral protocol for the reactivation of learned and unlearned CS representations in the BLA. **B.** Percent of time spent freezing in response to optical stimulation of the CS representation in the BLA (CS paired ChR2 25.22±2.25%, n=9; CS unpaired ChR2 9.93±1.40%, n=10; CS paired GFP 9.98±1.36%, n=6; CS unpaired GFP 9.59±1.50%, n=6. One-way ANOVA, $F_{3,26}$=20.10, P<0.00001). All error bars represent ± s.e.m.

Figure 11.

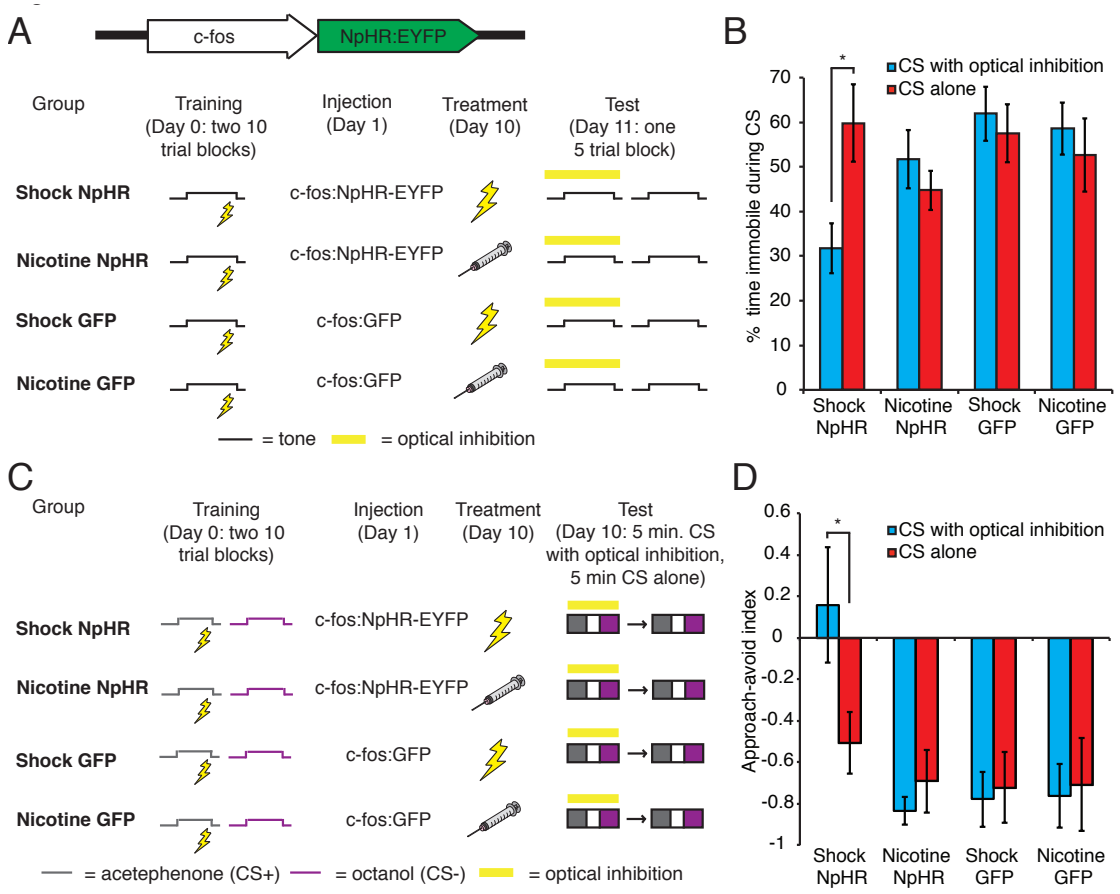
A
c-fos
NpHR:EYFP
Group
Training (Day 0: two 10 trial blocks)
Injection (Day 1)
Treatment (Day 10)
Test (Day 11: one 5 trial block)
Shock NpHR
c-fos:NpHR-EYFP
Nicotine NpHR
c-fos:NpHR-EYFP
Shock GFP
c-fos:GFP
Nicotine GFP
c-fos:GFP
= tone
= optical inhibition
B
CS with optical inhibition
CS alone
% time immobile during CS
Shock NpHR
Nicotine NpHR
Shock GFP
Nicotine GFP
C
Group
Training (Day 0: two 10 trial blocks)
Injection (Day 1)
Treatment (Day 10)
Test (Day 10: 5 min. CS with optical inhibition, 5 min CS alone)
Shock NpHR
c-fos:NpHR-EYFP
Nicotine NpHR
c-fos:NpHR-EYFP
Shock GFP
c-fos:GFP
Nicotine GFP
c-fos:GFP
= acetephenone (CS+)
= octanol (CS-)
= optical inhibition
D
CS with optical inhibition
CS alone
Approach-avoid index
Shock NpHR
Nicotine NpHR
Shock GFP
Nicotine GFP

Figure 11. Learning connects auditory and olfactory CS representations to US-responsive neurons in the BLA. A. Behavioral protocol for the silencing of US-responsive cells during auditory CS presentation. **B.** Percent immobility in response to the CS in the presence and absence of optical inhibition of footshock and nicotine-responsive cells (shock NpHR with yellow light 31.75±5.62%, without yellow light 59.84±8.72%, n=6; nicotine NpHR with yellow light 51.70±6.54%, without yellow light 44.73%±4.45%, n=9; shock GFP with yellow light 61.92±6.06%, without yellow light 57.59±6.55%, n=6; nicotine GFP with yellow light 58.59±5.84%, without yellow light 52.64±8.18%, n=6. Two-way ANOVA, group × optical inhibition interaction, $F_{3,46}$=3.16, P<0.05). **C.** Behavioral protocol for the silencing of US-responsive cells during olfactory CS presentation. **D.** Approach-avoid index in the presence and absence of optical inhibition of footshock and nicotine-responsive cells (shock NpHR with yellow light 0.16±0.28, without yellow light -0.51±0.15, n=6; nicotine NpHR with yellow light -0.83±0.07, without yellow light -0.69±0.15, n=6; shock GFP with yellow light -0.78±0.13, without yellow light -0.72±0.17, n=6; nicotine GFP with yellow light -0.76±0.15, without yellow light -0.71±0.22, n=6. Two-way ANOVA, group $F_{3,40}$=5.36, P<0.005). All error bars represent ± s.e.m.

Figure 12.

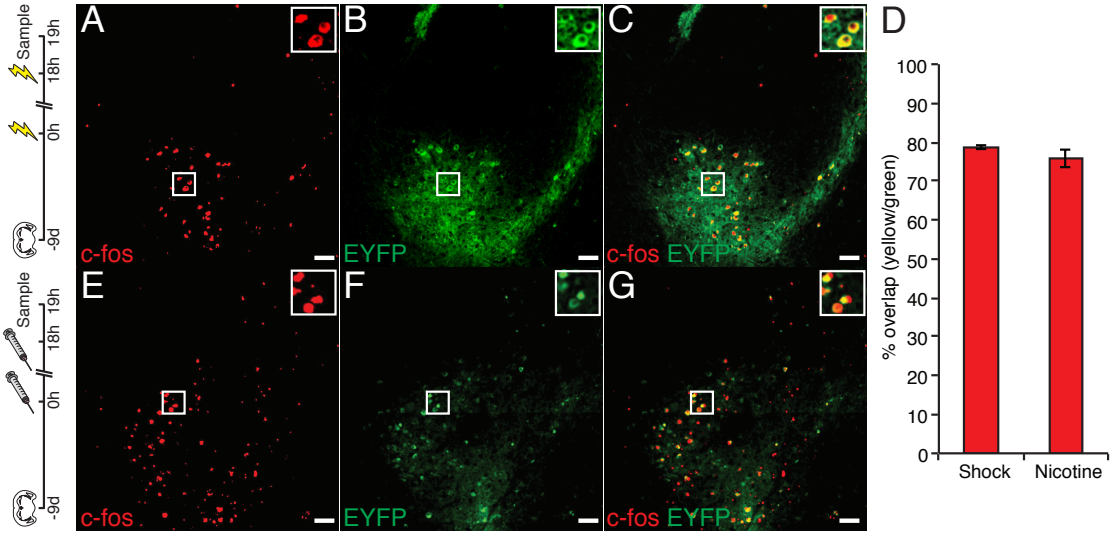
Sample
19h
18h
0h
-9d
A
B
C
D
c-fos
EYFP
c-fos EYFP
E
F
G
% overlap (yellow/green)
100
90
80
70
60
50
40
30
20
10
0
Shock
Nicotine

Figure 12. Halorhodopsin expression in US-responsive cells. A-C: Animals injected with lentivirus expressing NpHR-EYFP under the control of the *c-fos* promoter were treated with 2 sessions of footshock separated by 18 hours before being sacrificed 1 hour later and stained for c-Fos (**A**), EYFP (**B**), and merged (**C**). **D.** Percent overlap of EYFP positive and c-Fos positive neurons in the BLA (shock-shock 78.81±0.61%, n=4; nicotine-nicotine 75.83±2.31, n=4). **E-G:** Animals injected with lentivirus expressing NpHR-EYFP under the control of the *c-fos* promoter were treated with 2 sessions of i.p. nicotine separated by 18 hours before being sacrificed 1 hour later and stained for c-Fos (**E**), EYFP (**F**), and merged (**G**). Scale bars, 100μm. To visualize the entire BLA at 20x magnification, 16 tiled images were obtained and stitched together using the Zen imaging software (2009; version 5.5 SP1). A subset of contiguous tiles encompassing the BLA is presented. Lines in images are a result of the stitching process. All error bars represent ± s.e.m.

Figure 13.

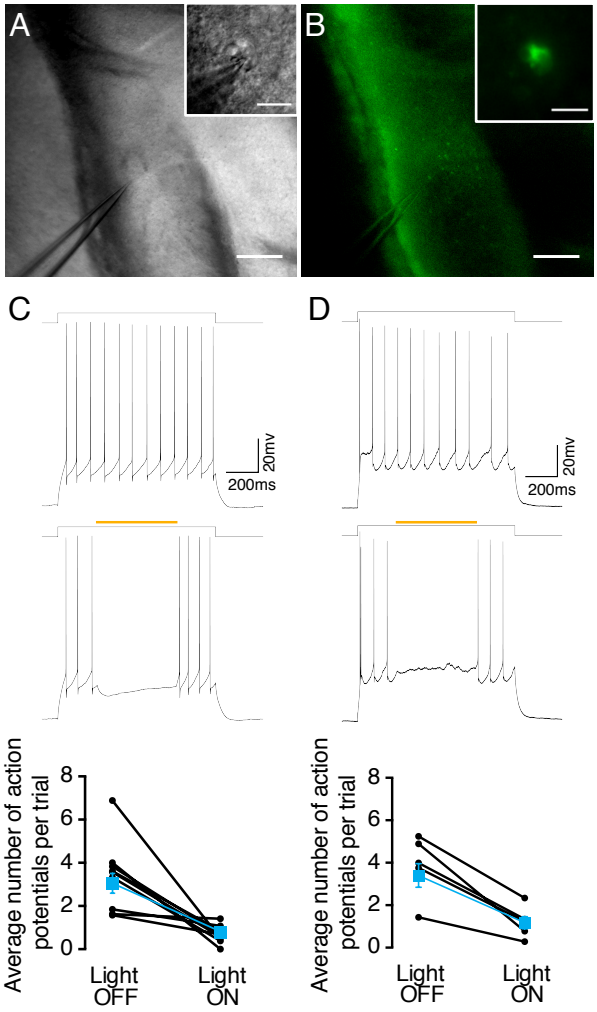
A
B
C
D
20mv
200ms
20mv
200ms
Average number of action potentials per trial
8
6
4
2
0
Light OFF
Light ON
Average number of action potentials per trial
8
6
4
2
0
Light OFF
Light ON

Figure 13. Yellow light reduces activity in BLA cells of mice that received shock or nicotine exposure the previous day. A. Differential interference contrast (DIC) image of a slice recording from cell expressing EYFP in the BLA after shock exposure (scale bar=200μm). Inset: magnified view of the recorded cell (scale bar=20μm). **B.** Epifluorescent image of BLA recording site and cells expressing EYFP in (**A**), (scale bar=200μm). Inset: EYFP fluorescence of recorded cell (scale bar=20μm). **C.** Top: Whole-cell, current-clamp recording from a cell expressing EYFP 18-hours after shock exposure. Current was injected to hold the cell at -70mV. A single, 1-second positive current step was applied to the cell to induce a train of action potentials. Current amplitude was selected as 50pA above rheobase. In this cell, rheobase was +131pA, and therefore, injected current was +181pA. Middle: Response to 500ms pulse of 595nm yellow light during current injection. Light OFF trials were interleaved with Light ON trials for all experiments. Bottom: Quantification of inhibition by 595nm light in shock-induced cells, 70 trials per cell (average number of action potentials during the middle 500ms of a 1s current step: light OFF 3.36±0.55, light ON 0.69±0.14, n=9 cells, p=0.0039, Wilcoxon matched-pairs signed-ranks test). **D.** Top: Whole-cell, current clamp recording of cell expressing EYFP as in (**C**), but 18 hours after nicotine exposure (rheobase 135pA, current step +185pA). Middle: Inhibition of firing with 595nm light. Bottom: Quantification of inhibition in nicotine-induced cells (average number of action potentials: light OFF 3.86±0.67, light ON 1.20±0.34, n=5 cells, p=0.0625, Wilcoxon matched-pairs signed-ranks test). Light-evoked photocurrents: shock 40.17±9.97pA, n=7; nicotine 24.52±3.05pA, n=5. All error bars represent ± s.e.m.

Figure 14.

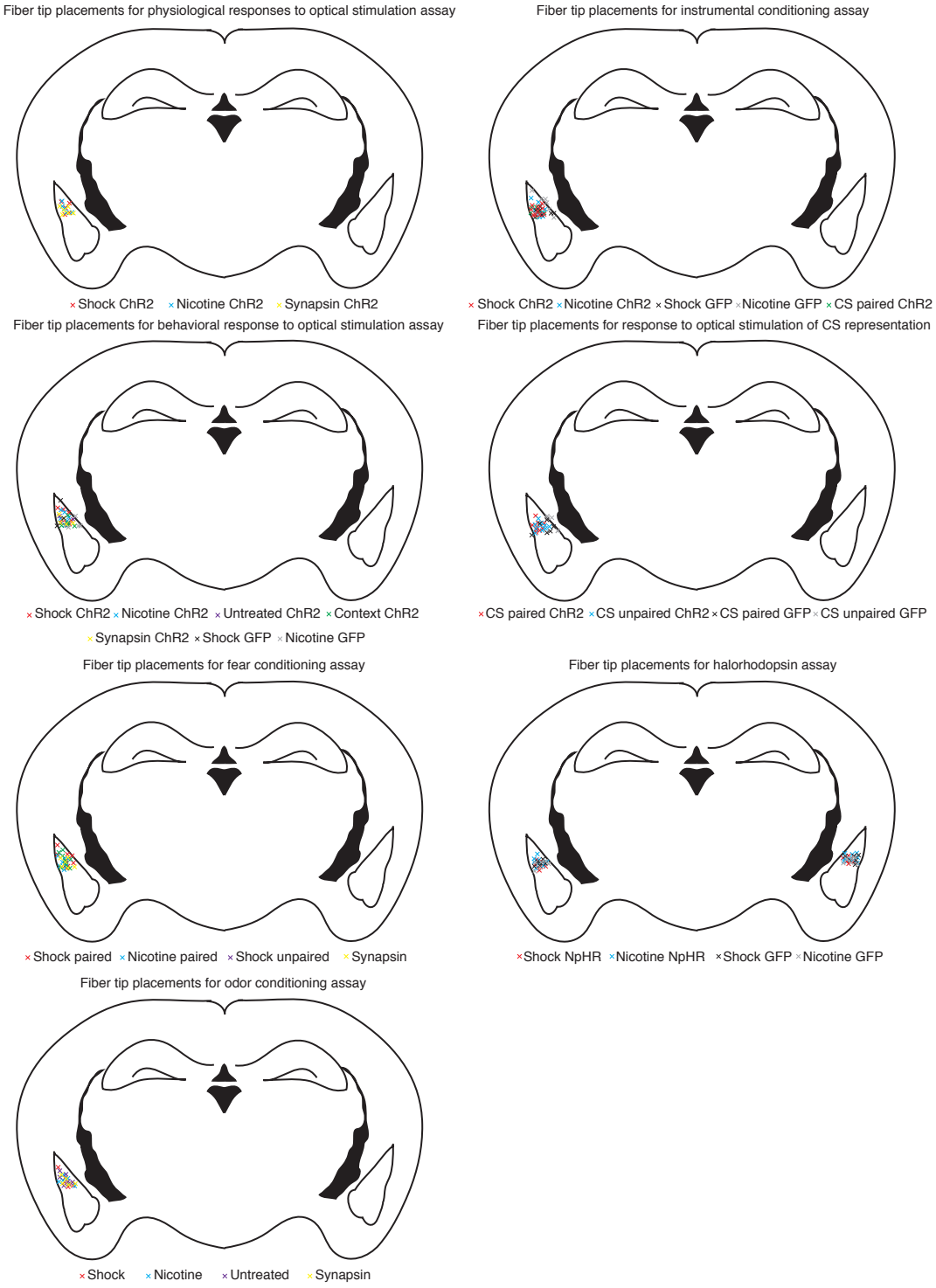
Fiber tip placements for physiological responses to optical stimulation assay
Shock ChR2
Nicotine ChR2
Synapsin ChR2
Fiber tip placements for instrumental conditioning assay
Shock ChR2
Nicotine ChR2
Shock GFP
Nicotine GFP
CS paired ChR2
Fiber tip placements for behavioral response to optical stimulation assay
Shock ChR2
Nicotine ChR2
Untreated ChR2
Context ChR2
Synapsin ChR2
Shock GFP
Nicotine GFP
Fiber tip placements for response to optical stimulation of CS representation
CS paired ChR2
CS unpaired ChR2
CS paired GFP
CS unpaired GFP
Fiber tip placements for fear conditioning assay
Shock paired
Nicotine paired
Shock unpaired
Synapsin
Fiber tip placements for halorhodopsin assay
Shock NpHR
Nicotine NpHR
Shock GFP
Nicotine GFP
Fiber tip placements for odor conditioning assay
Shock
Nicotine
Untreated
Synapsin

Figure 14. Fiber tip placements for behavioral assays.

CHAPTER 3

OLFACTORY FEAR LEARNING IS MEDIATED BY THE MONOSYNAPTIC PROJECTION FROM PIRIFORM CORTEX TO THE BASOLATERAL AMYGDALA

For many organisms the sense of smell is critical to survival. Some olfactory stimuli elicit innate responses that are mediated through hardwired circuits that have developed over long periods of evolutionary time. Most olfactory stimuli, however, have no inherent meaning. Instead, meaning must be imposed by learning during the lifetime of an organism. Despite the dominance of olfactory stimuli on animal behavior, the mechanisms by which odorants elicit learned behavioral responses remain poorly understood.

All odor-evoked behaviors are initiated by the binding of an odorant in the environment to olfactory receptors located on sensory neurons in the nasal epithelium (Buck and Axel, 1991, DeMaria and Ngai, 2010, Hayden and Teeling, 2014). Each olfactory sensory neuron expresses 1 of over 1000 olfactory receptors and every receptor can detect multiple odorants (Chess et al., 1994, Malnic et al., 1999, Shykind et al., 2004). Sensory neurons expressing a given receptor are randomly distributed within 4 zones of the olfactory epithelium (Ressler et al., 1993, Vassar et al., 1993) and order is only imparted on this system via the convergence of axons expressing like receptors on 2 spatially invariant glomeruli on the surface of the olfactory bulb (Mombaerts et al., 1996, Ressler et al., 1994, Vassar et al., 1994). As such, individual odorants evoke a stereotyped spatial map of glomerular activity (Bellucio and Katz, 2001, Bozza et al., 2004, Soucy et al., 2009).

The projection neurons of the olfactory bulb, the mitral and tufted cells, extend an apical dendrite into a single glomerulus and project their axons to numerous higher order structures that have been implicated in the generation of odor-evoked behaviors (Shepherd, 1994). Anatomical tracing reveals that mitral and tufted cells arising from individual glomeruli send diffuse projections across the whole of piriform cortex. These projections appear randomized, discarding the spatial order of the olfactory bulb (Ghosh et al., 2011, Sosulski et al., 2011). In addition, individual neurons in piriform cortex receive convergent input from multiple glomeruli (Davison and Ehlers, 2011, Miyamichi et al., 2011). This anatomical connectivity directly shapes odor-evoked responses in piriform: individual odorants evoke activity in sparse ensembles that are distributed over the extent of the piriform cortex and individual neurons exhibit discontinuous receptive fields, responding to structurally and perceptually similar and dissimilar odorants (Illig and Haberly, 2003, Poo and Isaacson, 2009, Rennaker et al., 2007, Stettler and Axel, 2009).

One model consistent with the anatomical and physiological data invokes the random convergence of mitral and tufted cell inputs onto piriform neurons such that each neuron in piriform cortex samples from a random combination of glomeruli (Choi et al., 2011, Davison and Ehlers, 2011, Sosulski et al., 2011). In this model, each odorant would evoke activity in an apparently random subset of piriform neurons such that each odorant representation in piriform would have no inherent meaning. Instead, meaning would be imposed by experience via the reinforcement of projections to valence-specific outputs.

In accord with this model, photoactivation of a random ensemble of piriform neurons can become entrained to both appetitive and aversive outcomes (Choi et al.,

2011) and lesions of posterior piriform cortex prevent retrieval of remote olfactory fear memories (Sacco and Sacchetti, 2010). Piriform cortex has therefore been implicated in olfactory fear learning. However how aversive meaning is imparted on disordered olfactory representations in piriform is unclear.

Piriform projects to numerous higher order brain structures that have been implicated olfactory learning, including the olfactory tubercle, cortical amygdala and the basolateral amygdala (BLA) (Shepherd, 1994, Sosulski et al., 2011). Prior studies have demonstrated that plasticity in the BLA is necessary for the acquisition of learned olfactory fear, and that activity in the BLA is required for the retrieval of olfactory fear memories (Cahill and McGaugh, 1990, Cousens and Otto, 1998, Kilpatrick and Cahill, 2003, Laviolette and Grace, 2006, Tan et al., 2011, Walker et al., 2005). Olfactory fear learning modulates odor-evoked responses in the BLA (Hegoburu et al., 2009, Rosenkranz and Grace, 2002, Rosenkranz et al., 2003, Sevelinges et al., 2004). Finally, we have previously identified a locus of olfactory convergence onto a representation of an unconditioned stimulus in the BLA that is necessary for the expression of learned olfactory fear (Gore et al., 2015a). These data suggest that connectivity between piriform and the BLA might provide an anatomical substrate through which aversive meaning is imparted on an odor.

We therefore manipulated the activity of the axonal projection from piriform cortex to the basolateral amygdala to determine its role in the generation of learned aversive behaviors. We demonstrate the existence of a monosynaptic projection from the posterior portion of piriform cortex to the BLA. Photoactivation of this projection can act as a conditioned stimulus and recall a fear memory. Moreover, inhibition of this

projection prevents the expression of learned olfactory behavior. Thus reinforcement of the projections of an odorant representation in piriform cortex to the basolateral amygdala provides a mechanism through which aversive meaning is imparted on disordered olfactory representation in piriform cortex.

Results

Representations of odor in piriform cortex are sparse and distributed, lacking any apparent spatial order (Poo and Isaacson, 2009, Stettler and Axel, 2009). Computational models suggest that this organization might facilitate associative learning (Marr, 1971). In addition, lesion studies have suggested that activity within posterior piriform cortex may be critically required for the expression of learned olfactory fear (Sacco and Sacchetti, 2010). We therefore confirmed the necessity of posterior piriform cortex for olfactory fear learning. Mice were injected bilaterally in posterior piriform cortex with an adeno-associated virus encoding the inhibitory DREADD, hM4Di, under the control of the synapsin promoter (AAV_5-hSyn-HA-hM4Di-IRES-mCitrine) (% infectivity: 73.49±4.30%, n=6. Figure 1A). Intraperitoneal (i.p.) delivery of the synthetic ligand clozapine-N-oxide reduced odor-evoked c-fos expression in piriform cortex compared to saline injected controls (% c-fos expressing cells: CNO 1.27±0.14%, n=3; Saline 4.68±0.13%, n=3. Figure 1A), suggesting that we were able to chemogentically silence piriform neurons. Animals were trained to associate an odor with footshock. Mice received 20 presentations of 1% acetephenone (CS+) that co-terminated with 2 seconds of footshock (0.7mA). Animals also received 20 randomly interleaved presentations of 2% octanol (CS-). Mice were then placed in the center of a 3-compartment chamber. CS+

and CS- odors were infused from opposite ends of the apparatus. When injected with saline, animals avoided the CS+ (approach-avoid index: -0.64±0.15, n=7. Figure 1C). However, when injected with CNO, the same animals showed diminished avoidance of the CS+ (approach-avoid index: -0.14±0.05, n=7. Figure 1C). Importantly, this was only true of animals in which piriform neurons were silenced as avoidance of the CS+ was unaffected by CNO application in animals injected with an AAV encoding GFP (approach-avoid index: saline -0.58±0.17, CNO: -0.54±0.17, n=4. Figure 1C). Thus activity in posterior piriform cortex is required for the expression of learned olfactory fear. Notably, silencing of the posterior portion of piriform cortex had no effect on a mouse's innate avoidance of the fox secretion 2,3,5-trimethyl-3-thiazoline (TMT) (approach-avoid index: saline -0.50±0.15, CNO -0.39±0.11, n=5. Figure 1C). These data demonstrate that activity in posterior piriform cortex is necessary for learned olfactory fear but dispensable for innate olfactory aversion.

To identify candidate structures downstream of piriform cortex that might mediate olfactory fear learning we conducted c-Fos immunostaining in response to either an odorant that had either been paired with no outcome (neutral odor) or an odorant that had been paired with footshock (learned aversive odor) (Figure 2A-C). Mice received 20 presentations of 1% acetephenone (neutral odor) or 20 presentations of 1% acetephenone paired with footshock (learned aversive odor). All mice were then exposed to acetephenone and were sacrificed 1 hour later. In animals that had received acetephenone paired with no outcome, we observed expression of c-Fos in numerous brain regions, including piriform cortex, the basolateral amygdala, and the cortical amygdala (% cells expressing c-Fos in response to neutral odor: piriform 3.99±0.35%, n=6; BLA

1.46±0.13%, n=6, cortical amygdala 4.07±0.40%, n=6. Figure 2A, C). Interestingly, in animals in which acetephenone had been paired with footshock, we observed an increase in the percentage of cells expressing c-Fos selectively in the basolateral amygdala (% cells expressing c-Fos in response to learned aversive odor: piriform 3.04±0.32%, n=6; BLA 3.49±0.51%, n=6; cortical amygdala 4.35±0.48, n=6. Figure 2B, C). Thus aversive conditioning increases the number of odor-responsive cells in the BLA, suggesting a role for the BLA in learned olfactory fear.

Prior anatomical studies have identified a modest monosynaptic projection from posterior piriform cortex to the BLA (McDonald, 1998, Sah et al., 2003). To confirm the existence of this projection, we injected the retrograde trace cholera toxin B subunit into the BLA. This revealed labeling of cell bodies in piriform cortex, primarily in the posterior subdivision (Figure 3A). Likewise, injection of an AAV expressing halorhodopsin fused to EYFP (AAV_5-hSyn-NpHR-EYFP) into posterior piriform cortex revealed labeling axon terminals in the BLA (Figure 3B). Thus there is a monosynaptic projection from posterior piriform cortex to the BLA. We therefore investigated the possibility that reinforcement of the monosynaptic projection from posterior piriform to the basolateral amygdala might be the anatomical substrate through which aversive meaning is imparted on the disordered odorant representation in piriform cortex.

We first asked whether the activity of the piriform-BLA projection was sufficient to recall an aversive memory. Animals were injected with an AAV encoding channelrhodopsin fused to EYFP (AAV_5-hSyn-ChR2-EYFP) to result in expression of ChR2-EYFP in a random ensemble of approximately 500 neurons in posterior piriform cortex (Choi et al., 2011). Optical fibers were placed over posterior piriform cortex, and a

beveled cannula was positioned over the BLA to allow region specific targeting of optical stimulation. Animals received 20 presentations of 10 seconds of photoactivation of piriform cell bodies that coterminated with 2 seconds of footshock (Figure 4A). In accordance with prior work, we observed that subsequent photoactivation of piriform cell bodies was able to elicit defensive behavior (% freezing: 52.49±4.54%, n=6. Figure 4B). We also asked in these same animals whether photoactivation specifically of the piriform terminals in the basolateral amygdala could recall the same fear memory. Photoactivation of piriform terminals in the BLA was able to elicit freezing (% freezing: 46.99±3.44%, n=6. Figure 4B) and moderate avoidance behavior (approach-avoid index: -0.20±0.08, n=6. Figure 4C). Freezing behavior was not elicited via antidromic stimulation of piriform cell bodies as simultaneous inhibition of piriform cell bodies did not attenuate freezing behavior evoked by stimulation of piriform terminals in the BLA (% freezing: 46.33±3.83%, n=6. Figure 4B). Notably, we have also demonstrated that photoactivation of piriform projections to other brain regions such as the cortical amygdala, is insufficient to recall aversive memories (% freezing in response to optical stimulation of piriform terminals in cortical amygdala: 20.62±5.43, n=5). Thus, while piriform cortex has multiple targets, its projection to the basolateral amygdala appears positioned to impart aversive meaning upon odorant representations.

These experiments suggest that the projection from posterior piriform to the BLA is a candidate pathway through which odorants can acquire aversive meaning. However, in this paradigm we activate many fewer neurons than a native odorant. We therefore asked whether this projection is required for learned behavior using real odors. Mice were injected bilaterally in posterior piriform cortex with an AAV expressing halorhodopsin

fused to EYFP (AAV_5-hSyn-NpHR-EYFP) and a cannula was positioned over each BLA to allow optical inhibition of the projection from posterior piriform to the BLA. Mice received 20 presentations of 1% acetephenone (CS+) that co-terminated with 2 seconds of footshock (0.7mA), and 20 randomly interleaved presentations of 2% octanol (CS-). Animals were then placed in the center of a 3-compartment chamber. CS+ and CS- odors were infused from opposite ends of the apparatus. In the absence of optical inhibition, animals avoided the aversive CS+ (approach-avoid index: -0.62±0.09, n=7. Figure 5A). However, in the presence of optical inhibition avoidance of the CS+ was attenuated (approach-avoid index: -0.23±0.12, n=7. Figure 5A). This effect was specific to silencing of the piriform to BLA projection as yellow light had no effect on avoidance of the CS+ in animals injected with a virus encoding GFP (approach-avoid index: in absence of yellow light -0.83±0.11, in presence of yellow light -0.80±0.09, n=5. Figure 5A). Notably, activity of this projection is not required for an olfactory discrimination task using the same odorants (fraction correct licks: in the absence of yellow light 0.93±0.02, n=7; in the presence of yellow light 0.90±0.02, n=7. Figure 5B) suggesting diminished avoidance behavior was not due to a generalized deficit in olfactory perception. In addition, silencing of the projection from piriform to BLA had no effect on an animal's innate avoidance of TMT (approach-avoid index: in absence of yellow light -0.68±0.11, n=6; in presence of yellow light -0.66±0.12, n=4, Figure 5A). Thus activity of the posterior piriform to BLA projection is specifically required for the expression of learned olfactory fear.

Discussion

Mitral and tufted cells innervate piriform cortex without any apparent spatial stereotypy such that individual piriform neurons sample from an apparently random subset of glomeruli (Apicella et al., 2010, Davison and Ehlers, 2011, Ghosh et al., 2011, Miyamichi et al., 2011, Sosulski et al., 2011). This anatomical connectivity directly shapes the representations of odorants in piriform: individual odorants evoke activity in sparse, distributed ensembles of neurons, and individual piriform neurons exhibit discontinuous receptive fields (Illig and Haberly, 2003, Poo and Isaacson, 2009, Rennaker at al., 2007, Stettler and Axel, 2009). This neural architecture makes it unlikely that odorant representations in piriform cortex possess an inherent meaning or valence. Instead meaning must be imparted on piriform representations via learning. Our data identify a monosynaptic projection from piriform cortex to the basolateral amygdala that can act as a conditioned stimulus in an aversive conditioning paradigm, and is necessary for the expression of learned olfactory fear. Aversive meaning is therefore imparted on disordered olfactory representations in piriform cortex via reinforcement of their projections to the BLA.

Photoactivation of a random ensemble of neurons in piriform cortex can be entrained to both appetitive and aversive outcomes (Choi et al., 2011). We demonstrate that the exogenous activation of the piriform to BLA projection can act as a conditioned stimulus and recall an aversive fear memory. In addition, activity of this projection is necessary for learned olfactory fear. This suggests that plasticity at the piriform to BLA synapse, or downstream, must mediate olfactory fear learning. Electrophysiological studies have identified US-responsive neurons in the BLA that respond to olfactory conditioned stimuli after learning (Rosenkranz and Grace, 2002, Rosenkranz et al., 2003,

Sevelinges et al., 2004). NMDA receptor blockade in the BLA prevents olfactory fear learning (Walker et al., 2005). Finally, activity of a footshock representation in the BLA can drive olfactory fear conditioning, and is required for the expression of learned behavior (Gore et al., 2015a). Taken together, these data suggest that the potentiation of piriform inputs that project either directly or indirectly to US representations in the basolateral amygdala must mediate olfactory fear learning.

One model in accord with these data suggests the existence of an unconditioned stimulus representation in the basolateral amygdala that is capable of generating innate defensive responses. Olfactory representations in piriform cortex send weak projections to the US representation in the BLA such that presentation of the odorant is insufficient to elicit postsynaptic activity in the US ensemble. Temporal pairing of an odorant with an unconditioned stimulus results in Hebbian potentiation of piriform inputs to the US representation such that subsequent presentations of the odorant activate the US ensemble to generate learned defensive responses. In this model reinforcement of the projections of a specific odorant representation in piriform onto the US representation in the BLA imparts aversive meaning exclusively onto the trained odorant, thus affording the discriminative capabilities that are observed in the animal kingdom.

This model assumes that the axon terminals of an odorant representation in piriform cortex directly synapse onto a US representation in the BLA. In this model, odorant identity would be encoded by the combination of synaptic inputs onto the US representation in the BLA and neurons in the BLA would only encode the learned valence of the odor. This would imply that through fear learning, a high dimensional representation of an odorant in piriform is reduced into a low dimensional representation

of valence at the synapse onto a US representation in the BLA. There is a huge convergence of olfactory information from piriform onto single cells in the BLA (approximately 100:1) and this may indeed place restrictions on the information content of odorant ensembles in the BLA. Moreover, electrophysiological recordings in rodents suggest that olfactory responses are broadly tuned and often reflect the hedonic properties of an odorant (Cain and Bindra, 1972, Schoenbaum et al., 1999). However our data cannot preclude the possibility that piriform projections to the BLA establish an olfactory representation in the BLA that is unique for each odorant and potentiation of projections from this BLA olfactory representation onto the US ensemble mediates fear learning. This would suggest that the BLA encodes odor identity, in addition to its learned valence. Support for this notion comes from electrophysiological studies in non-human primates that have identified neurons that are selective for different neutral conditioned stimuli (Paton et al., 2006).

We have demonstrated that activity of the projection from piriform to the BLA can act as a conditioned stimulus to recall a fear memory and is necessary for learned olfactory fear responses. It should be noted that the anatomical projection from piriform to the basolateral amygdala primarily originates in the posterior portion of piriform cortex (McDonald, 1998). In accord with our data, prior studies have demonstrated that lesions of posterior piriform impair the recall of an aversive olfactory memory (Sacco and Sacchetti, 2010). However, olfactory stimuli evoke activity throughout piriform cortex (Stettler and Axel, 2009) and random ensembles of neurons in anterior and posterior piriform are equally capable of becoming entrained to aversive outcomes (Choi et al., 2011). It is currently unclear how neural ensembles in anterior piriform engage the

projection from posterior piriform to generate learned aversive behaviors. Long-range excitatory projections have been identified in piriform cortex (Franks et al., 2011, Poo and Isaacson, 2011). These intracortical connections might provide a means by which ensembles in anterior piriform evoke activity in the projection from posterior piriform to the BLA.

We have demonstrated that activity of the projection from piriform to the BLA is necessary for the expression of learned olfactory fear. The activity of this same projection is not required for an appetitive discrimination task in which a mouse is trained to lick in response to an odor that predicts a water reward and to suppress licking to a second odor that predicts nothing. Photoactivation of a random ensemble of piriform neurons can, however, be entrained to an appetitive outcome (Choi et al., 2011). Piriform has dense projections to neural structures that have been implicated in reward learning, such as the olfactory tubercle (Murata et al., 2015). The activity of distinct projections of piriform cortex may therefore mediate appetitive olfactory learning. It is currently unclear whether the piriform neurons that project to the BLA circuits that mediate fear learning also project to structures that mediate appetitive conditioning. There appears to be no spatial bias in the ability of piriform ensembles to generate learned responses of different valence (Choi et al., 2011), however it remains possible that different subpopulations of piriform neurons target appetitive or aversive circuitry exclusively. The neural basis of appetitive olfactory discrimination therefore remains to be elucidated.

This notwithstanding, our data suggest that aversive meaning is imparted on a disordered representation of odor in piriform cortex via reinforcement of piriform projections to the BLA. A similar strategy may be implemented in the hippocampus, a 3-

layered paleocortex similar to piriform cortex, to mediate contextual fear conditioning. Contexts are encoded by the activity of distributed ensembles of place cells in the hippocampus. These ensembles lack any apparent spatial order such that the anatomical location of individual place cells has no apparent relationship to its receptive field in the external world (O'Keefe et al., 1998, Redish et al., 2001). Moreover, connectivity between representations of context in the hippocampus and representations of unconditioned stimuli in the BLA has been implicated in the generation of learned behavioral responses (Redondo et al., 2014). Thus reinforcement of sensory projections to US representations in the BLA might provide a generalized model by which meaning is imposed on disordered representations of the external world.

Odorants in the external environment are detected by receptors on sensory neurons that are randomly distributed in the olfactory epithelium (Buck and Axel, 1991, Ressler et al., 1993, Vassar et al., 1993). Olfactory sensory neurons expressing like receptors project with spatial precision to 2 specific glomeruli in the olfactory bulb, such that a given odorant activates a stereotyped spatial map of glomerular activity (Mombaerts et al., 1996, Ressler et al., 1994, Vassar et al., 1994, Bellucio and Katz, 2001, Bozza et al., 2004, Soucy 2009). This spatial order is presumably used for the generation of innate behaviors (Root et al., 2014). This order however is discarded in the projection to cortex: individual glomeruli send spatially diffuse, apparently random projections across the entire piriform cortex, such that the projection pattern of one glomerulus in piriform cortex is indistinguishable from another (Ghosh et al., 2011, Sosulski et al., 2011). This is reflected in odor-evoked responses in piriform where individual odorants activated sparse, distributed ensembles that have no apparent spatial

order (Poo and Isaacson, 2009, Stettler and Axel, 2009). The disordered odorant representation in piriform likely has no inherent meaning. Instead meaning must be imposed on this representation by learning. We have described a monosynaptic projection from piriform to the basolateral amygdala through which aversive meaning can be imparted on an odorant, thus restoring order to the olfactory world.

Figure 1.

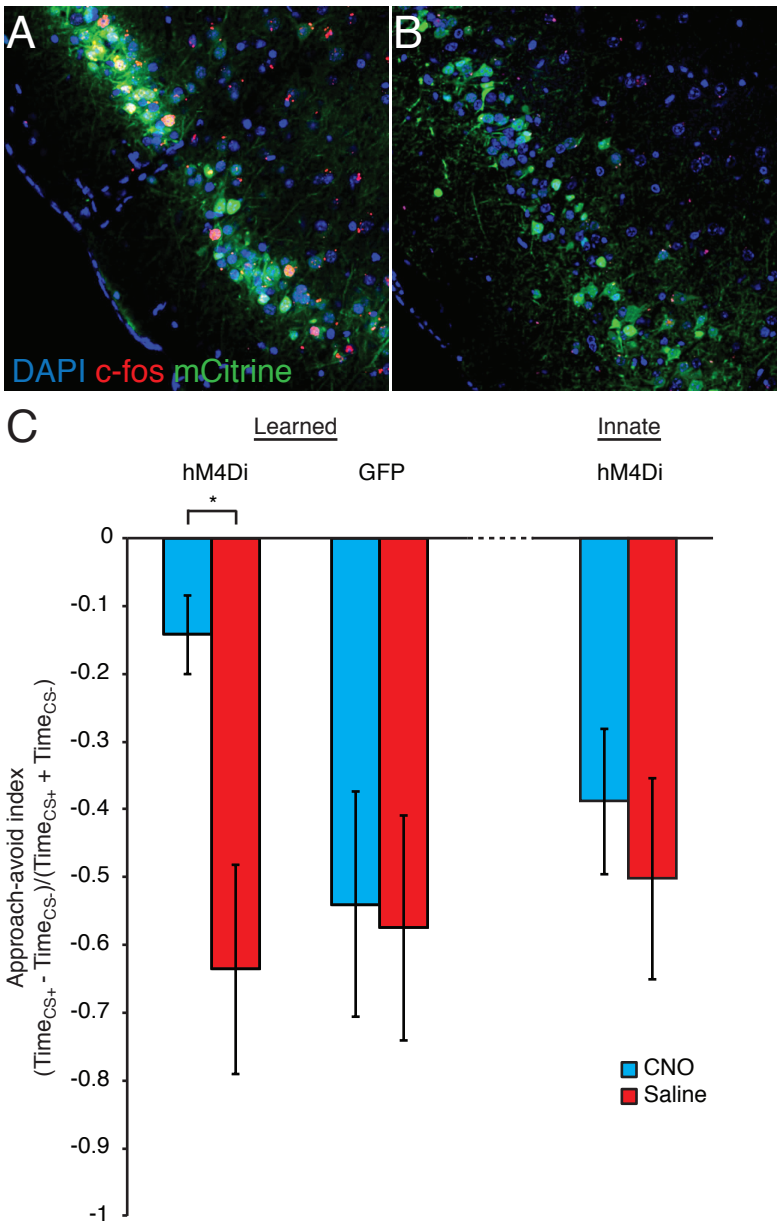
A
B
DAPI c-fos mCitrine
C
Learned
Innate
hM4Di
GFP
hM4Di
*
0
-0.1
-0.2
-0.3
-0.4
-0.5
-0.6
-0.7
-0.8
-0.9
-1
Approach-avoid index
(Time$_{CS+}$ - Time$_{CS-}$)/(Time$_{CS+}$ + Time$_{CS-}$)
CNO
Saline

Figure 1. Activity in posterior piriform cortex is necessary for the expression of learned olfactory fear. A-B. Animals were injected with AAV_5-hSyn-HA-hM4Di-IRES-mCitrine and exposed to acetephenone following CNO (**A**) or saline (**B**) administration before being sacrificed 1 hour later and stained for c-Fos. **C.** Approach-avoid index (difference in time spent in CS+ and CS- compartments of a 3 compartment chamber, divided by the time spent in both compartments) of learned aversive odorant and innately aversive odorant in the presence and absence of chemogenetic inhibition of posterior piriform cortex (learned: hM4Di CNO -0.14±0.05, saline -0.64±0.15, n=7; GFP CNO -0.54±0.17, saline -0.58±0.17, n=4. Innate: hM4Di CNO -0.39±0.11, saline -0.50±0.15, n=5. Two-way ANOVA, main effect of treatment, $F_{1,18}=8.58$, $P<0.001$). All error bars represent ± s.e.m.

Figure 2.

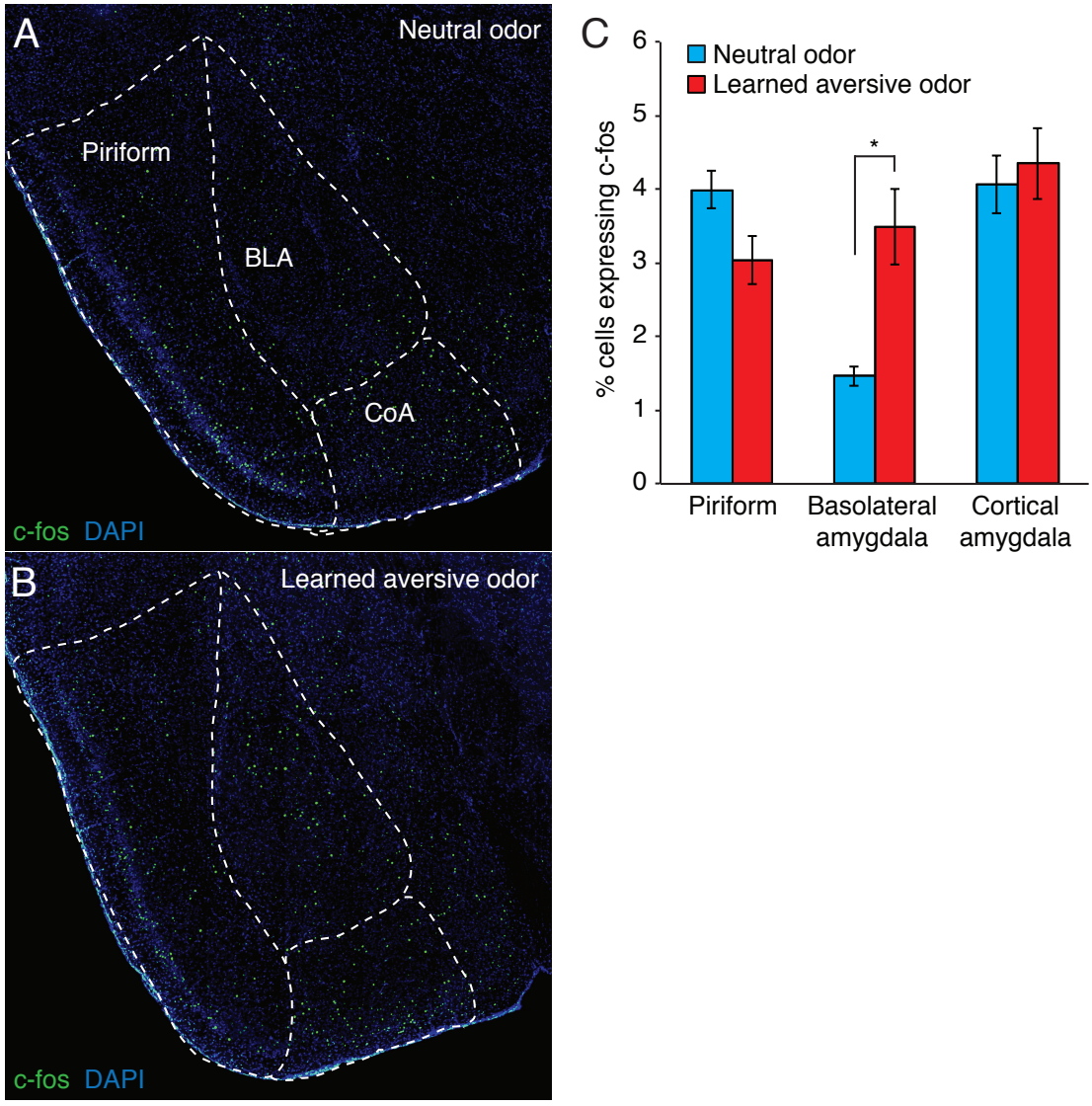
A
Neutral odor
Piriform
BLA
CoA
c-fos DAPI
B
Learned aversive odor
c-fos DAPI
C
Neutral odor
Learned aversive odor
% cells expressing c-fos
0
1
2
3
4
5
6
*
Piriform
Basolateral amygdala
Cortical amygdala

Figure 2. Olfactory fear conditioning increases c-Fos expression in the BLA. A. Animals were exposed to 20 presentations of acetephenone. The following day animals were exposed to 10 minutes of acetephenone (neutral odor) before being sacrificed 1 hour later and stained for c-Fos. **B.** Animals were exposed to 20 presentations of acetephenone all of which coterminated with 2 seconds of footshock. The following day animals were exposed to 10 minutes of acetephenone (learned aversive odor) before being sacrificed 1 hour later and stained for c-Fos. **C.** Percent of cells expressing c-Fos in piriform cortex, the basolateral amygdala, and the cortical amygdala in response to the neutral odor or the learned aversive odor (% cells expressing c-Fos in response to neutral odor: piriform 3.99±0.35%, n=6; BLA 1.46±0.13%, n=6, cortical amygdala 4.07±0.40%, n=6. % cells expressing c-Fos in response to learned aversive odor: piriform 3.04±0.32%, n=6; BLA 3.49±0.51%, n=6; cortical amygdala 4.35±0.48, n=6. Two-way ANOVA, group x area interaction, $F_{2,30}=8.09$, $P<0.005$). All error bars represent ± s.e.m.

Figure 3.

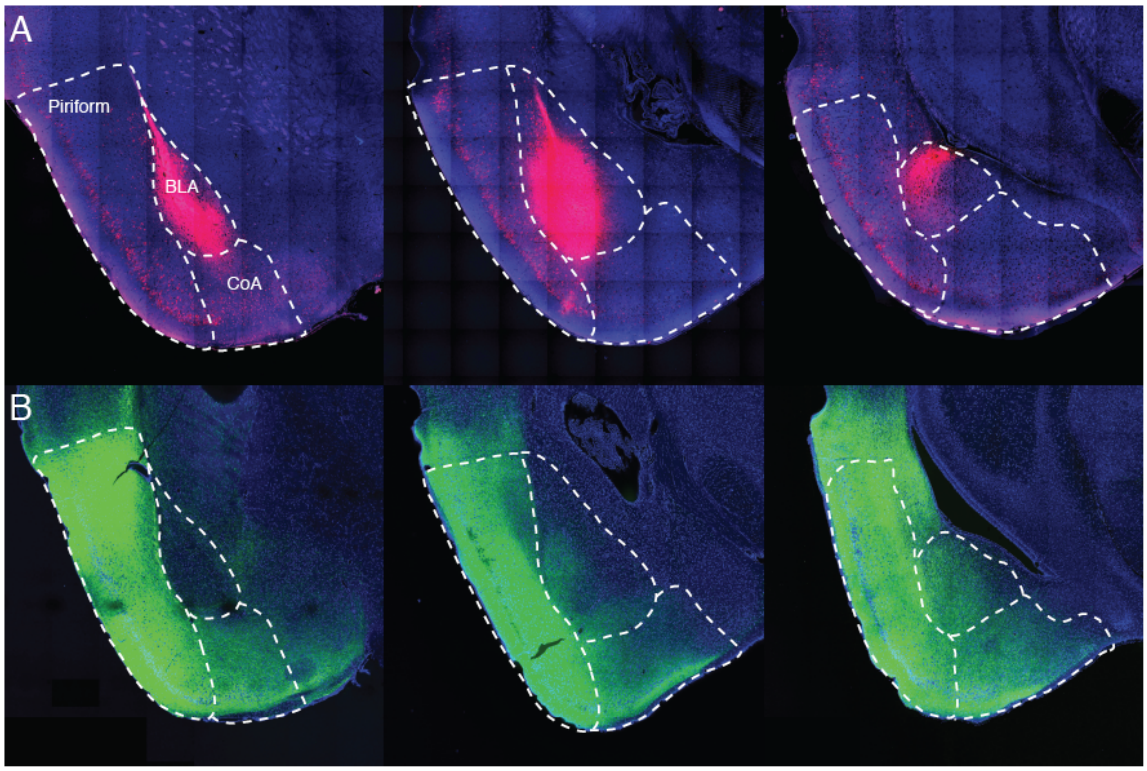

Figure 3. Identification of a monosynaptic projection from posterior piriform cortex to the basolateral amygdala. A. Animals were injected with the retrograde tracer cholera toxin B subunit, which is taken up by axon terminals and retrogradely transported to cell bodies, in the BLA and sacrificed 5 days later. **B.** Animals were injected with AAV-hSyn-NpHR-EYFP, which is taken up by cell bodies and transported to axon terminals, in posterior piriform cortex and sacrificed 3 weeks later.

Figure 4.

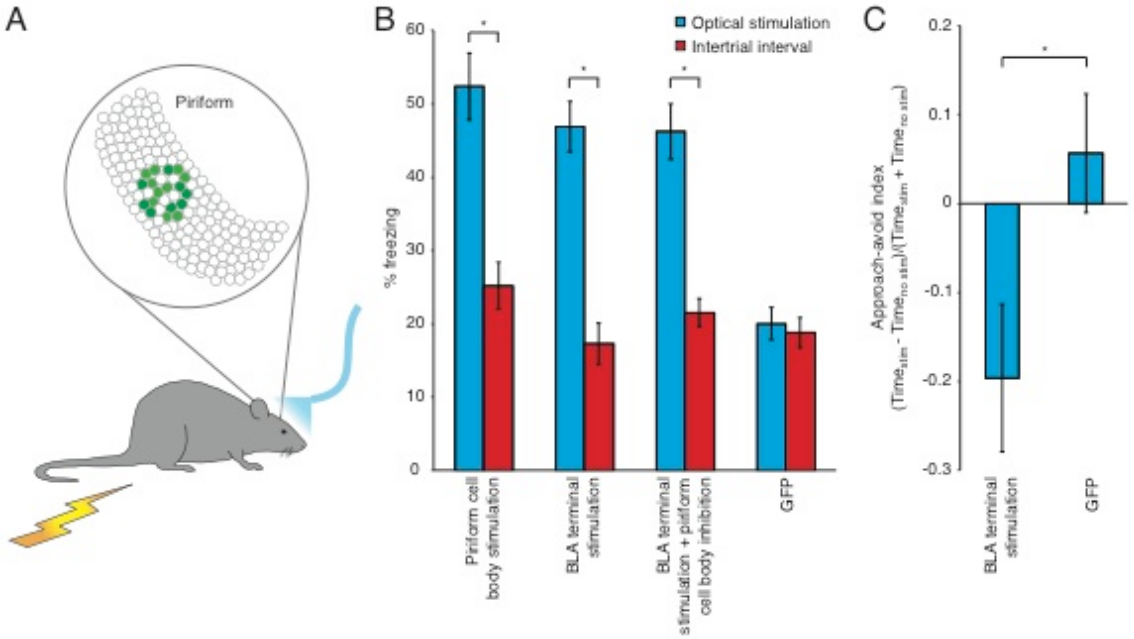
A
Piriform
B
Optical stimulation
Intertrial interval
% freezing
60
50
40
30
20
10
0
Piriform cell body stimulation
BLA terminal stimulation
BLA terminal stimulation + piriform cell body inhibition
GFP
C
Approach-avoid index
(Time_stim - Time_no stim)/(Time_stim + Time_no stim)
0.2
0.1
0
-0.1
-0.2
-0.3
BLA terminal stimulation
GFP

Figure 4. Photoactivation of the projection from posterior piriform cortex to the basolateral amygdala can act as a conditioned stimulus and recall a fear memory. A. Schematic of training process. Briefly, animals were injected with AAV-hsyn-ChR2-EYFP in posterior piriform cortex and trained to associate photoactivation of this ensemble with a footshock. **B.** Percent of time spent freezing in response to optical stimulation compared to the intertrial interval (ITI) (piriform cell body optical stimulation 52.49±4.54%, ITI 25.29±3.18% n=6; BLA terminal optical stimulation 46.99±3.44%, ITI 17.33±2.79 n=6; BLA terminal optical stimulation plus cell body inhibition 46.33±3.83%, ITI 21.63±1.91, n=6; GFP optical stimulation 20.10±2.23%, ITI 18.84±2.06%, n=11. Two-way ANOVA, group × optical stimulation interaction, $F_{3,54}$=6.87, P<0.001). **C.** Approach-avoid index (difference in time spent in "optical stimulation" and "no optical stimulation" of a 3 compartment chamber, divided by the time spent in both compartments) (BLA terminal stimulation -0.20±0.08, n=6, GFP 0.06±0.07, n=11. Student's t-test, P<0.05). All error bars represent ± s.e.m.

Figure 5.

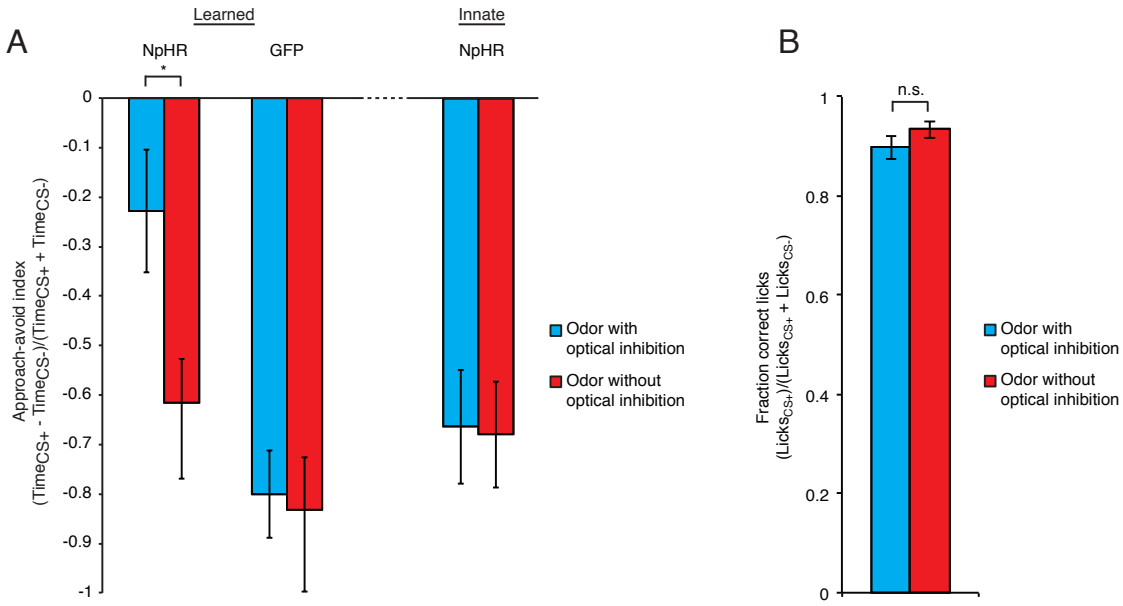
A
Learned
Innate
NpHR
GFP
NpHR
*
0
-0.1
-0.2
-0.3
-0.4
-0.5
-0.6
-0.7
-0.8
-0.9
-1
Approach-avoid index
(TimeCS+ - TimeCS-)/(TimeCS+ + TimeCS-)
Odor with optical inhibition
Odor without optical inhibition
B
n.s.
1
0.8
0.6
0.4
0.2
0
Fraction correct licks
(LicksCS+)/(LicksCS+ + LicksCS-)
Odor with optical inhibition
Odor without optical inhibition

Figure 5. Inhibition of the projection from posterior piriform cortex to the basolateral amygdala impairs the expression of learned olfactory fear. A. Approach-avoid index of a learned aversive odorant and an innately aversive odorant in the presence and absence of optical inhibition of the projection from posterior piriform to the BLA (learned: NpHR with yellow light -0.23±0.12, without yellow light -0.62±0.09, n=7; GFP with yellow light -0.80±0.09, without yellow light -0.83±0.11, n=5. Innate: NpHR with yellow light -0.66±0.12, without yellow light -0.68±0.11, n=4. Two-way ANOVA, group $F_{1,20}$=13.38, P<0.005). **B.** Fraction licks correct ($Licks_{CS+}$)/($Licks_{CS+}$ + $Licks_{CS-}$) for 100 trials in presence and absence of optical inhibition (odor with optical inhibition 0.90±0.02, odor without optical inhibition 0.93±0.02. Student's t-test, P>0.05). All error bars represent ± s.e.m.

CHAPTER 4

SUMMARY AND CONCLUSIONS

For many organisms the sense of smell is critical to survival. Some olfactory stimuli elicit innate responses that are mediated through hardwired circuits that have developed over long periods of evolutionary time. Most olfactory stimuli, however, have no inherent meaning. Instead meaning must be imposed by learning during the lifetime of an organism. Despite the dominance of olfactory stimuli on animal behavior, the mechanisms by which odorants elicit learned behavioral responses remain poorly understood.

All odor-evoked behaviors are initiated by the binding of an odorant to olfactory receptors located on sensory neurons in the nasal epithelium (Buck and Axel, 1991, DeMaria and Ngai, 2010, Hayden and Teeling, 2014). Olfactory sensory neurons transmit this information to the olfactory bulb via stereotyped axonal projections (Mombaerts et al., 1996, Ressler et al., 1994, Vassar et al., 1994) such that individual odorants evoke a stereotyped spatial map of glomerular activity (Belluscio and Katz, 2001, Bozza et al., 2004, Soucy et al., 2009). A subset of bulbar neurons, the mitral and tufted cells, relay olfactory information to higher brain structures that have been implicated in the generation of innate and learned behavioral responses (Choi et al., 2011, Ghosh et al., 2011, Miyamichi et al., 2011, Root et al., 2014, Sosulski et al., 2011, Shepherd, 1994).

Anatomical studies have demonstrated that the spatial stereotypy of the olfactory bulb is maintained in projections to the posterolateral cortical amygdala (Sosulski et al.,

2011), and behavioral studies have demonstrated that this projection is necessary for the generation of innate odor-evoked responses (Root et al., 2014).

The projections of mitral and tufted cells to piriform cortex however appear to discard the order of the olfactory bulb: each glomerulus sends spatially diffuse, apparently random projections across the entire cortex (Ghosh et al., 2011, Sosulski et al., 2011). This anatomy appears to constrain odor-evoked responses in piriform cortex: electrophysiological and imaging studies demonstrate that individual odorants activate sparse ensembles that are distributed across the extent of cortex, and individual piriform neurons exhibit discontinuous receptive fields such that they respond to structurally and perceptually similar and dissimilar odorants (Illig and Haberly, 2003, Poo and Isaacson, 2009, Rennaker et al., 2007, Stettler and Axel, 2009). It is therefore unlikely that olfactory representations in piriform have inherent meaning. Instead, these representations have been proposed to mediate olfactory learning.

In accord with a role for piriform cortex in associative learning, photoactivation of a random ensemble of piriform neurons can become entrained to both appetitive and aversive outcomes (Choi et al., 2011). In addition, lesions of posterior piriform cortex prevent the expression of a previously acquired olfactory fear memory (Sacco and Sacchetti, 2010) Olfactory representations in piriform cortex have therefore been implicated in the generation of learned responses; however how meaning is imparted on disordered olfactory representations in piriform remains largely unknown.

We developed a strategy to manipulate the neural activity of representations of conditioned and unconditioned stimuli in the basolateral amygdala, a downstream target of piriform cortex that has been implicated in the generation of learned olfactory

responses (Cousens and Otto, 1998, Rosenkranz and Grace, 2002, Rosenkranz et al., 2003). This strategy allowed us to demonstrate that distinct neural ensembles represent an appetitive and an aversive unconditioned stimulus in the BLA. Moreover, the activity of these representations can elicit innate responses as well as direct Pavlovian and instrumental learning. Finally activity of an aversive US representation in the basolateral amygdala is required for learned olfactory and auditory fear responses. These data suggest that both olfactory and auditory stimuli converge on US representations in the BLA to generate learned behavioral responses. Having identified a US representation in the BLA that receives convergent olfactory information to generate learned fear responses, we were then able to step back into the olfactory system and demonstrate that the BLA receives olfactory input via the monosynaptic projection from piriform cortex. These data suggest that aversive meaning is imparted on an olfactory representation in piriform cortex via reinforcement of its projections onto a US representation in the BLA.

One model in accord with these data suggests the existence of an unconditioned stimulus representation in the basolateral amygdala that is capable of generating innate defensive responses (Figure 1). Olfactory representations in piriform cortex send weak projections to the US representation in the BLA such that presentation of an odor is insufficient to elicit postsynaptic activity in the US ensemble. Temporal pairing of an odor with an unconditioned stimulus results in Hebbian potentiation of piriform inputs to the US representation such that subsequent presentations of the odor activates the US ensemble to generate learned defensive responses. In this model reinforcement of the projections of a specific odorant representation in piriform onto the US representation in

the BLA imparts aversive meaning exclusively onto the trained odorant, thus affording the discriminative abilities that are observed in the animal kingdom.

This model assumes axon terminals of an odor representation in piriform cortex directly synapse onto a US representation in the BLA. In this model, a high dimensional representation of an odorant in piriform is reduced into a low dimensional representation of valence at the synapse onto a US representation in the BLA. However our data cannot preclude the possibility that piriform projections to the BLA establish an olfactory representation in the BLA that is unique for each odorant and potentiation of projections of this BLA olfactory representation onto the US ensemble mediates fear learning. This would suggest that the BLA encodes odor identity, in addition to its learned valence. Determining the extent of olfactory information encoding in the BLA would require observing odor-evoked activity in large populations of BLA neurons in response to many odorants. Future studies are therefore aimed at conducting calcium imaging of odor-evoked responses in the BLA of awake mice to determine the extent to which olfactory representation is encoded in the BLA.

This notwithstanding, our data suggest that aversive meaning is imparted on a disordered representation of odor in piriform cortex via reinforcement of piriform projections to the BLA. A similar strategy of fear learning may be implemented by the hippocampus, a 3-layered paleocortex similar to piriform cortex, to mediate contextual fear conditioning. Contexts are encoded by the activity of distributed ensembles of place cells in the hippocampus. These ensembles lack any apparent spatial order such that the anatomical location of individual place cells has no apparent relationship to its receptive field in the external world (O'Keefe et al., 1998, Redish et al., 2001). Moreover,

connectivity between representations of context in the hippocampus and representations of footshock in the BLA has been implicated in the generation of learned behavioral responses (Redondo et al., 2014). Thus reinforcement of sensory projections to the BLA might provide a generalized model by which meaning is imposed on disordered representations of the external world.

Our data suggest that aversive meaning is imparted on an odorant representation in piriform by reinforcement of its projections to an aversive US representation in the BLA. However, odorants can become associated with both rewards and punishments, and prior work has demonstrated that piriform ensembles can become entrained to both appetitive and aversive outcomes. The downstream circuitry that mediates appetitive conditioning has not been fully elucidated. We have demonstrated that photoactivation of nicotine-responsive cells in the BLA can reinforce olfactory conditioning, however the necessity for this representation has not been demonstrated. Moreover, pharmacological inactivation studies indicate that the BLA is not necessary for the formation of simple CS-appetitive US associations in other sensory modalities (Hatfield et al., 1996 and Holland, 1997). Finally, we demonstrate that activity of the piriform to BLA projection is not required for an appetitive discrimination task. These data suggest that distinct piriform targets might mediate appetitive learning. It is currently unclear whether all piriform neurons project to both appetitive and aversive downstream structures. There appears to be no spatial bias in the ability of piriform ensembles to generate learned responses of different valence (Choi et al., 2011), however it remains possible that different subpopulations of piriform neurons target appetitive or aversive circuitry exclusively. The use of optogenetic techniques to selectively manipulate the outputs of

odorant representations in piriform cortex therefore promises to advance the understanding of appetitive olfactory learning.

We have demonstrated that associative fear learning results in a previously neutral stimulus eliciting behavioral responses through the activity of US representations in the BLA. However, learning has also been reported to modulate the sensory perception of a conditioned stimulus. Indeed, olfactory fear conditioning reduces the threshold for detection of a conditioned stimulus and improves discriminability (Li et al., 2008). Fear learning increases the size of the representation of a conditioned odor in the olfactory bulb, and narrows the receptive fields of neurons in piriform cortex (Chen et al., 2011, Dias and Ressler, 2014, Funk and Amir, 2000, Jones et al., 2008, Kass et al., 2013, Li et al., 2008, Morrison et al., 2015, Sevelinges et al., 2004). This plasticity might facilitate the detection and discrimination of biologically significant odorants. However how plasticity in either piriform or the olfactory bulb arises is unclear. Piriform receives reciprocal input from the BLA (McDonald, 1998, Sah et al., 2003) and plasticity in the basolateral amygdala precedes that observed in piriform cortex (Hegoburu et al., 2009). Finally, amygdala-cortical connectivity has previously been shown to modulate cortical activity (Chavez et al., 2013, Garcia et al., 1999). Understanding how representations of learned aversive odorants in the BLA might modulate primary sensory representations could therefore provide insight into the mechanisms that enhance the perception of biologically significant stimuli.

The mouse olfactory system is characterized by a series of transformations. Odorants are detected by randomly distributed receptors located on sensory neurons in the nasal epithelium. Order is imparted on this system via the convergence of neurons

expressing like receptors on 2 spatially invariant glomeruli in the olfactory bulb such that each odorant evokes a stereotyped spatial map of glomerular activity. This spatial map is presumably used for the generation of innate responses. The order of the olfactory bulb is discarded in the projection to piriform cortex, such that every odorant is represented by a unique, apparently random ensemble of neurons distributed across the extent of cortex. We have used a combination of molecular and behavioral techniques to elucidate how order is restored to this system. We have identified a projection from piriform cortex to representations of unconditioned stimuli in the basolateral amygdala that imparts aversive meaning on an odorant, thus restoring order to the olfactory world. The simplicity of the olfactory system in concert with its complex behavioral repertoire makes it an invaluable model system for understanding how animals learn to associate sensory stimuli with specific outcomes and events. Continued investigation of its function will impact tremendously on our understanding of the neural origins of motivated behavior.

Figure 1.

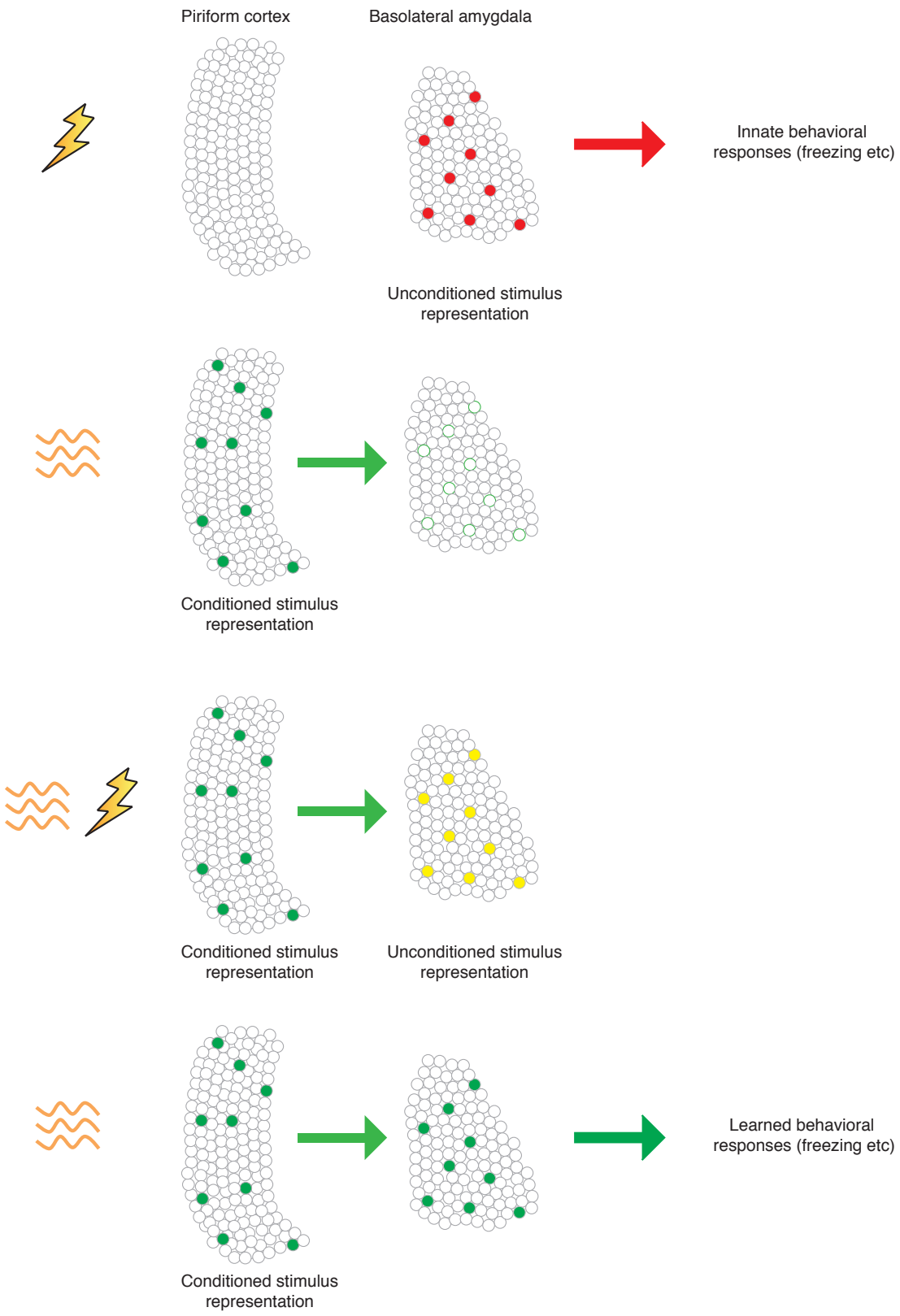
Piriform cortex
Basolateral amygdala
Innate behavioral responses (freezing etc)
Unconditioned stimulus representation
Conditioned stimulus representation
Conditioned stimulus representation
Unconditioned stimulus representation
Conditioned stimulus representation
Learned behavioral responses (freezing etc)

Figure 1. Model of olfactory fear learning. An unconditioned stimulus representation exists in the basolateral amygdala that is capable of generating innate defensive responses. Olfactory representations in piriform cortex send weak projections to this US representation such that presentation of an odor is insufficient to elicit postsynaptic activity in the US ensemble. Temporal pairing of an odor with an unconditioned stimulus results in Hebbian potentiation of piriform inputs to the US representation such that subsequent presentations of the odor activates the US ensemble to generate learned defensive responses.

REFERENCES

Afraz, S.R., Kiani, R. and Esteky, H. (2006). Microstimulation of inferotemporal cortex influences face categorization. Nature *442*, 692-695.

Amano, T., Duvarci, S., Popa, D., and Paré, D. (2011). The fear circuit revisited: contributions of the basal amygdala nuclei to conditioned fear. J Neurosci *31*, 15481-15489.

Amaral, D., Price, J., Pitkanen, A., and Carmichael, S. (1992). In The Amygdala: Neurobiological Aspects of Emotion, Memory, and Mental Dysfunction, J. Aggleton, ed. (Wiley-Liss, New York), pp. 1-66.

Ambroggi, F., Ishikawa, A., Fields, H. L., and Nicola, S. M. (2008). Basolateral amygdala neurons facilitate reward-seeking behavior by exciting nucleus accumbens neurons. Neuron *59*, 648-661.

Anglada-Figueroa, D., and Quirk, G.J. (2005). Lesions of the basal amygdala block expression of conditioned fear but not extinction. J Neurosci *25*, 9680-9685.

Apicella, A., Yuan, Q., Scanziani, M. and Isaacson, J.S. (2010). Pyramidal cells in piriform cortex receive convergent input from distinct olfactory bulb glomeruli. J Neurosci *30*, 14255-14260.

Balderston, N.L., Schultz, D.H. and Helmstetter, F.J. (2011). The human amygdala plays a stimulus specific role in the detection of novelty. Neuroimage *55*, 1889-1898.

Balleine, B. W., and Killcross, S. (2006). Parallel incentive processing: an integrated view of amygdala function. Trends Neurosci *29*, 272-279.

Barot, S. K., Yasuhiro, K., Clark, E. W. and Bernstein, I. L. (2008). Visualizing stimulus convergence in amygdala neurons during associative learning. Proc Natl Acad Sci USA *105*, 20959-20963.

Bartel, D.P., Sheng, M. Lau, L.F. and Greenberg, M.E. (1989). Growth factors and membrane depolarization activate distinct programs of early response gene expression: dissociation of fos and jun induction. Genes Dev *3*, 304-313.

Bito, H., Deisseroth, K. and Tsien, R.W. (1996). CREB phosphorylation and dephosphorylation: a Ca(2+)- and stimulus duration-dependent switch for hippocampal gene expression. Cell *87*, 1203-1214.

Belkin, D.A. (1968). Bradycardia in response to threat. American Zoologist *8*, 775.

Belluscio, L. and Katz, L.C. (2001). Symmetry, stereotypy and topography of odorant representations in mouse olfactory bulbs. J Neurosci *6*, 2113-2122.

Belova, M.A., Paton, J.J., Morrison, S.E., and Salzman, C.D. (2007). Expectation modulates neural responses to pleasant and aversive stimuli in primate amygdala. Neuron *55*, 970-984.

Belova, M.A., Paton, J.J., and Salzman, C.D. (2008). Moment-to-moment tracking of state value in the amygdala. J Neurosci *28*, 10023-10030.

Berlucchi, G. (2010). The contributions of neurophysiology to clinical neurology an exercise in contemporary history. Handb Clin Neurol *95*, 169-188.

Bermudez, M.A., and Schultz, W. (2010). Reward magnitude coding in primate amygdala neurons. J Neurophysiol *104*, 3424-3432.

Blundell, P., Hall, G., and Killcross, S. (2001). Lesions of the basolateral amygdala disrupt selective aspects of reinforce representation in rats. J Neurosci *21*, 9018-9026.

Bozza, T., McGann, J.P., Mombaerts, P. and Wachowiak, M. (2004). In vivo imaging of neuronal activity by targeted expression of a genetically encoded probe in the mouse. Neuron *42*, 9-21.

Brindley, G.S. and Lewin, W.S. (1968). The sensations produced by electrical stimulation of the visual cortex. J Physiol *196*, 479-493.

Britten, K.H. and van Wezel, R.J. (1998). Electrical microstimulation of cortical area MST biases heading perception in monkeys. Nat Neurosci *1*, 59-63.

Buck, L. and Axel, R. (1991). A novel multigene family may encode odorant reecptors: a molecular basis for odor recognition. Cell *65*, 175-187.

Cahill, L. and McGaugh, J.L. (1990). Amygdaloid complex lesions differentially affect retention of tasks using appetitive and aversive reinforcement. Behav Neurosci *104,* 532-543.

Cain, D.P. and Bindra, D. (1972). Responses of amygdala single units to odors in the rat. Exp Neurol *1*, 98-110.

Cajal, S.R. (1909). Histologie du systeme nerveux de l'homme et des vertebres. A. Maloine, Paris.

Calu, D.L., Roesch, M.R., Stalnaker, T.A. and Schoenbaum, G. (2007). Associative encoding in posterior piriform cortex during odor discrimination and reversal learning. Cereb Cortex *17*, 1342-1349.

Campeau, S. and Davis, M. (1995) Involvement of the central nucleus and basolateral complex of the amygdala in fear conditioning measured with fear-potentiated startle in rats trained concurrently with auditory and visual conditioned stimuli. J Neurosci *15*, 2301-2311.

Cardinal, R.N., Parkinson, J.A., Hall, J., and Everitt, B.J. (2002). Emotion and motivation: the role of the amygdala, ventral striatum, and prefrontal cortex. Neurosci Biobehav Rev *26*, 321-352.

Celebrini, S. and Newsome, W.T. (1995). Microstimulation of extrastriate area MST influences performance on a direction discrimination task. J Neurophysiol *73*, 437-448.

Chavez, C.M., McGaugh, J.L. and Weinberger, N.M. (2013). Activation of the basolateral amygdala induces long-term enhancements of memory representations in the cerebral cortex. Neurobiol Learn Mem *101*, 8-18.

Chen, C.F., Barnes, D.C. and Wilson, D.A. (2011). Generalizaed vs. stimulus-specific learned fear differentially modifies stimulus encoding in primary sensory cortex of awake rats. J Neurophysiol *106*, 3136-3144.

Chess, A., Simon, I., Cedar, H. and Axel, R. (1994). Allelic inactivation regulates olfactory receptor gene expression. Cell *78*, 823-834.

Choi, G.B., Stettler, D.D., Kallman, B.R., Bhaskar, S.T., Fleischmann, A. and Axel, R. (2011). Driving opposing behaviors with ensembles of piriform neurons. Cell *146*, 1004-1015.

Cicmil, N and Krug, K. (2015). Playing the electric light orchestra – how electrical stimulation of visual cortex elucidates the neural basis of perception. Philos Trans R Soc Lond B Biol Sci *370*, 20140206.

Clark, K.L., Armstrong, K.M. and Moore, T. (2011). Probing neural circuitry and function with electrical microstimulation. Proc Biol Sci *278*, 1121-1130.

Clowney, E.J., Magklara, A., Colquitt, B.M., Pathak, N., Lane, R.P. and Lomvardas, S. (2011). High-throughput mapping of the promoters of the mouse olfactory receptor genes reveals a new type of mammalian promoter and provides insight into olfactory receptor gene regulation. Genome Res *21*, 1249-1259.

Cohen, M.R. and Newsome, W.T. (2004). What electrical microstimulation has revealed about the neural basis of cognition. Curr Opin Neurobiol *14*, 169-177.

Corbit, L.H., and Balleine, B.W. (2005). Double dissociation of basolateral and central amygdala lesions on the general and outcome-specific forms of pavlovian-instrumental transfer. J Neurosci *25*, 962-970.

Cousens, G. and Otto, T. (1998). Both pre- and posttraining excitotoxic lesions of the basolateral amygdala abolish the expression of olfactory and contextual fear conditioning. Behav Neurosci *112*, 1092-1103.

Cruikshank, S.J., Edeline, J.M. and Weinberger, N.M. (1992). Stimulation at a site of auditory-somatosensory convergence in the medial geniculate nucleus is an effective unconditioned stimulus for fear conditioning. Behav Neurosci *106*, 471-183.

Cruz, F.C., Koya, E., Guez-Barber, D.H., Bossert, J.M., Lupica, C.R., Shaham, Y. and Hope, B.T. (2013). New technologies for examining the role of neuronal ensembles in drug addiction and fear. Nat Rev Neurosci *14*, 743-754.

Dalton, R.P. and Lomvardas, S. (2015). Chemosensory receptor specificity and regulation. Annu Rev Neurosci *38*, 331-349.

Davis, M. (1998). Anatomic and physiologic substrates of emotion in an animal model. J Clin Neurophysiol *15*, 378-387.

Davison, I. G. and Ehlers, M.D. (2011). Neural circuit mechanisms for pattern detection and feature combination in olfactory cortex. Neuron *70*, 82-94.

DeMaria, S. and Ngai, J. (2010). The cell biology of smell. J Cell Biol *3*, 443-452.
Hayden, S. and Teeling, E.C. (2014). The molecular biology of vertebrate olfaction. Anat Rec *297*, 2216-2226.

Dias, B.G. and Ressler, K.J. (2014). Parental olfactory experience influences behavior and neural structure in subsequent generations. Nat Neursci *17*, 89-96.

Doron, G. and Brecht, M. (2015). What single cell stimulation has told us about neural coding. Philos Trans R Soc Lond B Biol Sci *370*, 20140204.

Everitt, B. J., Cardinal, R. N., Parkinson, J. A., and Robbins, T. W. (2003). Appetitive behavior: impact of amygdala-dependent mechanisms of emotional learning. Ann N Y Acad Sci *985*, 233-250.

Fanselow, M. S. (1980). Conditional and unconditional components of post-shock freezing. Pav J Bio Sci *15*, 177-182.

Feinstein, P., Bozza, T., Rodriguez, I., Vassalli, A. and Mobaerts, P. (2004). Axon guidance of mouse olfactory sensory neurons by odorant receptors and the beta2 adrenergic receptor. Cell *117*, 833-846.

Felix-Ortiz, A.C., Beyeler, A., Seo, C., Leppla, C.A., Wildes, C.P., and Tye., K.M. (2013). BLA to vHPC inputs modulate anxiety-related behaviors. Neuron *79*, 658-664.

Felix-Ortiz, A.C., Burgos-Robles, A., Bhagat, N.D., Leppla, C.A. and Tye, K.M. (2015). Bidirectional modulation of anxiety-related and social behaviors by amygdala projections to the medial prefrontal cortex. Neuroscience *S0306-4522*, 655-657.

Felix-Ortiz, A.C. and Tye, K.M. (2014). Amygdala inputs to the ventral hippocampus bidirectionally modulate social behavior. J Neurosci *34*, 586-595.

Fendt, M., and Fanselow, M.S. (1999). The neuroanatomical and neurochemical basis of conditioned fear. Neurosci Biobehav Rev *23*, 743-760.

Franks, K.M., Russo, M.J., Sosulski, D.L., Mulligan, A.A., Siegelbaum, S.A. and Axel, R. (2011). Recurrent circuitry dynamically shapes the activation of piriform cortex. Neuron *72*, 49-56.

Funk, D. and Amir, S. (2000). Enhanced fos expression within the primary olfactory and limbic pathways induced by an aversive conditioned odor stimulus. Neuroscience *98*, 403-406.

Gallagher, M., and Holland, P.C. (1994). The amygdala complex: multiple roles in associative learning and attention. Proc Natl Acad Sci USA *91*, 11771-11776.

Gallo, M., Roldan, G. and Bures, J. (1992). Differential involvement of gustatory insular cortex and amygdala in the acquisition and retrieval of conditioned taste aversion in rats. Behav Brain Res *52*, 91-97.

Garcia, R., Vouimba, R.M., Baudry, M. and Thompson, R.F. (1999). The amygdala modulates prefrontal cortex activity relative to conditioned fear. Nature *402*, 294-296.

Ghosh, S., Larson, S.D., Hefzi, H., Marnoy, Z., Cutforth, T., Dokka, K. and Baldwin, K.K. (2011). Sensory maps in the olfactory cortex defined by long-range viral tracing of single neurons. Nature *472*, 217-220.

Gore, F., Schwartz, E.C., Brangers, B.C., Aladi, S., Stujenske, J.M., Likhtik, E., Russo, M.J., Gordon, J.A., Salzman, C.D. and Axel, R. (2015a). Neural representations of unconditioned stimuli in the basolateral amygdala mediate innate and learned responses. Cell, *162*, 1-12.

Gore, F., Schwartz, E.C. and Salzman, C.D. (2015b). Manipulating neural activity in physiologically classified neurons: triumphs and challenges. Philos Trans R Soc Lond B Biol Sci *370*, 20140216.

Graziano, M. (2006). The organization of behavioral repertoire in motor cortex. Annu Rev Neurosci *29*, 105-134.

Greenberg, M.E. and Ziff, E.B. (1984). Stimulation of 3T3 cells induces transcription of c-fos proto-oncogene. Nature *311,* 433-438

Gschwend, O., Abraham, N.M., Lagier, S., Begnaud, F., Rodriguez, I. and Carleton, A. (2015). Neuronal pattern separation in the olfactory bulb improves odor discrimination learning. Nat Neurosci *18*, 1474-1482.

Gu, Y., DeAngelis, G.C. and Angelaki, D.E. (2012). Causal links between dorsal medial superior temporal area neurons and multisensory heading perception. J Neurosci *32*, 2299-2313.

Guzowski, J.F. and Worley, P.F. (2001). Cellular compartment analysis of temporal activity by fluorescence in situ hybridization (catFISH). Curr Protoc Neurosci Chapter 1: Unit 1.8. (doi: 10.1002/0471142301.ns0108s15)

Haberly, L.B. and Price, J.L. (1977). The axonal projection patterns of the mitral and tufted cells of the olfactory bulb in the rat. Brain Res *129*, 152-157.

Han, J.H., Kushner, S.A., Yiu, A.P., Hsiang, H.L., Buch, T., Waisman, A., Bontempi, B., Neve, R.L., Frankland, P.W. and Josselyn, S.A. (2009). Selective erasure of a fear memory. Science *323*, 1492-1496.

Han, J.H., Kushner, S.A., Yiu, A.P., Cole, C.J., Matynia, A., Brown, R.A., Neve, R.L., Guzowski, J.F., Silva, A.J. and Josselyn, S.A. (2007). Neuronal competition and selection during memory formation. Science *316*, 457-460.

Hanks, T.D., Ditterich, J. and Shadlen, M.N. (2006). Microstimulation of macaque area LIP affects decision-making in a motion discrimination task. Nat Neurosci *9*, 682-689.

Hatfield, T., Hans, J.S., Conley, M., Gallagher, M., and Holland, P. (1996). Neurotoxic lesions of the basolateral, but not central, amygdala interfere with Pavlovian second-order conditioning and reinforce devaluation effects. J Neurosci *16*, 5256-5265.

Hegoburu, C., Sevelinges, Y., Thévenet, M., Gervais, R., Parrot, S. and Mouly, A.M. (2009). Differential dynamics of amino acid release in the amygdala and olfactory cortex during fear acquisition as revealed with simultaneous high temporal resolution microdialysis.. Learn Mem *16*, 687-697.

Herry, C., Ciocchi, S., Senn, V., Demmou, L., Müller, C., Lüthi, A. (2008). Swtiching on and off fear by distinct neural circuits. Nature *454*, 600-606.

Histed, M.H., Ni, A.M. and Maunsell, J.H. (2013). Insights into cortical mechanisms of behavior from microstimulation experiments. *Prog Neurobiol 103*, 115-130.

Holland, P.C. (1997). Brain mechanisms for changes in processing of conditioned stimuli in Pavlovian conditioning: implications for behavior theory. Anim Learn Behav *25*, 373-399.

Holland, P.C. (1990). Event representation in Pavlovian conditioning: image and action. Cognition *37*, 105-131.

Hsiang, H.L., Epp, J.R., van den Oever, M.C., Yan, C., Rashid, A.J., Insel, N., Ye, L., Deisseroth, K., Frankland, P.W. and Josselyn, S.A. (2014). Manipulating a "cocaine engram" in mice. J Neurosci *34*, 14115-14127.

Hubel, D.H. and Weisel, T.N. (1959). Receptive fields of single neurones in the cat's striate cortex. J Physiol *148*, 574-591.

Illig, K.R., and Haberly, L.B. (2003). Odor-evoked activity is spatially distributed in piriform cortex. J Comp Neurol *457*, 361-373.

Janak, P.H., and Tye, K.M. (2015). From circuits to behaviour in the amygdala. Nature *517*, 284-292.

Jarrel, T.W., Gentile, C.G., Romanski, L.M., McCabe, P.M. and Schneiderman, N. (1987). Involvement of cortical and thalamic auditory regions in retention of differential bradycardiac conditioning to acoustic stimuli in rabbits. Brain Res *412*, 285-294.

Johansen, J. P., Cain, C. K., Ostroff, L. E. and LeDoux, J. E. (2011). Molecular mechanisms of fear learning and memory. Cell *147*, 509-524.

Johansen, J.P., Hamanaka, H., Monfils, M.H., Behnia, R., Deisseroth, K., Blair, H.T., and LeDoux, J.E. (2010). Optical activation of lateral amygdala pyramidal cells instructs associative fear learning. Proc Natl Acad Sci USA *107*, 12692-12697.

Johansen, J.P., Tarpley, J.W., LeDoux, J.E. and Blair, H.T. (2010). Neural substrates for expectation-modulated fear learning in the amygdala and periaqueductal gray. Nat Neurosci *13*, 979-986.

Jones, S.V., Choi, D.C., Davis, M. and Ressler, K.J. (2008). Learning-dependent structural plasticity in the adult olfactory pathway. J Neurosci *28*, 13106-13111.

Kass, M.D., Rosenthal, M.C., Pottackal, J. and McGann, J.P. (2013). Fear learning enhances neural responses to threat-predictive sensory stimuli. Science *342*, 1389-1392.

Kawashima, T., Okuno, H. and Bito, H. (2014). A new era for functional labeling of neurons: activity-dependent promoters have come of age. Front Neural Circuits *8*, 37.

Kikuta, S., Fletcher, M.L., Homma, R., Yamasoba, T. and Nagayama, S. (2013). Odorant response properties of individual neurons in an olfactory glomerular module. Neuron *77*, 1122-1135.

Kilpatrick, L. and Cahill, L. (2003). Modulation of memory consolidation for olfactory learning by reversible inactivation of the basolateral amygdala. Behav Neurosci *117*, 184-188.

Kim, S.Y., Adhikari, A., Lee, S.Y., Marshel, J.H., Kim, C.K., Mallory, C.S., Lo, M., Pak, S., Mattis, J., Lim, B.K., et al. (2013). Diverging neural pathways assemble a behavioral state from separable features in anxiety. Nature *496*, 219-223.

Kim, J., Kwon, J.T., Kim, H.S., Josselyn, S.A. and Han, J.H. (2014). Memory recall and modifications by activating neurons with elevated CREB. Nat Neurosci *17*, 65-72.

Kim, D., Paré, D., Nair, S.S. (2013). Assignment of model amygdala neurons to the fear memory trace depends on competitive synaptic interactions. J Neurosci *33*, 14343-14358.

Knapska, E., Radwanska, K., Werka, T., and Kaczmarek, L. (2007). Functional internal complexity of amygdala: focus on gene activity mapping after behavioral training and drugs of abuse. Physiol Rev *87*, 1113-1173.

Kobayakawa, K., Kobayakawa, R., Matsumoto, H., Oka, Y., Imai, T., Okabe, M., Ikeda, T., Itohara, S., Kikusui, T., Mori, K. and Sakano, H. (2007). Innate versus learned odour processing in the mouse olfactory bulb. Nature *450*, 503-508.

Lanuza, E., Nader, K. and LeDoux, J.E. (2004). Unconditioned stimulus pathways to the amygdala: effects of posterior thalamic and cortical lesions of fear conditioning. Neuroscience *125*, 305-315.

Lanuza, E., Moncho Bogani, J. and LeDoux, J.E. (2008). Unconditioned stimulus pathways to the amygdala: effects of lesions of the posterior intralaminar thalamus on foot-shock-induced c-Fos expression in the subdivisions of the lateral amygdala. Neuroscience *155*, 959-968.

Lang, P.J., and Davis, M. (2006). Emotion, motivation, and the brain: reflex foundations in animals and human research. Prog Brain Res *156*, 3-29.

Laviolette, S.R. and Grace, A.A. (2006). Cannabinoids potentiate emotional learning plasticity in neurons of the medial prefrontal cortex through basolateral amygdala inputs. J Neurosci *26*, 6458-6468.

LeDoux, J. E. (2000). Emotion circuits in the brain. Annu Rev Neurosci *23*, 155-184.

Lee, H.W., Hong, S.B., Seo, D.W., Tae, W.S. and Hong, S.C. (2000). Mapping of functional organization in human visual cortex: electrical cortical stimulation. Neurology *54*, 849-854.

Lewcock, J.W. and Reed, R.R. (2004). A feedback mechanism regulates monoallelic odorant receptor expression. Proc Natl Acad Sci USA *4*, 1069-1074.

Li, W., Howard, J.D., Parrish, T.B. and Gottfried, J.A. (2008). Aversive learning enhances perceptual and cortical discrimination of indiscriminable odor cues. Science *319*, 1842-1845.

Lin, D., Boyle, M.P., Dollar, P., Lee, H., Lein, E.S., Perona, P., and Anderson, D.J. (2011). Functional identification of an aggression locus in the mouse hypothalamus. Nature *470*, 221-226.

Lin, da Y., Shea, S.D. and Katz, L.C. (2006). Representation of natural stimuli in the rodent main olfactory bulb. Neuron *50*, 937-949.

Liu, X., Ramirez, S. and Tonegawa, S. (2013). Inception of a false memory by optogenetic manipulation of a hippocampal memory engram. Philos Trans R Soc Lond B Biol Sci *369*, 20130242.

Livneh, U., and Paz, R. (2012). Aversive-bias and stage-selectivity in neurons of the primate amygdala during acquisition, extinction, and overnight retention. J Neurosci *32*, 8592-8610.

London, B.M., Jordan, L.R., Jackson, C.R. and Miller, L.E. (2008). Electrical stimulation of the proprioceptive cortex (area 3a) used to instruct a behaving monkey. IEEE Trans Neural Syst Rehabil Eng *16*, 32-36.

Luskin, M.B., and Price, J.L. (1983). The topographic organization of associational fibers of the olfactory system in the rat, including centrifugal fibers to the olfactory bulb. J Comp Neurol *216*, 264-291.

Malnic, B., Hirono, J., Sato, T. and Buck, L.B. (1999). Combinatorial receptor codes for odors. Cell *96*, 713-723.

Maren, S., and Quirk, G.J. (2004). Neuronal signaling of fear memory. Nat Rev Neurosci *5*, 844-852.

Maren, S., Yap, S.A., and Goosens, K.A. (2001). The amygdala is essential for the development of neuronal plasticity in the medial geniculate nucleus during auditory fear conditioning in rats. J Neurosci *21*, RC135.

Markenscoff-Papadimitriou, E., Allen, W.E., Colquitt, B.M., Goh, T., Murphy, K.K., Monahan, K., Mosley, C.P., Ahituv, N. and Lomvardas, S. (2014). Enhancer interaction networks as a means for singular olfactory receptor expression. Cell *159*, 543-557.

Marr, D. (1971). Simple memory: a theory for archicortex. Philos Trans R Soc Lond B Biol Sci *841*, 23-81.

Mayford, M. (2013). The search for a hippocampal engram. Philos Trans R Soc Lond B Biol Sci *369*, 20130161.

McDonald, A.J. (1998). Cortical pathways to the mammalian amygdala. Prog Neurobiol *55*, 257-332.

McNally, G.P., Johansen, J.P. and Blair, H.T. (2011). Placing prediction into the fear circuit. Trend Neurosci *34*, 283-292.

Merritt, L. L., Martin, B. R., Walters, C., Lichtman, A. H. and Damaj, M. I. (2008). The endogenous cannabinoid system modulates nicotine reward and dependence. J Pharmacol Exp Ther *326*, 483-492.

Miyamichi, K., Amat, F., Moussavi, F., Wang, C., Wickersham, I., Wall, N.R., Taniguchi, H., Tasic, B., Huang, Z.J., He, Z., Callaway, E.M., Horowitz, M.A. and Luo, L. (2011). Cortical representations of olfactory input by trans-synaptic tracing. Nature *472*, 191-196.

Mombaerts, P., Wang, F., Dulac, C., Chao, S.K., Nemes, A., Mendelsohn, M., Edmondson, J. and Axel, R. (1996). Visualizing an olfactory sensory map. Cell *87*, 675-686.

Mombaerts, P. (2006). Axonal wiring in the mouse olfactory system. Annu Rev Cell Dev Biol *22*, 713-737.

Moore, T. and Armstrong, K.M. (2003). Selective gating of visual signals by microstimulation of frontal cortex. Nature *421*, 370-373.

Moore, T. and Fallah, M. (2004). Microstimulation of the frontal eye field and its effects on covert spatial attention. J Neurophysiol *91*, 152-162.

Morgan, J.I., Cohen, D.R., Hempstead, J.L, and Curran, T. (1987). Mapping patterns of c-fos expression in the central nervous system after seizure. Science *237*, 192-197.

Morrison, F.G., Dias, B.G. and Ressler, K.J. (2015). Extinction reverse olfactory fear-conditioned increases in neuron number and glomerular size. Proc Natl Acad Sci USA *112*, 12846-12851.

Mountcastle, V.B. (1957). Modality and topographic properties of single neurons of cat's somatic sensory cortex. J Neurophysiol *4*, 408-434.

Morrison, S.E., Saez, A., Lau, B., and Salzman. (2011). Different time course for learning-related changes in amygdala and orbitofrontal cortex. Neuron *71*, 1127-1140.

Muramoto, K., Ono, T., Nishijo, H., and Fukuda, M. (1993). Rat amygdaloid neuron responses during auditory discrimination. Neuroscience *52*, 621-636.

Murasugi, C.M., Salzman, C.D. and Newsome, W.T. (1993a). Microstimulation in visual area MT: effects of varying pulse amplitude and frequency. J Neurosci *13*, 1719-1729.

Murasugi, C.M., Salzman, C.D. and Newsome, W.T. (1993b). Microstimulation of visual area MT: effects on choice behavior in the absence of moving visual stimuli. In: Brain mechanisms of perception and memory: from neurons to behavior. (Ono, T., Squire, L.E., Raichle, M.E., Perrett, M.E. and Fukuda, M. Eds), pp 200-215. Oxford: Oxford UP.

Murata, K., Kanno, M., Ieki, N., Mori, K. and Yamaguchi, M. (2015). Mapping of learned odor-induced motivated behaviors in the mouse olfactory tubercle. J Neursci *35*, 10581-10599.

Nabavi, S., Fox, R., Proulx, C.D., Lin, J.Y., Tsien, R.Y. and Manilow, R. (2014). Engineering a memory with LTD and LTP. Nature *511*, 348-352.

Nachman, M. and Ashe, J.H. (1974). Effects of basolateral amygdala lesions on neophobia, learned taste aversions, and sodium appetitive in rats. J Comp Physiol Psychol *87*, 622-643.

Nagayama, S., Takahasi, Y.K., Yoshihara, Y. and Mori, K. (2004). Mitral and tufted cells differ in the decoding manner of odor maps in the rat olfactory bulb. J Neurophysiol *6*, 2532-2540.

Namburi, P., Beyeler, A., Yorozu, S., Calhoon, G.G., Halbert, S.A., Wichmann, R., Holden, S.S., Mertens, K.L., Anahtar, M., Felix-Ortiz, A.C., Wickersham, I.R., Gray, J.M., and Tye, K.M. (2015). A circuit mechanism for differentiating positive and negative associations. Nature *520*, 675-678.

Nguyen, M.Q., Zhou, Z., Marks, C.A., Ryba, N.J. and Belluscio, L. (2007). Prominent roles for odorant receptor coding sequences in allelic exclusion. Cell *131*, 1009-1017.
Rodriguez, I. (2007). Odorant and pheromone receptor gene regulation in vertebrates. Curr Opin Genet Dev *17*, 465-470.

O'Keefe, J., Burgess, N., Donnett, J.G., Jeffery, K.J. and Maguire, E.A. (1998). Place cells, navigational accuracy, and the human hippocampus. Philos Trans R Soc Lond B Biol Sci *353*, 1333-1340.

Pape, H. C., and Paré, D. (2010). Plastic synaptic networks of the amygdala for the acquisition, expression, and extinction of conditioned fear. Physiol Rev *90*, 419-463.

Paton, J. J., Belova, M. A., Morrison, S. E., and Salzman, C. D. (2006). The primate amygdala represents the positive and negative value of visual stimuli during learning. Nature *439*, 865-870.

Pavlov, I.P. (1927). Conditioned Reflexes. (Oxford University Press, London).

Penfield, W. and Jasper, H. (1954). Epilepsy and the functional anatomy of the human brain. Little, Brown, Boston.

Penfield, W. and Perot, P. (1963). The brain's record of auditory and visual experience. A final summary and discussion. Brain *86*, 595-696.

Penfield, W. and Rasmussen, T. (1950). The Cerebral Cortex of Man: A Clinical Study of Localization of Function. New York: Macmillan.

Peron, S.P., Freeman, J., Iyer, V., Guo, C. and Svoboda, K. (2015). A cellular resolution map of barrel cortex activity during tactile behavior. Neuron *86*, 783-799.

Pickens, C.L., and Holland, P.C. (2004). Conditioning and cognition. Neurosci Biobehav Rev *28*, 651-661.

Poo, C. and Isaacson, J.S. (2009). Odor representations in olfactory cortex: "sparse" coding, global inhibition and oscillations. Neurons *62*, 850-861.

Quirk, G.J., Armony, J.L. and LeDoux, J.E. (1997). Fear conditioning enhances the temporal componenets of tone-evoked spike trains in auditory cortex and lateral amygdala. Neuron *19*, 613-624.

Quirk, G.J., Repa, C., and LeDoux, J.E. (1995). Fear conditioning enhances short-latency auditory responses of lateral amygdala neurons: parallel recordings in the freely behaving rat. Neuron *15*, 1029-1039.

Ramirez, S., Tonegawa, S. and Liu, X. (2014). Identification and optogenetic manipulation of memory engrams in the hippocampus. Front Behav Neurosci *7*, 226.

Redish, A.D., Battaglia, F.P., Chawla, M.K., Ekstrom, A.D., Gerrard, J.L., Lipa, P., Rosenzweig, E.S., Worley, P.F., Guzowski, J.F., McNaughton, B.L. and Barnes, C.A. (2001). Independence of firing correlates of anatomically proximate hippocampal pyramidal cells. J Neurosci *21*, RC134.

Redondo, R.L., Kim, J., Arons, A.L., Ramirez, S., Liu, X., and Tonegawa, S. (2014). Bidirectional switch of the valence associated with a hippocampal contextual memory engram. Nature *513*, 426-430.

Rennaker, R.L., Chen, C.F., and Ruyle, A.M., Sloan, A.M., and Wilson, D.A. (2007). J Neurosci *27*, 1534-1542.

Repa, J.C., Muller, J., Apergis, J., Desrochers, T.M., Zhou, Y., and LeDoux, J.E. (2001). Two different lateral amygdala cell populations contribute to the initiation and storage of memory. Nat Neurosci *4*, 724-731.

Rescorla, R.A. and Wagner, A.R. (1972). A theory of Pavlovian conditioning: Variations in the effectiveness of reinforcement and nonreinforcement. In A.H. Black and W.F. Prokasy (Eds.). Classical conditioning II: Current research and theory (pp. 64-99). New York: Appleton-Century-Crofts.

Rescorla, R.A. (1988). Behavioral studies of Pavlovian conditioning. Annu Rev Neurosci *11*, 329-352.

Ressler, K.J., Sullivan, S.L. and Buck, L.B. (1993). A zonal organization of odorant receptor gene expression in the olfactory system. Cell *73*, 597-609.

Ressler, K.J., Sullivan, S.L. and Buck, L.B. (1994). Information coding in the olfactory system: evidence for a stereotyped and highly organized epitope map in the olfactory bulb. Cell *79*, 1245-1255.

Rinberg, D., Koulakov, A. and Gelperin, A. (2006). Sparse odor coding in awake behaving mice. J Neurosci *34*, 8857-8865.

Roesch, M.R., Stalnaker, T.A. and Schoenbaum, G. (2007). Asssociative encoding in anterior piriform cortex versus orbitofrontal cortex during odor discrimination and reversal learning. Cereb Cortex *17*, 643-652.

Rogan, M.T., Stäubli, U.V., and LeDoux, J.E. (1997). Fear conditioning induces associative long-term potentiation in the amygdala. Nature *390*, 604-607.

Romanski, L.M. and LeDoux, J.E. (1992). Equipotentiality of thalamo-amygdala and thalamo-cortico-amygdala circuits in auditory fear conditioning. J Neurosci *12*, 4501-4509.

Romanski, L. M., Clugnet, M.C., Bordi, F., and LeDoux, J.E. (1993). Somatosensory and auditory convergence in lateral nucleus of the amygdala. Behav Neurosci *107*, 444-450.

Romo, R., Hernández, A., Zainos, O., Brody, C.D. and Lemus, L. (2000). Sensing without touching: psychophysical performance based on cortical microstimulation. Neuron *26*, 273-278.

Root, C.M., Denny, C.A., Hen, R. and Axel, R. (2014). The participation of cortical amygdala in innate, odour-driven behavior. Nature *515*, 269-273.

Rosen, J.B. (2004). The neurobiology of conditioned and unconditioned fear: a neurobehavioral system analysis of the amygdala. Behav Cogn Neurosci Rev *3*, 23-41.

Rosenkranz, J.A., and Grace, A.A. (2002). Dopamine-mediated modulation of odour-evoked amygdala potentials during pavlovian conditioning. Nature 417, 282-287.

Rosenkranz, J.A., Moore, H. and Grace, A.A. (2003). The prefrontal cortex regulates lateral amygdala neuronal plasticity and responses to previously conditioned stimuli. J Neurosci *23*, 11054-11064.

Rosenkranz, J.A., and Grace, A.A. (2002). Dopamine-mediated modulation of odour-evoked amygdala potentials during pavlovian conditioning. Nature 417, 282-287.

Rothschild, G., Nelken, L. and Mizrahi, A. (2010). Functional organization and population dynamics in the mouse primary auditory cortex. Nat Neurosci *3,* 353-360.

Russchen, F.T., Bakst, I., Amaral, D.G., and Price, J.L. (1985). The amygdalostriatal projections in the monkey. An anterograde tracing study. Brain Res *329*, 241-257.

Sacco, T. and Sacchetti, B. (2010). Role of secondary sensory cortices in emotional memory storage and retrieval and rates. Science *329*, 649-656.

Saez, A., Rigotti, M., Ostojic, S., Fusi, S. and Salzman, C.D. (2015). Abstract context representations in primate amygdala and prefrontal cortex. Neuron *87*, 869-881.

Sah, P., Faber, E.S., Lopez De Armentia, M., and Power, J. (2003). The amygdaloid complex: anatomy and physiology. Physiol Rev *83*, 803-834.

Sah, P., Westbrook, R. F., and Luthi, A. (2008). Fear conditioning and long-term potentiation in the amygdala: what really is the connection? Ann NY Acad Sci *1129*, 88-95.

Salzman, C.D., Britten, K.H. and Newsome, W.T. (1990). Cortical microstimulation influences perceptual judgements of motor direction. Nature *346*, 174-177.

Salzman, C. D., and Fusi, S. (2010). Emotion, cognition, and mental state representation in amygdala and prefrontal cortex. Annu Rev Neurosci *33*, 173-202.

Salzman, C.D., Murasugi, C.M., Britten, K.H. and Newsome, W.T. (1992). Microstimulation in visual area MT: effects on direction discrimination performance. J Neurosci *12*, 2331-2355.

Salzman, C.D. and Newsome, W.T. (1994). Neural mechanisms for forming a perceptual decision. Science *264*, 231-237.

Sarter, M., and Markowitsch, H.J. (1985). Involvement of the amygdala in learning and memory: a critical review, with emphasis on anatomical relations. Behav Neurosci *99*, 342-380.

Schoenbaum, G., Chiba, A.A., and Gallagher, M. (1998). Orbitofrontal cortex and basolateral amygdala encode expected outcomes during learning. Nat Neurosci *1*, 155-159.

Schultz, W. (2001). Reward signaling by dopamine neurons. Neuroscientist *7*, 293-302.

Schultz, W. (2006). Behavioral theories and the neurophysiology of reward. Annu Rev Psychol *57*, 87-115.

Schwabe, K., Ebert, U., and Loscher, W. (2004). The central piriform cortex: anatomical connections and anticonvulsant effect of GABA elevation in the kindling model. Neurosci *126*, 727-741.

Serizawa, S., Miyamichi, K., Nakatani, H., Suzuki, M., Saito, M., Yashihara, Y. and Sakano, H. (2003). Negative feedback regulation ensures the one receptor-one olfactory neurons rule in mouse. Science *302*, 2088-2094.

Sevelinges, Y., Gervais, R., Messaoudi, B., Granjon, L. and Mouly, A.M. (2004). Olfactory fear conditioning induces field potential potentiation in rat olfactory cortex and amygdala. Learn Mem *11,* 761-769.

Seymour, B., and Dolan, R. (2008). Emotion, decision making, and the amygdala. Neuron *58*, 662, 671.

Shabel, S. J., and Janak, P.H. (2009). Substantial similarity in amygdala neuronal activity during conditioned appetitive and aversive emotional arousal. Proc Natl Acad Sci USA *106*, 15031-15036.

Shepherd, G.M., ed. (2004). The synaptic organization of the brain, 5th ed. New York: Oxford University Press.

Shi, C. and Davis, M. (2001). Visual pathways involved in fear conditioning measured with fear-potentiated startle: behavioral and anatomic studies. J Neurosci *21*, 9844-9855.

Shykind, B.M., Rohani, S.C., O'Donnell, S., Nemes, A., Mendelsohn, M., Sun, Y., Axel, R. and Barnea, G. (2004). Gene switching and the stability of odorant receptor gene choice. *177*, 801-815.

Sosulski, D.L., Bloom, M.L., Cutforth, T., Axel, R. and Datta, S.R. (2011). Distinct representations of olfactory information in different cortical centres. Nature *472*, 213-216.

Soucy, E.R., Albeanu, D.F., Fantana, A.L., Murthy, V.N. and Meister, M. (2009). Precision and diversity in an odor map in the olfactory bulb. Nat Neurosci *2*, 210-220.

Stettler, D.D. and Axel, R. (2009). Representations of odor in the piriform cortex. Neuron *63*, 854-864.

Stuber, G. D., Sparta, D.R., Stamatakis, A.M., van Leeuwen, W.A., Hardjoprajitno, J.E., Cho, S., Tye, K.M., Kempadoo, K.A., Zhang, F., Deisseroth, K., and Bonci, A. (2011). Excitatory transmission from the amygdala to nucleus accumbens facilitates reward seeking. Nature *475*, 377-380.

Tan, H., Lauzon, N.M., Bishop, S.F., Chi, N., Bechard, M. and Laviolette, S.R. Cannabinoid transmission in the basolateral amygdala modulates fear memory formation via functional inputs to the prelimbic cortex. J Neurosci *31*, 5300-5312.

Tan, J., Savigner, A., Ma, M. and Luo, M. (2010). Odor information processing by the olfactory bulb analyzed in gene-targeted mice. Neuron *6*, 912-926.

Tehovnik, E.J. and Slocum, W.M. (2007). Phosphene induction by microstimulation of macque V1. Brain Res Rev *53*, 337-343.

Touhara, K. and Vosshall, L.B. (2009). Sensing odorants and pheromones with chemosensory receptors. Annu Rev Physiol *71*, 307-332.

Tye, K.M., Prakash, R., Kim, S.Y., Fenno, L.E., Grosenick, L., Zarabi, H., Thompson, K.R., Gradinaru, V., Ramakrishnan, C., and Deisseroth, K. (2011). Amygdala circuitry mediating reversible and bidirectional control of anxiety. Nature *471*, 358-362.

Tye, K.M., Stuber, G.D, de Ridder, B., Bonci, A., and Panak, P.H. (2008). Rapid strengthening of thalamo-amygdala synapses mediates cue-reward learning. Nature *453*, 1253-1257.

Uwano, T., Nishijo, H., Ono, T., and Tamura, R. (1995). Neuronal responsiveness to various sensory stimuli, and associative learning in the rat amygdala. Neuroscience *68*, 339-361.

Vassalli, A., Rothman, A., Feinstein, P., Zapotocky, M. and Mombaerts, P. (2002). Minigenes impart odorant receptor-specific axon guidance in the olfactory bulb. Neuron *35*, 681-696.

Vassar, R., Ngai, J. and Axel, R. (1993). Spatial segregation of odorant receptor expression in the mammalian olfactory epithelium. Cell *74*, 309-318.

Vassar, R., Chao, S.K., Sitcheran, R., Nuñez, J.M., Vosshall, L.B. and Axel, R. (1994). Topographic organization of sensory projections to the olfactory bulb. Cell *79*, 981-991.

Walker, D.L., Paschall, G.Y. and Davis, M. (2005). Glutamate receptor antagonist infusions into the basolateral and medial amygdala reveal differential contributions to olfactory vs. context fear conditioning and expression. Learn Mem *12*, 120-129.

Wolff, S.B., Gründermann, J., Tovote, P., Krabbe, S., Jacobson, G.A., Müller, C., Herry, C., Ehrlich, I., Freidrich, R.W., Letzkus, J.J., and Lüthi, A. (2014). Amygdala interneuron subtypes control fear learning through disinhibition. Nature *509*, 453-458.

Wurtz, R. (2015). Using perturbations to identify the brain circuits underlying active vision. Philos Trans R Soc Lond B Biol Sci *370,* 20140205.

Yamamoto, T., Azuma, S. and Kawamura, Y. (1984). Functional relations between the cortical gustatory area and the amygdala: electrophysiological and behavior studies in rats. Exp Brain Res *56*, 23-31.

Yamamoto, T., Fujimoto, Y., Shimura, T. and Sakai, N. (1995). Conditioned taste aversion in rats with excitotoxic brain lesions. Neurosci Res *22*, 31-49.

Yau, J.M., DeAngelis, G.C. and Angelaki, D.E. (2015). Dissecting the neural circuits for multisensory integration and crossmodal processing. Philos Trans R Soc Lond B Biol Sci *370*, 20140203.

Yiu, A.P., Mercaldo, V., Yan, C., Richards, B., Rashid, A.J., Hsiang, H.L., Pressey, J., Tran, M.M., Kushner, S.A., Woodin, M.A., Frankland, P.W. and Josselyn, S.A. (2014). Neuron *83*, 722-735.

Yokoi, M., Mori, K. and Nakanishi, S. (1995). Refinement of odor molecule tuning by dendrodendritic synaptic inhibition in the olfactory bulb. Proc Natl Acad Sci USA *8*, 3371-3375.

Zhang, T. and Britten, K.H. (2011). Parietal area VIP causally influences heading perception during pursuit eye movements. J Neurosci *31*, 2569-2575.

Zhang, F., Gradinaru, V., Adamantidis, A.R., Durand, R., Airan, R.D., de Lecea, L., and Deisseroth, K. (2010). Optogenetic interrogation of neural circuits: technology for probing mammalian brain structures. Nat Protoc *5*, 439–456.

APPENDIX A

CHAPTER 2 METHODS

Constructs and viruses: Codon-optimized lentiviral vector expressing ChR2-EYFP under the control of the human *synapsin* promoter was a kind gift from Dr. Karl Deisseroth. To generate the hsyn:ChR2-EYFP-2A-mCherry construct, ChR2-EYFP was replaced by codon optimized ChR2-EYFP-T2A-mCherry (synthesized by Genewiz, Inc.). To generate the c-fos:ChR2-EYFP-2A-mCherry construct, a 720 nucleotide fragment of the *c-fos* promoter (residues 85493280-85473999 of mus musculus chromosome 12; ascension NC_000078.6) replaced the *synapsin* promoter. To generate the c-fos:NpHR-EYFP construct, NpHR-EYFP was PCR amplified from pAAV-EF1a-DIO-eNpHR 3.0-EYFP (also a gift from Dr. Karl Deisseroth) and this was used to replace ChR2-EYFP-T2A-mCherry in the c-fos:ChR2-EYFP-2A-mCherry construct. c-fos:GFP was generated by replacing the ChR2-EYFP-2A-mCherry construct with a codon optimized EGFP construct (synthesized by Genewiz, Inc.). Lentiviruses for *in vivo* injection were produced as previously described (Zhang et al., 2010).

Experimental subjects and stereotactic surgery: Adult (25-30g) male C57BL/6J mice (Jackson laboratory) were group-housed until surgery. Animals were anaesthetized with ketamine/xylazine (100mgkg^{-1} or 10mgkg^{-1}, respectively, Henry Schein) and placed in a stereotactic frame (Kopf Instruments). Custom-made microinjection needles (Drummond) were then inserted (coordinates from Bregma: -1.55AP, +3.3ML, -4.75 DV) and each BLA was injected with 1µl of lentivirus over 0.5µm (from -4.75DV to -4.25DV). A 6mm guide cannula (Plastics One) was placed 250µm above the virus

injection site and fixed in place using a small amount of dental cement (Parkell Inc.). Buprenorphine (0.05mgkg^{-1}, Henry Schein) was administered. As exclusion criteria, we only included mice with viral expression confined to the BLA, and cannula placement above the BLA (Supplemental Figure 7). All experiments were conducted according to approved protocols at Columbia University.

Footshock and nicotine treatment: Footshock-treated animals were removed from their homecage and placed into a standard Med-Associates operant chamber equipped with a grid floor and aversive stimulator. Animals received 20 1.5mA footshocks over 10 minutes before being returned to their homecage. Nicotine treated animals were removed from their homecage and administered an intraperitoneal (i.p.) injection of nicotine hydrogen tartrate (0.7mgkg^{-1} free base, Sigma-Aldrich), prepared in saline, before being returned to their homecage. Both unconditioned stimuli were used at higher intensities than were used in studies that have previously reported little induction of c-Fos expression in the BLA in response to either footshock or nicotine (Knapska et al., 2007).

Histological processing: Mice were killed by transcardial perfusion with 13ml PBS, followed by 10ml 4% paraformaldehyde. Brains were extracted and coronal sections of the BLA (100μm) were cut on a vibratome. The slices were labeled with the following primary antibodies: goat anti-GFP (Abcam), rabbit anti-DsRed (Clontech), rabbit anti-c-Fos (Santa Cruz) and goat anti-c-Fos (Santa Cruz). The following fluorophore-conjugated secondary antibodies were used: Alexa 488 donkey anti-goat (Invitrogen), Alexa 594 donkey anti-rabbit (Invitrogen). Slices were counterstained with DAPI (Vector Laboratories). All images were taken using a Zeiss LSM-710 confocal microscope system. To visualize the entire BLA at 20x magnification, 16 tiled images were obtained

and stitched together using the Zen imaging software (2009; version 5.5 SP1). A subset of contiguous tiles encompassing the BLA is presented. Lines in images are a result of the stitching process.

***In situ* hybridization:** *In situ* hybridization was conducted by the *in situ* hybridization core at UNC Neuroscience Center. catFISH experiments were conducted as described previously (Guzowski and Worley, 2001). Briefly, we utilized an intronic *c-fos* probe to detect nuclear localized intronic RNA present 5 minutes after US exposure, and an exonic *c-fos* probe to detect cytoplasmic exonic RNA present 45 minutes after US exposure. This provides 2 time-points at which to label active cells using only endogenous *c-fos* activation. The *c-fos* exonic probe spans the first 2 exons of the *c-fos* gene. The fluorescein-labeled *c-fos* exonic probe was detected using a horseradish peroxidase-conjugated anti-fluorescien antibody (Roche) on 20μm frozen sections. The signal was amplified using DNP-conjugated tyramide (Perkin Elmer) and subsequently visualized using Alexa 488-conjugated anti-DNP antibody (Life Technologies). The *c-fos* intronic probe was a kind gift from Dr D. Lin and contains the entire first intron of the *c-fos* gene (Lin et al., 2011). The digoxigenin-labeled *c-fos* intronic probe was detected using an alkaline phosphatase-conjugated anti-DIG antibody (Roche) on 20μm frozen sections. The signal was amplified and detected using the HNPP Fast Red system (Roche).

Cell counts: To quantify the number of cells expressing fluorophores and *c-fos*, we acquired images from a single z plane across 3 adjacent slices. The mean background intensity of each image was subtracted and DAPI, *c-fos*, EYFP and mCherry positive nuclei were counted manually (ImageJ). All histological procedures were conducted by

an individual who was blind to the experimental condition. For cell counts, N refers to number of animals.

Data analysis: Statistical significance was assessed using *t*-tests or analysis of variance (ANOVA), followed by post-hoc tests (Bonferroni test for difference between means, unless otherwise stated) when applicable, using α tests. Data were analyzed using Microsoft Excel with the Statplus plugin. All error bars are ± standard error of the mean (s.e.m.).

Conditioned place preference: A biased design for conditioned place preference was used, in which a positive valence of nicotine was tested by its ability to increase the time spent in the initially non-preferred chamber. The apparatus consisted of a rectangular chamber split into 2 compartments (120×165×200mm per compartment) connected by a 50×50mm opening. Each compartment had distinct olfactory (1% acetephenone or 2% octanol), tactile (rough or smooth flooring) and visual (vertical or no stripes on walls) cues. Singly housed animals were removed from their homecage and placed in the center of the conditioning apparatus and allowed to explore for 10 minutes (pre-test). After the pre-test an initial compartment preference for each mouse was recorded. The following day animals were assigned to either saline or nicotine groups. Animals in the nicotine group were given an i.p. injection of nicotine and confined to their initially non-preferred compartment for 20 minutes. Animals in the saline group were given an i.p. injection of saline and confined to their initially non-preferred compartment for 20 minutes. 5 hours later, animals of both groups were given an i.p. injection of saline and confined to their initially preferred compartment for 20 minutes. The following day animals were placed in the center of the conditioning apparatus and allowed to explore for 10 minutes to

determine any change in compartment preference as a result of conditioning. The time spent in each compartment was scored manually by individuals who were blind to the experimental conditions.

***In vivo* electrophysiology:** Animals were injected with virus expressing c-fos:ChR2-EYFP-2A-nCherry. Nine days later animals were treated with either footshock or nicotine to induce ChR2 expression. Eighteen hours later animals were anaesthetized with urethane (1800mg/kg) and placed in a stereotactic system with 1% oxygen delivery throughout the recording. An optrode consisting of 16 stereotrodes (25µm Formvar-coated tungsten microwire (California Fine Wire)) glued to a 200µm optical fiber (0.37 NA, Thor labs), with the tip of the stereotrodes extending 300-500µm beyond the tip of the fiber, was used for simultaneous optical stimulation and extracellular recordings. The optical fiber was connected to a 473nm laser (Shanghai Laser and Optics Century), which was controlled by a stimulator (Master-8, A.M.P.I.). The power intensity of light emitted from the optrode was adjusted to 18mW prior to recordings. The optrode was lowered to the BLA. Light pulses of 100ms were delivered at 0.1Hz at recording sites throughout the BLA. After light-responsive cells were detected two types of optical stimulation were delivered: 100ms pulses delivered every 10s (100-120 sweeps), and bursts of 200, 10ms light pulses at 20Hz delivered every 40s (3-5 sweeps). Recordings were obtained via a unitary gain head-stage preamplifier attached to a fine wire cable (Neuralynx). Multi- and single-unit recordings were obtained by lowering stereotrodes through the BLA in 100µm steps from -4.2 to -4.7 DV. Signals were amplified, bandpass filtered and acquired by a Digital Lynx SX programmable amplifier (Neuralynx) on a personal computer running Cheetah data acquisition software (Neuralynx). Spikes were bandpass filtered (600-6000

Hz) and recorded at 32 kHz with 30μV threshold. Single units were clustered using Klustakwik (by Ken Harris, http://klustakwik.sourceforge.net/), using the first two principal components, energy, and peak of the action potentials. Data were analyzed with custom software written in Matlab. The response latency of single units to light pulses was quantified as the most likely first spike time across all sweeps, corresponding with the onset of the light-evoked response.

***Ex vivo* slice electrophysiology:** Acute brain slices were made from mice 18 hours after shock or nicotine induction. Mice were anesthetized with isoflurane and transcardially perfused with ice-cold artificial cerebrospinal fluid (aCSF, in mM: 125 NaCl, 2.5 KCl, 1.25 NaH_2PO_4, 25 $NaHCO_3$, 20 glucose, 2 $CaCl_2$, 1 $MgCl_2$, 2 Na-pyruvate; equilibrated with 95% O_2 and 5% CO_2). After perfusion, brains were removed and submerged in an ice-cold, isotonic solution for sectioning (in mM: 10 NaCl, 2.5 KCl, 0.5 $CaCl_2$, 7 $MgSO_4$, 1.25 NaH_2PO_4, 25 $NaHCO_3$, 10 glucose, and 195 sucrose; equilibrated with 95% O_2 and 5% CO_2). Coronal sections (350μm) of the forebrain were cut with a vibrating microtome (VT1200, Leica), and were immediately placed into aCSF. Slices were incubated in aCSF at 35°C for 25 minutes, and then maintained at room temperature until transfer to the recording chamber beneath an upright microscope (Olympus Optical) with a 40X objective (LUMPLFLN 40XW, 0.8 N.A.). Slices were perfused with fresh aCSF at 33-35°C during all recordings. Glass patch microelectrodes (2-5 MΩ) contained (in mM): 135 $KMeSO_4$, 5 KCl, 2 NaCl, 10 HEPES, 10 Na_2-phosphocreatine, 5 MgATP, 0.4 Na_2GTP, 0.2 EGTA, and 0.2% biocytin. The BLA was located under differential interference contrast (DIC) microscopy and cells expressing EYFP were located under epifluorescent illumination with a 470nm LED source (pE-100, CoolLED) at low power,

and a 520Δ50 BP emission filter (Chroma). Optogenetic stimulation was with the same 470nm LED source (14.7 mW) or a 595nm LED (9.6 mW), delivered through the objective. Voltage-clamp and current-clamp responses were recorded with a Multiclamp 700A amplifier (Molecular Devices), low-pass filtered at 2-4 kHz, and digitized at 20 kHz (Digidata 1440A, Instrutech). Series resistance upon whole-cell configuration was typically 10-12 MΩ, and cells that had initial series resistance ≥ 15 MΩ or for which series resistance increased by ≥ 5 MΩ during the course of experiment were excluded from analysis. In voltage-clamp experiments, series resistance was compensated with the correction circuit (≥95%) of the amplifier. Microelectrode voltage drop (bridge) was compensated at the beginning of each current-clamp experiment with the automatic feature of the amplifier. We did not correct for liquid junction potential. Data were collected and analyzed using Axograph X and Matlab (Mathworks). For halorhodopsin experiments, current was injected to generate spike trains 50 pA above rheobase (minimum current to induce firing), with rheobase first determined for each cell by a ramp protocol (Δ400pA/s). This ensured that all cells were perithreshold. Small amounts of current were injected to hold all cells at the same resting voltage of -70mV. All light OFF vs. light ON data were collected from interleaved trials.

Assay for physiologic responses to optical stimulation: Respiration and heart rate were measured using a pulse oximeter (MouseOx, Starr Life Sciences) connected to a computer that was equipped with MouseOx software. Recordings were made using a collar sensor. Mice were shaved around the neck and acclimated to the collar sensor for 30 minutes. Heart rate (beats per minute) was reported as a moving average across 5 heartbeats. Breath rate (breaths per minute) was reported as a moving average across 10

breath cycles. Eighteen hours after footshock or nicotine treatment animals were prepared for assessment of their response to optical stimulation. Stylets were removed from the guide cannulae and a flat-cut 300μm diameter fiber-optic cable, coupled to a 473nm laser (Shanghai Laser and Optics Century) outside of the operant chamber, was inserted through the guide cannula and positioned directly above the BLA. Immediately before this the power of the laser was adjusted to 18mW. The collar sensor was then attached. Mice were placed into a clean home cage and were acclimated to the cage for 10 minutes. After this, heart and respiration rate were recorded for 3 minutes to establish a baseline. Animals then received three 3 minute presentations of optical stimulation (18mW, 20Hz, 20% duty cycle). Heart and respiration rate were computed as the percent difference in rate during optical stimulation compared to baseline.

Assay for freezing response to optical stimulation: Mice were placed into an illuminated Med-Associates operant chamber equipped with nosepoke portals, audio stimulus generator, infra-red light source and a house light (the testing chamber), and behavior was recorded using a modified web cam capable of detecting infra-red light (Logitech). Upon initiation of a 500 second session the house light was dimmed and animals received 5 presentations of 10 seconds of optical stimulation. Upon completion of the session the house light was illuminated and animals were returned to their home cage. All stimuli were presented and all timestamp data recorded using Med-PC software. Freezing behavior was defined as the cessation of all movements except those caused by respiration and was scored manually by individuals who were blind to the experimental conditions.

Self-administration assay: Upon initiation of a 60 minute session the house light was dimmed and nosepoke entries into the active and inactive nosepoke portals, detected by breakage of an infrared beam across each portal, were separately recorded. Entry into the active portal resulted in 5 seconds of optical stimulation (18mW, 20Hz, 20% duty cycle). Entry into the inactive portal had no consequence. Upon completion of the session, the house light was illuminated and animals were returned to their home cages.

Fear conditioning assay: Upon initiation of a 1000 second training session the house-light was dimmed and animals receiving paired training received 10 randomly presented 10-second 1.5kHz tones, all of which coterminated with 2 seconds of optical stimulation (18mW, 20Hz, 20% duty cycle). Animals receiving unpaired training received 10 randomly presented 10-second 1.5kHz tones and 10 randomly presented 2 seconds of optical stimulation. Upon completion of the training session the house light was illuminated and the animals were returned to their home cage. 3 hours later animals received a second training session identical to the first. 3 hours after this, animals were exposed to a 500 second test session in which they received 5 presentations of the 10-second CS. Upon completion of the test session the house light was illuminated and animals were returned to their home cage. Freezing behavior during the training and test sessions was recorded.

Context assay: Animals were removed from their homecage and placed into a standard Med-Associates operant chamber equipped with a grid floor and aversive stimulator. Animals received 20 1.5mA footshocks over 10 minutes before being returned to their homecage. The following day animals were injected and cannulated as described previously. 9 days later animals were removed from their homecage and returned to the

footshock chamber. Upon initiation of a 500 second session the house light was dimmed. After 500 seconds of context exposure, the house light was illuminated and animals were returned to their homecage. Freezing behavior was scored during the first 2 minutes of exposure to context. 18 hours later animals were assayed for their response to optical stimulation.

Odor assay: Animals were placed into a Med Associates operant chamber that had air passing through it at 1 liter/minute, with a vacuum removing air at an equal rate. Acetephenone (1%) and octanol (2%) were dissolved in mineral oil and their entry into the chamber was controlled manually. Over a 1000 second session animals received 10 presentations of 10 seconds of acetephenone that always coterminated with 2 seconds of optical stimulation (18mW, 20Hz, 20% duty cycle), and 10 presentations of 10 seconds of octanol, randomly interleaved. When the session was complete animals were returned to their home cage. 3 hours later animals received a second identical training session. 3 hours after this, animals were placed into the center of a 3-compartment chamber (Med Associates) comprising a central compartment with opaque walls and 2 extreme compartments with Perspex walls. Animals were left to explore the chamber for 5 minutes. Animals were then removed and the two odors were presented from opposite ends of the chamber at a rate of 1 liter/minute. Animals were returned to the central compartment and left to explore the chamber for a further 5 minutes. Behavior was recorded using a camcorder (Sony) and the amount of time spent in each compartment during the 'without odor' and 'with odor' epochs was scored manually by individuals who were blind to the experimental conditions.

CS assay: Animals were removed from their homecage and placed into a standard Med-Associates operant chamber equipped with a grid floor and aversive stimulator. Upon initiation of a 1000 second training session the house-light was dimmed and animals receiving paired training received 10 randomly presented 10-second 1.5kHz tones, all of which coterminated with 2 seconds of 1.5mA footshock. Animals receiving unpaired training received 10 randomly presented 10-second 1.5kHz tones and 10 randomly presented 2 seconds of 1.5mA footshock. Upon completion of the training session the house light was illuminated and the animals were returned to their home cage. 3 hours later animals received a second training session identical to the first. The following day animals were injected and cannulated as described previously. 9 days later animals were removed from their homecage and placed into the testing chamber. Upon initiation of a 500 second session the house light was dimmed and animals received 5 presentations of the 10-second 1.5kHz tone. Upon completion of the session the house light was illuminated and animals were returned to their homecage. 18 hours later animals were either assayed for their response to optical stimulation.

Assay for effect of optical inhibition on response to auditory CS: Animals were removed from their homecage and placed into a standard Med-Associates operant chamber equipped with a grid floor and aversive stimulator. Upon initiation of a 1000 second training session the house-light was dimmed and animals received 10 randomly presented 10-second 1.5kHz tones, all of which coterminated with 2 seconds of 1.5mA footshock. Upon completion of the training session the house light was illuminated and the animals were returned to their home cage. 3 hours later animals received a second training session identical to the first. The following day animals were bilaterally injected

with lentivirus expressing c-fos:NpHR-EYFP and bilaterally cannulated 250μm above the BLA. 9 days later animals were treated with either footshock or nicotine as previously described. 18 hours later animals were prepared for assessment of their response to the CS in the presence and absence of optical inhibition. Stylets were removed from the guide cannulae and a flat-cut 300μm diameter fiber-optic cable, coupled to a 593nm laser (Shanghai Laser and Optics Century) outside of the operant chamber, was inserted through each guide cannula and positioned directly above each BLA. Immediately before this the power of each laser was adjusted to 10mW. Mice were then placed into the testing chamber. Upon initiation of a 500 second session the house light was dimmed, the lasers were turned on and animals received 5 presentations of the 10-second 1.5kHz tone. Upon completion of the session the house light was illuminated and lasers were turned off. Immediately following this a second 500 second session was initiated. The house light was dimmed and the animals received 5 10 second presentations of the 1.5kHz tone. Upon completion of the session, the house light was illuminated and animals were returned to their homecage.

Assay for effect of optical inhibition on response to olfactory CS: Animals were placed into a Med Associates operant chamber that had air passing through it at 1 liter/minute, with a vacuum removing air at an equal rate. Acetephenone (1%) and octanol (2%) were dissolved in mineral oil and their entry into the chamber was controlled manually. Over a 1000 second session animals received 10 presentations of 10 seconds of acetephenone that always coterminated with 2 seconds of 1.5mA footshock, and 10 presentations of 10 seconds of octanol, randomly interleaved. When the session was complete animals were returned to their home cage. 3 hours later animals received a

second identical training session. The following day animals were bilaterally injected with lentivirus expressing c-fos:NpHR-EYFP and bilaterally cannulated 250μm above the BLA. 9 days later animals were treated with either footshock or nicotine as previously described. 18 hours later animals were prepared for assessment of their response to the CS in the presence and absence of optical inhibition. Stylets were removed from the guide cannulae and a flat-cut 300μm diameter fiber-optic cable, coupled to a 593nm laser (Shanghai Laser and Optics Century), was inserted through each guide cannula and positioned directly above each BLA. Immediately before this the power of each laser was adjusted to 10mW. Animals were then placed into the center of a 3-compartment chamber. Animals were left to explore the chamber for 5 minutes. Animals were then removed and the two odors were presented from opposite ends of the chamber at a rate of 1 liter/minute and the lasers were turned on. Animals were returned to the central compartment and left to explore the chamber for 5 minutes. Animals were then removed and the lasers were turned off. Animals were returned to the central compartment and left to explore the chamber for a further 5 minutes. Behavior was recorded using a camcorder (Sony) and the amount of time spent in each compartment during the 'without yellow light' and 'with yellow light' odor epochs was scored manually by individuals who were blind to the experimental conditions.

Supplementary References

Lin, D., Boyle, M.P., Dollar, P., Lee, H., Lein, E.S., Perona, P., and Anderson, D.J. (2011). Functional identification of an aggression locus in the mouse hypothalamus. Nature *470*, 221-226.

APPENDIX B

CHAPTER 3 METHODS

Experimental subjects and stereotactic surgery: Adult (25-30g) male C57BL/6J mice (Jackson laboratory) were group-housed until surgery. Animals were anaesthetized with isoflurane (1-2%) and placed in a stereotactic frame (Kopf Instruments). Custom-made microinjection needles (Drummond) were then inserted. For hM4Di and NpHR experiments piriform coordinates from Bregma: -4 AP, -1 ML, -5.2 DV; -4.25 AP, -2 ML, -5.7 DV; -4 AP, 1 ML, -5.2 DV; -4.25 AP, 4.25 ML, -5.7 DV. Each site was injected with 1.5µl of AAV. For NpHR experiments a 6mm guide cannula (Plastics One) was placed 250µm above each BLA (coordinates from bregma: -1.55 AP, -3,3 ML, -4 DV; -1.55 AP, 3.3 ML, -4 DV) and fixed in place using a small amount of dental cement (Parkell Inc.). For ChR2 experiments 0.5µl AAV was injected into piriform cortex (-4.25 AP, 4.25 ML, -5.6 DV). An optical fiber (200µm, 0.39 numerical aperture, Thorlabs) was epoxied to 1.25mm stainless steel ferrules (Precision Fibre products), and polished to achieve a minimum of 85% transmission. This was inserted at 10° (-4.95 AP, 4.25 ML, -5.45 DV) and placed 100µm above the injection site. A 6mm beveled cannula (Plastics One) was placed 250µm above the BLA. Buprenorphine (0.05mgkg^{-1}, Henry Schein) was administered. As exclusion criteria, we only included mice with viral expression confined to piriform cortex, fiber placement in piriform and cannula placement above the BLA. All experiments were conducted according to approved protocols at Columbia University.

Histological processing: Mice were killed by transcardial perfusion with 13ml PBS, followed by 10ml 4% paraformaldehyde. Brains were extracted and coronal sections of the BLA (100μm) were cut on a vibratome. The slices were labeled with the following primary antibodies: goat anti-GFP (Abcam), rabbit anti-DsRed (Clontech), rabbit anti-c-Fos (Santa Cruz) and goat anti-c-Fos (Santa Cruz). The following fluorophore-conjugated secondary antibodies were used: Alexa 488 donkey anti-goat (Invitrogen), Alexa 594 donkey anti-rabbit (Invitrogen). Slices were counterstained with DAPI (Vector Laboratories). All images were taken using a Zeiss LSM-710 confocal microscope system.

Cell counts: To quantify the number of cells expressing fluorophores and *c-fos*, we acquired images from a single z plane across 3 adjacent slices. The mean background intensity of each image was subtracted and DAPI, *c-fos*, EYFP and mCherry positive nuclei were counted manually (ImageJ). All histological procedures were conducted by an individual who was blind to the experimental condition.

Retrograde tracing: Animals were unilaterally in the BLA with 0.5μl cholera toxin B subunit conjugated to Alexa Fluorophore 555. 5 days later animals were sacrificed.

Olfactory fear conditioning assay: Animals were placed into a Med Associates operant chamber that had air passing through it at 1 liter/minute, with a vacuum removing air at an equal rate. Acetephenone (1%) and octanol (2%) were dissolved in mineral oil and their entry into the chamber was controlled by a custom made olfactometer. Over a 2000 second session animals received 10 presentations of 10 seconds of acetephenone that always coterminated with 2 seconds of 0.7mA footshock, and 10 presentations of 10 seconds of octanol, randomly interleaved. When the session was complete animals were

returned to their home cage. 3 hours later animals received a second identical training session. The following day animals were placed into the center of a 3-compartment chamber (Med Associates) comprising a central compartment with opaque walls and 2 extreme compartments with Perspex walls. Animals were left to explore the chamber for 5 minutes. Animals were then removed and the two odors were presented from opposite ends of the chamber at a rate of 1 liter/minute. Animals were returned to the central compartment and left to explore the chamber for a further 5 minutes. For hM4Di experiments, animals were administered CNO (Sigma Aldrich, 0.3mg/kg dissolved in saline) 30 minutes prior to the test session. The following day animals were administered an equal volume of saline 30 minutes prior to an identical testing session. For NpHR experiments, stylets were removed from the guide cannulae and a flat-cut 300μm diameter fiber-optic cable, coupled to a 593nm laser (Shanghai Laser and Optics Century), was inserted through each guide cannula and positioned directly above each BLA. Immediately before this the power of each laser was adjusted to 10mW. Animals then received one testing session with the lasers turned on followed by an identical testing session with the lasers turned off. Behavior was recorded using a camcorder (Sony) and the amount of time spent in each compartment during the 'without odor' and 'with odor' epochs was scored manually by individuals who were blind to the experimental conditions.

Optical stimulation fear conditioning assay (freezing): Animals were removed from their homecage and the ferrule positioned above piriform cortex was coupled to a 473nm laser (Shanghai Laser and Optics Century) via a custom-made patch cord. The power of the laser was adjusted such that the power coming out of the ferrule was approximately

18mW. Animals were then placed into a standard Med-Associates operant chamber equipped with a grid floor and aversive stimulator. Upon initiation of a 1000 second training session the house-light was dimmed and animals received 10 randomly presented 10-second presentations of optical stimulation (18mW, 20Hz, 20% duty cycle), all of which coterminated with 2 seconds of 0.7mA footshock. Upon completion of the training session the house light was illuminated and the animals were returned to their home cage. 3 hours later animals received a second training session identical to the first. The following day animals were habituated to a different Med-Associates operant chamber that had distinct visual and tactile cues. Habituation consisted of 2 20 minutes exposures to the new context. Animals were then prepared for assessment of their response to optical stimulation. Stylets were removed from the guide cannulae and a flat-cut 300μm diameter fiber-optic cable, coupled to a 473nm laser (Shanghai Laser and Optics Century) outside of the operant chamber, was inserted through the guide cannula and positioned directly above the BLA. Immediately before this the power of the laser was adjusted to 18mW. Upon initiation of a 500 second session the house light was dimmed and animals received 5 presentations of 10 seconds of optical stimulation. A subset of animals received concurrent optical inhibition via the ferrule (10mW, constant illumination) throughout the entire testing session to control for effects of antidromic activation. Upon completion of the session the house light was illuminated. Animals were removed from the chamber, and the fiber optic cable was removed. The ferrule positioned above piriform cortex was then coupled to a 473nm laser via a custom-made patch cord. The power of the laser was adjusted such that the power coming out of the ferrule was approximately 18mW. Animals then received a second identical testing session. Upon

completion of the session the house light was illuminated and animals were returned to their home cage. All stimuli were presented and all timestamp data recorded using Med-PC software. Behavior was monitored and recorded using a modified webcam capable of detecting infrared light. Freezing behavior was defined as the cessation of all movements except those caused by respiration and was scored manually by individuals who were blind to the experimental conditions.

Optical stimulation fear conditioning assay (avoidance): Animals were removed from their homecage and the ferrule positioned above piriform cortex was coupled to a 473nm laser (Shanghai Laser and Optics Century) via a custom-made patch cord. The power of the laser was adjusted such that the power coming out of the ferrule was approximately 18mW. Animals were then placed into a standard Med-Associates operant chamber equipped with a grid floor and aversive stimulator. Upon initiation of a 1000 second training session the house-light was dimmed and animals received 10 randomly presented 10-second presentations of optical stimulation (18mW, 20Hz, 20% duty cycle), all of which coterminated with 2 seconds of 0.7mA footshock. Upon completion of the training session the house light was illuminated and the animals were returned to their home cage. 3 hours later animals received a second training session identical to the first. The following day stylets were removed from the guide cannulae and a flat-cut 300μm diameter fiber-optic cable, coupled to a 473nm laser (Shanghai Laser and Optics Century) outside of the operant chamber, was inserted through the guide cannula and positioned directly above the BLA. Animals were placed in the center of the 3 compartment chamber and allowed to explore for 5 minutes. Animals were then removed and placed back in the center of the chamber. Upon entry into one of the 2 most extreme

compartments animals received optical stimulation that was only terminated upon exiting of the compartment. This continued for 5 minutes before animals were removed and returned to their homecage.

Innate avoidance assay: Animals were placed into the center of a 3-compartment chamber (Med Associates) comprising a central compartment with opaque walls and 2 extreme compartments with Perspex walls. Animals were left to explore the chamber for 5 minutes. Animals were then removed and 2,3,5-trimethyl-3-thiazoline (TMT) and air were presented from opposite ends of the chamber at a rate of 1 liter/minute. Animals were returned to the central compartment and left to explore the chamber for a further 5 minutes. For hM4Di experiments, animals were administered CNO (Sigma Aldrich, 0.3mg/kg dissolved in saline) 30 minutes prior to the test session. The following day animals were administered an equal volume of saline 30 minutes prior to an identical testing session. For NpHR experiments, stylets were removed from the guide cannulae and a flat-cut 300μm diameter fiber-optic cable, coupled to a 593nm laser (Shanghai Laser and Optics Century), was inserted through each guide cannula and positioned directly above each BLA. Immediately before this the power of each laser was adjusted to 10mW. Animals then received one testing session with the lasers turned on followed by an identical testing session with the lasers turned off. Behavior was recorded using a camcorder (Sony) and the amount of time spent in each compartment during the 'without odor' and 'with odor' epochs was scored manually by individuals who were blind to the experimental conditions.

Discrimination assay: Animals were restricted to 1.5ml water/day and body weight was monitored daily to ensure mice maintained 85% of their initial body weight. Animals

were removed from their homecage and placed in a modified Med Associates operant chamber equipped with portal containing a sipper for water delivery. Air was infused into the bottom of the sipper portal at 1 liter/minute and removed via a vacuum at the top of the sipper portal at an equal rate. Entries into the sipper portal were detected by breakage of 2 infrared beams at the front of the portal. Licks were detected by a contact lickometer. All stimuli were presented and all timestamp data recorded using custom Python code. Animals were initially trained on a progressive ratio schedule to lick to obtain water in the presence of an odorant (1% isoamyl acetate, dissolved in mineral oil). Initially, animals received 20 trials in which entry into the sipper portal resulted in 5µl water with no odor. Each trial was followed by a 5 second time out after which animals could initiate another trial by entering the sipper portal. Following the completion of 20 trials, animals received 20 trials in which entry into the sipper portal resulted in 2 seconds of odor presentation. Delivery of 5µl water occurred at the end of this 2 second period if animals displayed at least one lick during odor delivery. After the completion of 20 successful trials, animals received 20 trials in which water was only delivered if animals displayed at least one lick in final 0.66 seconds of odor delivery. Following the completion of 20 successful trials, animals received 120 trials in which water was only delivered if animals displayed at least one lick in the final 0.66 seconds of odor delivery and either the first or middle 0.66 seconds. Following the completion of 160 successful trials animals were deemed to have learned to lick for water delivery. Training sessions were limited to 1 hour so this often took several days. After the successful acquisition of anticipatory licking behavior, animals received discrimination training. Animals were placed into the chamber and entry into the sipper portal initiated 2 seconds of odor presentation. Odors

were 1% acetephenone or 2% octanol dissolved in mineral oil. Presentation of acetephenone (CS+) always coterminated with presentation of 5µl water, whereas presentation of octanol (CS-) had no consequence. Odors were presented in a pseudorandom order. The number of licks was recorded during the 2 seconds of odor delivery, prior to the delivery of water. Animals were trained until criterion performance was achieved (($licks_{CS+}$)/($licks_{CS+}$ + $licks_{CS-}$) > 0.8). Training sessions were limited to 1 hour so this often took several days. When criterion had been achieved, stylets were removed from the guide cannulae and a flat-cut 300µm diameter fiber-optic cable, coupled to a 593nm laser (Shanghai Laser and Optics Century) outside of the operant chamber, was inserted through each guide cannula and positioned directly above each BLA. Animals were placed in the chamber. Animals completed approximately 15 acclimation trials. These were discarded. The laser was turned on and animals completed 100 trials, before the laser was turned off and animals completed another 100 trials. Fraction correct (($licks_{CS+}$)/($licks_{CS+}$ + $licks_{CS-}$)) was computed for laser on and laser off epochs.